ISSN 2500-316X (Online)

RUSSIAN TECHNOLOGICAL JOURNAL

РОССИЙСКИЙ ТЕХНОЛОГИЧЕСКИЙ ЖУРНАЛ

Information systems.
Computer sciences.
Issues of information security

Multiple robots (robotic centers) and systems.
Remote sensing and non-destructive testing

Modern radio engineering and telecommunication systems

Micro- and nanoelectronics.
Condensed matter physics

Analytical instrument engineering and technology

Mathematical modeling

Economics of knowledge-intensive and high-tech enterprises and industries.
Management in organizational systems

Product quality management. Standardization

Philosophical foundations of technology and society

12+
www.rtj-mirea.ru

12(3) 2024

ISSN 2500-316X (Online)

RUSSIAN TECHNOLOGICAL JOURNAL

РОССИЙСКИЙ ТЕХНОЛОГИЧЕСКИЙ ЖУРНАЛ

- Information systems. Computer sciences. Issues of information security
- Multiple robots (robotic centers) and systems. Remote sensing and non-destructive testing
- Modern radio engineering and telecommunication systems
- Micro- and nanoelectronics. Condensed matter physics
- Analytical instrument engineering and technology
- Mathematical modeling
- Economics of knowledge-intensive and high-tech enterprises and industries. Management in organizational systems
- Product quality management. Standardization
- Philosophical foundations of technology and society

- Информационные системы. Информатика. Проблемы информационной безопасности
- Роботизированные комплексы и системы. Технологии дистанционного зондирования и неразрушающего контроля
- Современные радиотехнические и телекоммуникационные системы
- Микро- и наноэлектроника. Физика конденсированного состояния
- Аналитическое приборостроение и технологии
- Математическое моделирование
- Экономика наукоемких и высокотехнологичных предприятий и производств. Управление в организационных системах
- Управление качеством продукции. Стандартизация
- Мировоззренческие основы технологии и общества

Russian Technological Journal
2024, Vol. 12, No. 3

Russian Technological Journal
2024, том 12, № 3

https://www.rtj-mirea.ru

https://doi.org/10.32362/2500-316X

ISSN 2500-316X (Online)

Russian Technological Journal
2024, Vol. 12, No. 3

Publication date May 31, 2024.

The peer-reviewed scientific and technical journal highlights the issues of complex development of radio engineering, telecommunication and information systems, electronics and informatics, as well as the results of fundamental and applied interdisciplinary researches, technological and economical developments aimed at the development and improvement of the modern technological base.

Periodicity: bimonthly.
The journal was founded in December 2013. The titles were «Herald of MSTU MIREA» until 2016 (ISSN 2313-5026) and «Rossiiskii tekhnologicheskii zhurnal» from January 2016 until July 2021 (ISSN 2500-316X).

Founder and Publisher:
Federal State Budget
Educational Institution of Higher Education
«MIREA – Russian Technological University»
78, Vernadskogo pr., Moscow, 119454 Russia.

The journal is included into the List of peer-reviewed science press of the State Commission for Academic Degrees and Titles of Russian Federation. The Journal is included in Russian State Library (RSL), Russian Science Citation Index, eLibrary, Socionet, Directory of Open Access Journals (DOAJ), Directory of Open Access Scholarly Resources (ROAD), Google Scholar, Ulrich's International Periodicals Directory.

Editor-in-Chief:
Alexander S. Sigov, Academician at the Russian Academy of Sciences, Dr. Sci. (Phys.–Math.), Professor, President of MIREA – Russian Technological University (RTU MIREA), Moscow, Russia.
Scopus Author ID 35557510600, ResearcherID L-4103-2017, sigov@mirea.ru.

Editorial staff:
Managing Editor — Cand. Sci. (Eng.) Galina D. Seredina
Scientific Editor — Dr. Sci. (Eng.), Prof. Gennady V. Kulikov
Executive Editor — Anna S. Alekseenko
Technical Editor — Darya V. Trofimova
86, Vernadskogo pr., Moscow, 119571 Russia.
Phone: +7 (499) 600-80-80 (#31288).
E-mail: seredina@mirea.ru.

The registration number ПИ № ФС 77 - 81733 was issued in August 19, 2021 by the Federal Service for Supervision of Communications, Information Technology, and Mass Media of Russia.

The subscription index of *Pressa Rossii*: **79641**.

Russian Technological Journal
2024, том 12, № 3

Дата опубликования 31 мая 2024 г.

Научно-технический рецензируемый журнал освещает вопросы комплексного развития радиотехнических, телекоммуникационных и информационных систем, электроники и информатики, а также результаты фундаментальных и прикладных междисциплинарных исследований, технологических и организационно-экономических разработок, направленных на развитие и совершенствование современной технологической базы.

Периодичность: один раз в два месяца.
Журнал основан в декабре 2013 года. До 2016 г. издавался под названием «Вестник МГТУ МИРЭА» (ISSN 2313-5026), а с января 2016 г. по июль 2021 г. под названием «Российский технологический журнал» (ISSN 2500-316X).

Учредитель и издатель:
федеральное государственное бюджетное образовательное учреждение высшего образования «МИРЭА – Российский технологический университет»
119454, РФ, г. Москва, пр-т Вернадского, д. 78.

Журнал входит в Перечень ведущих рецензируемых научных журналов ВАК РФ, в которых должны быть опубликованы основные научные результаты диссертаций на соискание ученой степени кандидата наук и доктора наук, индексируется в РГБ, РИНЦ, eLibrary, Соционет, Directory of Open Access Journals (DOAJ), Directory of Open Access Scholarly Resources (ROAD), Google Scholar, Ulrich's International Periodicals Directory.

Главный редактор:
Сигов Александр Сергеевич, академик РАН, доктор физ.-мат. наук, профессор, президент ФГБОУ ВО МИРЭА – Российский технологический университет (РТУ МИРЭА), Москва, Россия.
Scopus Author ID 35557510600, ResearcherID L-4103-2017, sigov@mirea.ru.

Редакция:
Зав. редакцией — к.т.н. Г.Д. Середина
Научный редактор — д.т.н., проф. Г.В. Куликов
Выпускающий редактор — А.С. Алексеенко
Технический редактор — Д.В. Трофимова
119571, г. Москва, пр-т Вернадского, 86, оф. Л-119.
Тел.: +7 (499) 600-80-80 (#31288).
E-mail: seredina@mirea.ru.

Регистрационный номер и дата принятия решения о регистрации СМИ ПИ № ФС 77 - 81733 от 19.08.2021 г. СМИ зарегистрировано Федеральной службой по надзору в сфере связи, информационных технологий и массовых коммуникаций (Роскомнадзор).

Индекс по объединенному каталогу «Пресса России» **79641**.

https://www.rtj-mirea.ru

Editorial Board

Редакционная коллегия

Contents

Содержание

Information systems. Computer sciences. Issues of information security
Информационные системы. Информатика. Проблемы информационной безопасности

UDC 004.657
https://doi.org/10.32362/2500-316X-2024-12-3-7-24
EDN BNQNDI

RESEARCH ARTICLE

Evaluation of connection pool *PgBouncer* efficiency for optimizing relational database computing resources

Anton S. Boronnikov @,
Pavel S. Tsyngalev,
Victor G. Ilyin,
Tatiana A. Demenkova

MIREA – Russian Technological University, Moscow, 119454 Russia
@ Corresponding author, e-mail: boronnikov-anton@mail.ru

Abstract

Objectives. The aim of the research is to investigate the possibilities of using the *PgBouncer* connection pool with various configurations in modern database installations by conducting load testing with diverse real-world like scenarios, identifying critical metrics, obtaining testing results, and interpreting them in the form of graphs.

Methods. The research utilized methods of experimentation, induction, testing, and statistical analysis.

Results. The main features, architecture and modes of operation of the *PgBouncer* service are considered. Load testing was carried out on a virtual machine deployed on the basis of an open cloud platform with different configurations of computing resources (CPU, RAM) and according to several scenarios with different configurations and different numbers of balancer connections to the database, during which the following main indicators were investigated: distribution of processor usage, utilization of RAM, disk space, and CPU. The interpretation of the data obtained and the analysis of the results obtained by highlighting critical parameters are performed. On the basis of results analysis, conclusions and recommendations are formulated on the use of a connection balancer in real high-load installations for optimizing the resources utilized by the server on which the database management system (DBMS) is located. A conclusion is presented on the usefulness of using the *PgBouncer* query balancer along with proposed configuration options for subsequent use in real installations.

Conclusions. The degree of influence of the use of the *PgBouncer* connection balancer on the performance of the system as a whole deployed in a virtualized environment is investigated. The results of the work showed that the use of *PgBouncer* allows significantly optimization of the computing resources of a computing node for a DBMS server, namely, load on the CPU decreased by 15%, RAM—by 25–50%, disk subsystem—by 20%, depending on the test scenarios, the number of connections to the database, and the configuration of the connection balancer.

Keywords: PgBouncer, PostgreSQL, connection pool, balancer, databases, optimization, monitoring, virtual machines, cloud technologies

• **Submitted:** 13.06.2023 • **Revised:** 06.12.2023 • **Accepted:** 09.04.2024

For citation: Boronnikov A.S., Tsyngalev P.S., Ilyin V.G., Demenkova T.A. Evaluation of connection pool *PgBouncer* efficiency for optimizing relational database computing resources. *Russ. Technol. J.* 2024;12(3):7–24. https://doi.org/10.32362/2500-316X-2024-12-3-7-24

Financial disclosure: The authors have no a financial or property interest in any material or method mentioned.

The authors declare no conflicts of interest.

НАУЧНАЯ СТАТЬЯ

Оценка эффективности балансировщика соединений *PgBouncer* для оптимизации вычислительных ресурсов реляционных баз данных

А.С. Боронников [@], **П.С. Цынгалёв**, **В.Г. Ильин**, **Т.А. Деменкова**

МИРЭА – Российский технологический университет, Москва, 119454 Россия
[@] *Автор для переписки, e-mail: boronnikov-anton@mail.ru*

Резюме

Цели. Целью работы является исследование возможностей использования балансировщика подключений *PgBouncer* с различными конфигурациями в современных инсталляциях баз данных (БД) путем проведения нагрузочного тестирования с различными сценариями, максимально приближенными к реальной нагрузке, определение критичных показателей, получение результатов тестирования и интерпретация их в виде графиков.

Методы. В ходе исследования использовались методы эксперимента, индукции, тестирования и статистического анализа.

Результаты. Рассмотрены основные возможности, архитектура и режимы работы сервиса *PgBouncer*. Проведено нагрузочное тестирование на виртуальной машине, развернутой на базе открытой облачной платформы, с различной конфигурацией затрачиваемых вычислительных ресурсов – центрального процессора (CPU) и оперативной памяти (RAM) и использованием нескольких сценариев с разной конфигурацией и разным количеством подключений балансировщика к БД. В ходе тестирования были исследованы основные показатели: распределение использования процессора, утилизация оперативной памяти, дискового пространства и центрального процессора. Выполнены интерпретация полученных данных и анализ полученных результатов путем выделения критических параметров. Сформулированы выводы и рекомендации по использованию балансировщика подключения в реальных высоконагруженных инсталляциях для оптимизации утилизируемых ресурсов сервером, на котором расположена система управления базами данных (СУБД). Сформировано заключение о полезности использования балансировщика запросов *PgBouncer* и предложены варианты конфигурации для последующего использования в реальных инсталляциях.

Выводы. Исследована степень влияния использования балансировщика соединений *PgBouncer* на производительность системы в целом, развернутой в виртуализированной среде. Результаты работы показали, что применение *PgBouncer* позволяет существенно оптимизировать затрачиваемые вычислительные ресурсы вычислительного узла под сервер СУБД, а именно: уменьшилась нагрузка на CPU на 15%, на RAM – на 25–50%, на дисковую подсистему – на 20%, в зависимости от сценариев тестов, количества подключений к БД, конфигурации балансировщика подключений.

Ключевые слова: PgBouncer, PostgreSQL, пуллер, балансировщик, база данных, оптимизация, мониторинг, виртуальная машина, облачные технологии

• **Поступила:** 13.06.2023 • **Доработана:** 06.12.2023 • **Принята к опубликованию:** 09.04.2024

Для цитирования: Боронников А.С., Цынгалёв П.С., Ильин В.Г., Деменкова Т.А. Оценка эффективности балансировщика соединений *PgBouncer* для оптимизации вычислительных ресурсов реляционных баз данных. *Russ. Technol. J*. 2024;12(3):7–24. https://doi.org/10.32362/2500-316X-2024-12-3-7-24

Прозрачность финансовой деятельности: Авторы не имеют финансовой заинтересованности в представленных материалах или методах.

Авторы заявляют об отсутствии конфликта интересов.

INTRODUCTION

Databases (DB) are an integral part of modern applications. They are used to store, manage, and process large scopes of information. However, one of the main problems faced by applications is managing multiple DB connections.

Connection to a DB involves the process of establishing a link between a client application and the DB server. Since each client application establishes its own connection to the DB, excessive loads on the DB server can decrease the application performance. In addition, each DB connection requires certain resources such as memory and CPU time. If a significant number of client applications establish a DB connection at the same time, it may overload the server and degrade the application performance.

In order to solve this problem, the DB management system (DBMS) can be optimized by configuring its parameters at the infrastructure startup stage [1–3] or using third-party services such as DB connection balancers. Such tools manage client connections in such a way as to maximize the use of DB server resources, thus improving application performance. There are several types of balancers [4]. This article discusses the main features of a tool that belongs to the application-level balancing type known as a *connection pooler* or *pooler*.

1. DB QUERY PATH

Implementation of the pooler leads to significant changes in working with the DB. In order to notice them, it is necessary to study the standard query passing route. In the usual client-server architecture, the following standard interaction principle takes place as shown in Fig. 1.

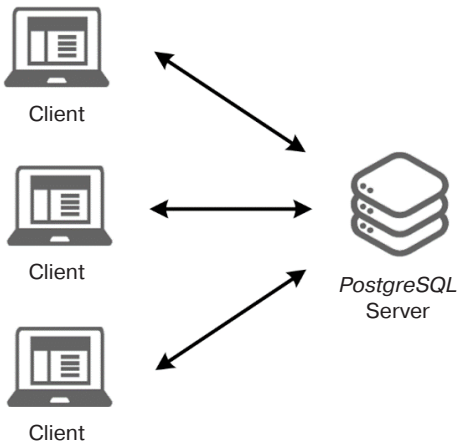

Fig. 1. Regular client-server connection[1]

[1] *PostgreSQL*. https://www.postgresql.org/. Accessed April 18, 2023.

When a new session is established, the client application requests a connection to the server and goes through the authentication process. The server responds by creating a separate system process to handle the connection and session operation. The initialization of the session state is based on various configuration parameters defined at server, DB, and user levels. Within a single session, the client performs the required operations. The operation continues until the client terminates the session by disconnecting. After the session is terminated, the server destroys the corresponding system process responsible for processing this session.

The main disadvantages of a regular client-server connection can be highlighted as follows:

1) creating, managing and deleting connection processes takes time and consumes resources;
2) as the number of connections on the server increases, so does the need for resources to manage them. In addition, memory utilization on the server increases as clients perform operations;
3) since a single session serves only one client, clients can change the state of a DB session and expect those changes to persist in subsequent transactions.

When using a pooler, clients connect to the puller that has already established a connection to the server (Fig. 2). This changes the model of the standard connection principle to a client-proxy-server architecture.

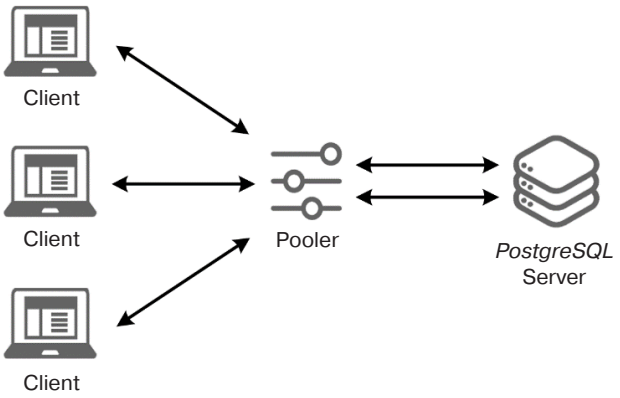

Fig. 2. Client-proxy-server connection

Now the connection of a client to a server is independent of the lifetime of the connection and the process on the server. The pooler is responsible for accepting and managing connections from the client, establishing and maintaining connections to the server, and assigning server connections to client connections.

PostgreSQL [5–9] is an excellent choice in terms of the quality of the DBMS. One of the main factors is *PostgreSQL*'s status as open-source software. There are several decent *PostgreSQL* connection

poolers [6, 10–12] such as *PgBouncer*[2], *Pgpool-II*[3], and *Odyssey*[4]. In this paper, the main features, architecture, and modes of operation of *PgBouncer* are considered.

2. *PgBouncer* CONNECTION POOL

PgBouncer is a pooler that allows you to manage connections to a *PostgreSQL* DB. It works as a proxy server that processes DB connection requests and redirects them to the appropriate server. *PgBouncer* can be installed on the same machine as *PostgreSQL* or on a separate one.

This pooler widely used in many *PostgreSQL*-based applications is for solving various tasks related to performance, scalability and security. This balancer is actively used in products of such large companies as Alibaba[5], Huawei[6], Instagram[7] (banned in the Russian Federation), Skype[8], as well Russian companies[9] such as Yandex[10], Avito[11], Sberbank[12], Gazpromneft[13], etc.

One of the main tasks of *PgBouncer* is connection management. This allows the creation of connection pools that can be used by multiple clients, which reduces load on the DB server and improves application performance.

2.1. Architecture

In the official documentation of *PgBouncer* there is no description of the balancer architecture. After analyzing the libraries of this pooler and investigating its functionality, we propose a *PgBouncer* balancer architecture based on our own reverse-engineering (Fig. 3).

Listener plays an important role in handling client connections to *PostgreSQL* DB. Providing an entry point for client connections (called a socket), it acts as an intermediary between the client and the server. The listener still includes a protocol that defines the format of data exchange between the client and the server over the socket. *PgBouncer* uses the same protocol as *PostgreSQL*, but has its own additional extensions and commands.

Authentication provides verification of the client's authenticity when an attempt is made to connect to it. Various methods such as md5, trust, plain, cert, etc. are supported.

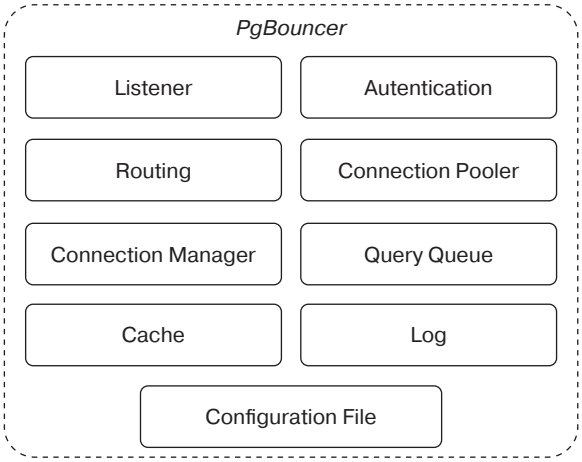

Fig. 3. *PgBouncer* architecture

Routing determines the modes of pooler operation. There are four types: session pooling, transaction pooling, statement pooling, and combined pooling. They are discussed in more detail in Section 2.2.

Connection pool is a set of available connections that can be used by the client to perform operations in the DB. If a connection is free, the client can take it from the pool. If there is no connection, the pooler can create a new one.

Connection manager is responsible for managing the lifecycle of each connection in the pool. It tracks the state of each active connection to the DB, including opening, closing and reusing free connections.

Query queue manages queries coming from clients when all connections are busy. This ensures fair processing of queries and avoids DB blocking or overloading. The query queue has customizable parameters that enable controlling the number and waiting time of queries in the queue.

Cache is an additional component that stores the results of previous queries so that when a query is executed again, the results are returned directly from the cache instead of accessing the DB. Cache saves time and resources for query execution, especially if the queries are often repeated and their results do not change.

Event log keeps a record of events such as establishing and breaking connections, executing requests and other operations, etc. It can be used to analyze and track the operation of the pooler, detect various errors and

[2] Official documentation *PgBouncer*. https://www.pgbouncer.org/. Accessed April 02, 2023.

[3] *Pgpool* Wiki. https://pgpool.net/mediawiki/index.php/Main_Page. Accessed April 15, 2023.

[4] *Odyssey* – Yandex Technologies. https://yandex.ru/dev/odyssey/ (in Russ.). Accessed April 15, 2023.

[5] https://www.alibaba.com/. Accessed April 15, 2023.

[6] https://www.huawei.com/. Accessed April 15, 2023.

[7] https://www.instagram.com/. Accessed April 15, 2023.

[8] https://www.skype.com/ru/ (in Russ.). Accessed April 15, 2023.

[9] Why the largest companies in Russia and the world choose Postgres. Results of PgConf.Russia 2017. http://www.interface.ru/home.asp?artId=39028 (in Russ.). Accessed April 10, 2023.

[10] https://yandex.ru/ (in Russ.). Accessed April 15, 2023.

[11] https://www.avito.ru/ (in Russ.). Accessed April 15, 2023.

[12] http://www.sberbank.ru/ (in Russ.). Accessed April 15, 2023.

[13] https://www.gazprom-neft.ru/ (in Russ.). Accessed April 15, 2023.

Table 1. Comparison of *PgBouncer* operating modes

Comparison of *PgBouncer* operating modes	Isolation of transactions	Connection pool	Capacity
Session mode	Full	Assigned for the duration of the session	Decrease due to creation and deletion of the connections
Transaction mode	Full	Assigned for the duration of the transaction	Decrease due to creation and deletion of the connections
Statement mode	Partial	Assigned for the duration of the query	Increase due to reuse of the connections
Combined mode	Balance	Depending on the type of the query	Balance between capacity and insulation

warnings, monitor performance, and perform debugging activities.

This is followed directly by the *configuration file*, where settings can be configured and specified for all the architecture components discussed in this section.

When these elements are properly configured, they ensure efficient use of server resources, improve performance and performance of applications that use *PostgreSQL*.

2.2. Operating modes

Operating modes determine how the pooler will manage connections. In different modes, *PgBouncer* can have different effects on system performance and functionality.

Session mode, representing the standard approach, consists of assigning a single server connection to each client for as long as the client remains connected. When a client disconnects, this server connection is returned back to the pool. This is the default method of operation. The mode can be useful for applications that have many client requests that are not frequent, but are executed in long sessions.

Transaction mode means that the client is assigned a connection to the server only for the duration of the transaction. When transaction completion is detected, *PgBouncer* returns the connection back to the pool. This mode can be useful in applications that have many short transactions.

Statement mode is the most aggressive approach, which assumes that the connection to the server will be returned to the pool immediately after each request is completed. In this mode, transactions with multiple statements are prohibited. This mode can be useful for applications that have many repetitive queries or use queries with the same structure.

Combined mode is an approach that combines transaction and operator modes. *PgBouncer* will use statement mode for queries that do not start a new transaction, and transaction mode for queries that do start a new transaction. This method can be useful for applications that run many repetitive queries and require transactions. It can also be effective for applications that have a large number of unique queries, but where transactions may be repeated.

PgBouncer operation modes were compared according to the following criteria: transaction isolation, connection pooling and performance. The results of the study are shown in Table 1.

2.3. Features of use

Some key features of *PgBouncer* will be emphasized in order to avoid mistakes when working with it.

The first key feature is the limitation on query types. Some queries, such as DB creation or deletion, cannot be routed through the pool and must be executed directly on the *PostgreSQL* server. It is also worth considering the configuration of the DBMS itself, since some parameters, such as those related to caching, may affect the performance of the pooler itself. In this case, additional configuration of the *PostgreSQL* server will be required for optimal operation in conjunction with the pooler.

In order to avoid pooler overloading, it is necessary to control the size of the balancer connection pool otherwise overflow may occur to exhaust system resources such as central processing unit (CPU) and random-access memory (RAM) utilization. An overflowed pool can cause performance degradation or application failures.

When configuring extensions, it should be taken into account that some of them may not be compatible with *PgBouncer*, as they may create their own connections to the *PostgreSQL* server, which will harm the performance of the system as a whole. When using this balancer, it is also necessary to ensure that it is compatible with other

tools and technologies used in the application, such as the ORM-framework[14] used.

Version support will be required when using with *PgBouncer*, since some versions of the pooler may not support the latest versions of *PostgreSQL*.

3. TESTING AND EVALUATION OF THE RESULTS OBTAINED

Testing was conducted on two virtual machines (VM) with the following characteristics:

- VM with DBMS: 8 virtual central processing units (vCPU), 16 GB of random access memory (RAM), external SSD 32 GB (under system), 500 Mbps, 320 IOPS[15], 120 GB (under DB), 500 Mbps, 1200 IOPS, Ubuntu 22.04 operating system (OS);
- VM with the pooler: 2 vCPU, 4 GB RAM, 120 GB SSD external drive, 500 Mbps, 1200 IOPS, Ubuntu 22.04 OS.

In order to collect and display metrics, the software *pgwatch2*[16], *Grafana*[17] and *PostgreSQL* were used. These were run in a docker container [13–15]. 2 GB of RAM, 1 vCPU was allocated for system performance. During testing, the performance of the test bench VMs was increased, since some tests utilized all available resources.

Testing was performed using several connection scenarios: directly to the DB and through the pooler. The pooler was set to session mode. The scenarios themselves included a gradual increase in the number of connections (100, 500, 1000) and query complexity with an active session size of 10 min.

The queries were of the following nature:

- simple queries to an empty DB;
- crud queries (create, read, update, delete) with application of temporary tables to the DB containing test data.

The following metrics were highlighted for the analysis:

1. CPU utilization distribution:
   - idle—free resources;
   - user—expenditures on the use of the system by users;
   - system—system expenditures;
   - iowait—waiting on the disk subsystem;
   - other—other CPU operations;
   - irqs—CPU core interruptions.
2. Utilization of CPU.
3. Utilization of RAM.
4. Utilization of the disk subsystem (disk).

3.1. Read queries

As a part of this testing, a read request to the DB (obtaining the DBMS version) was performed in parallel.

This test was chosen to evaluate the session's impact on DB resources as fairly as possible (it is most strongly reflected in RAM utilization).

Metrics for the direct connections with simple queries are depicted in Fig. 4 (100 connections), Fig. 5 (500 connections), Fig. 6 (1000 connections), where the time segments shown in the graph reflect the change of parameters during the testing period in real time in the *hours:minutes* format.

Metrics for connections via pooler with simple queries are shown in Fig. 7 (100 connections), Fig. 8 (500 connections), Fig. 9 (1000 connections).

During testing, an anticipated strong impact of idle connections on the resources reserved for the DB was noted.

If CPU and disk utilization can be attributed to the error and influence of external factors, RAM should be considered in more detail. The following utilization was obtained for the tests:

1) 100 connections, 230 MB (2.3 MB/connection);
2) 500 connections, 1180 MB (2.36 MB/connection);
3) 1000 connections, 1810 MB (1.81 MB/connection).

RAM utilization rates when tested via pooler were extremely low and did not fluctuate depending on the number of connections, remaining at an extremely low level (~30 MB on all tests).

It is also worth noting that a single connection had the greatest impact on the resources consumed when there were 500 parallel connections.

[14] Object relation mapping is a programming technology that connects DBs with the concepts of object-oriented programming languages, creating a virtual object DB.

[15] IOPS—input/output operations per second.

[16] PGWatch: Optimized PostgreSQL monitoring. https://pgwatch.com. Accessed April 15, 2023.

[17] Grafana Labs. https://grafana.com. Accessed April 12, 2023.

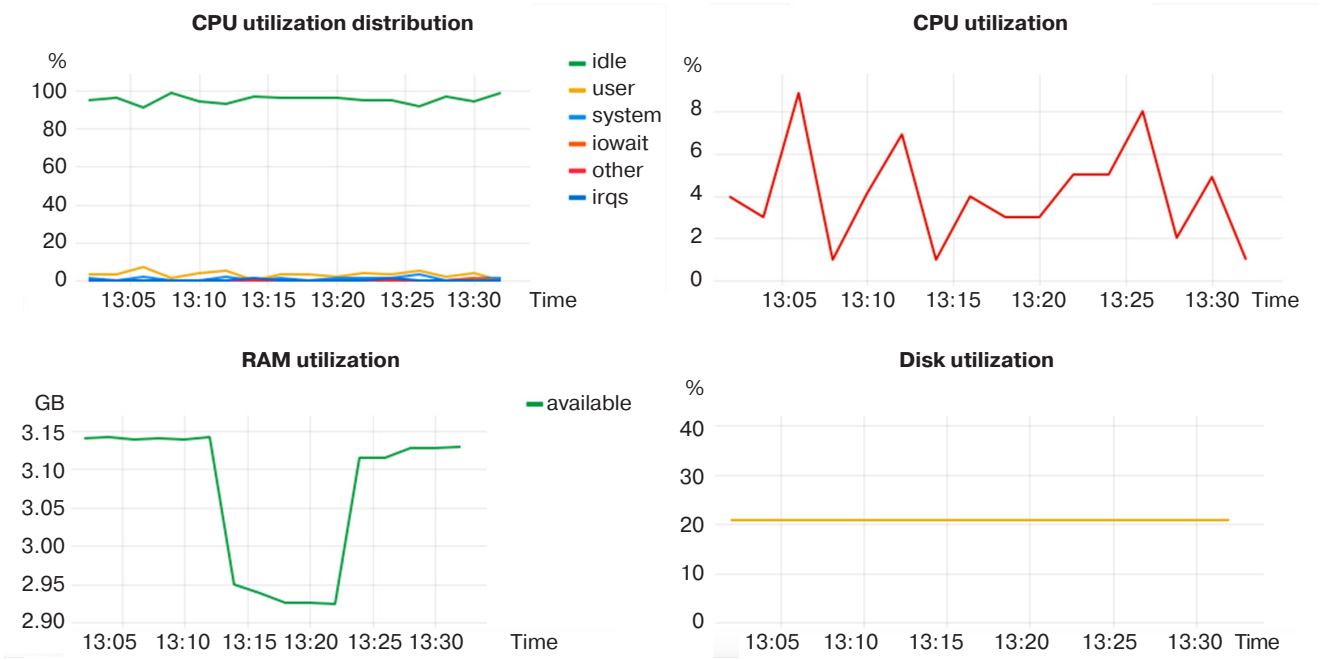

Fig. 4. Performing load testing with simple queries with 100 connections directly to an empty DB

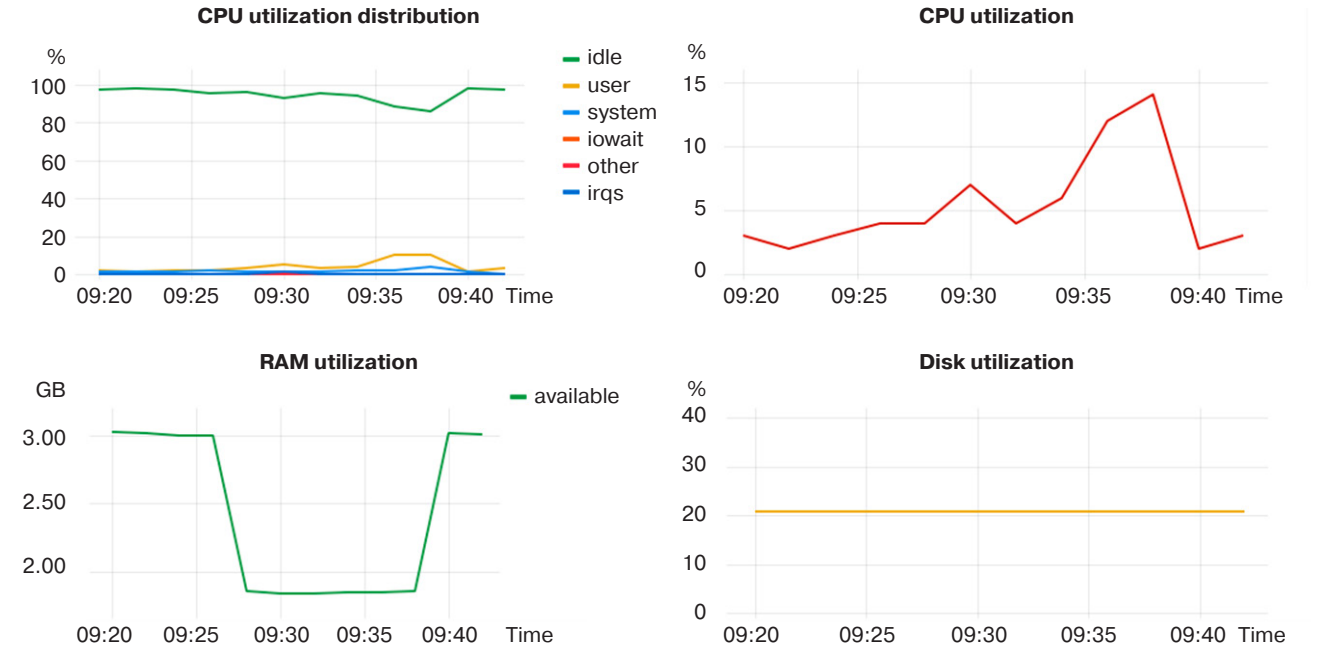

Fig. 5. Load testing with simple queries with 500 connections directly to an empty DB

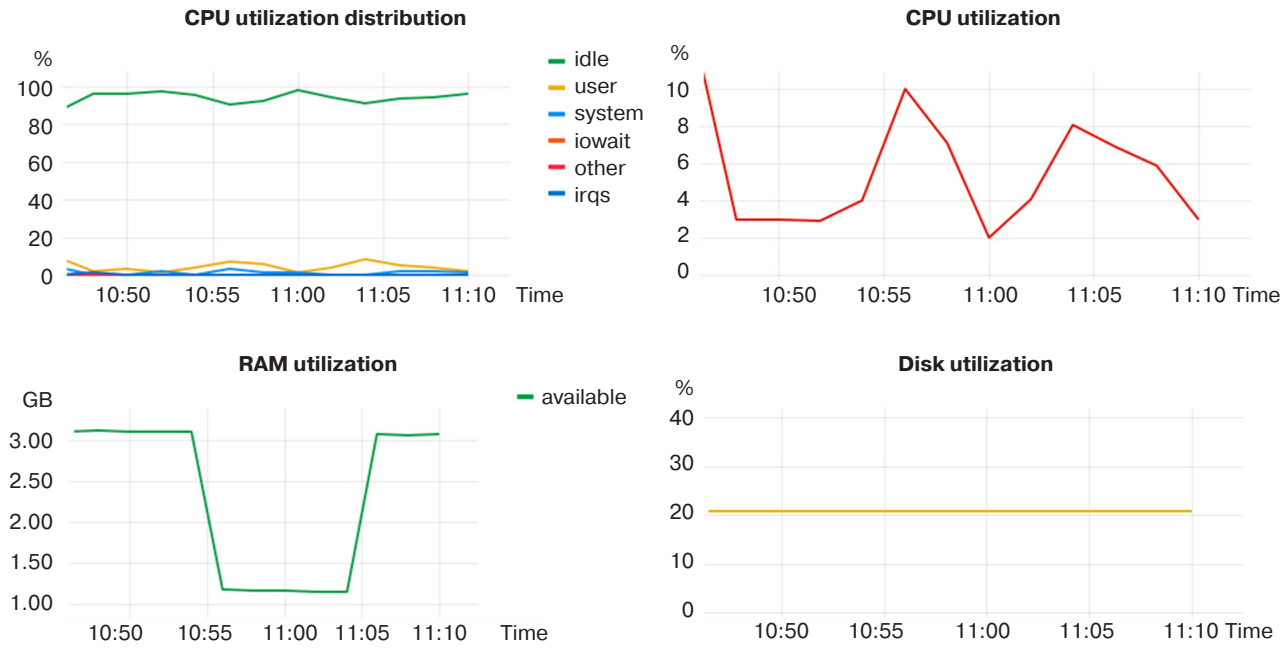

Fig. 6. Performing load testing with simple queries and 1000 connections directly to an empty DB

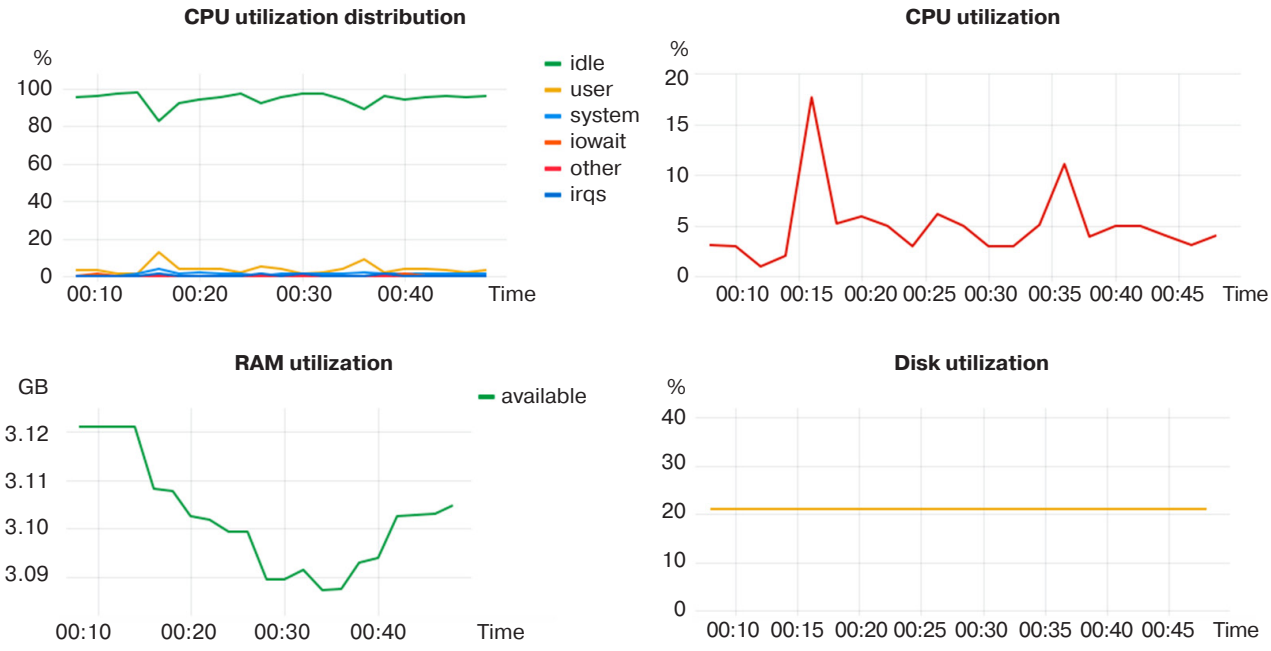

Fig. 7. Load testing with simple queries with the number of 100 connections through the pooler to an empty DB

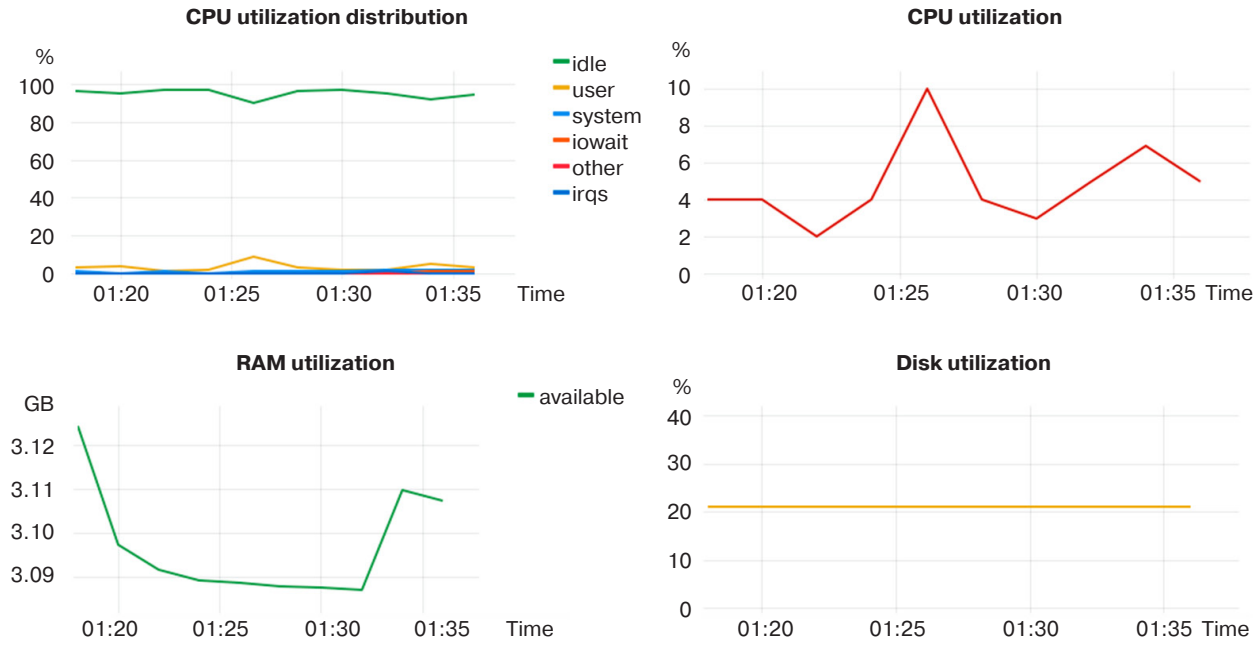

Fig. 8. Performing load testing with simple queries with the number of 500 connections through the pooler to an empty DB

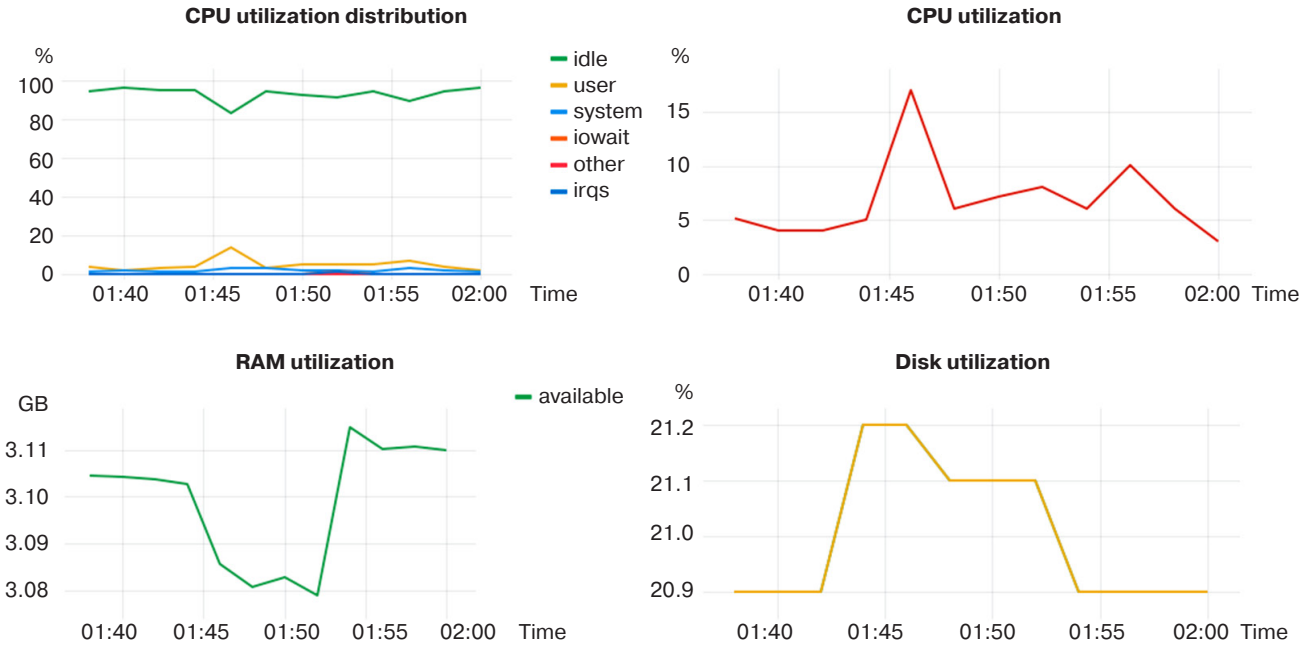

Fig. 9. Carrying out load testing with simple queries with 1000 connections through the pooler to an empty DB

3.2. Complicated queries

Within the framework of this testing, a query for writing to the DB, creating, filling, deleting a table (2 columns, 1000000 rows, with the *text* value type) was executed in parallel.

This test was chosen because it allows us to evaluate possible CPU and disk resource savings when using the request pooler.

The metrics for direct connections by complex queries are depicted in Fig. 10 (100 connections), Fig. 11 (500 connections), and Fig. 12 (1000 connections), where the time segments shown in the graph represent the change in metrics during the testing period in real time in the *hours:minutes* format.

Metrics for connections via pooler with complex queries are shown in Fig. 13 (100 connections), Fig. 14 (500 connections), and Fig. 15 (1000 connections).

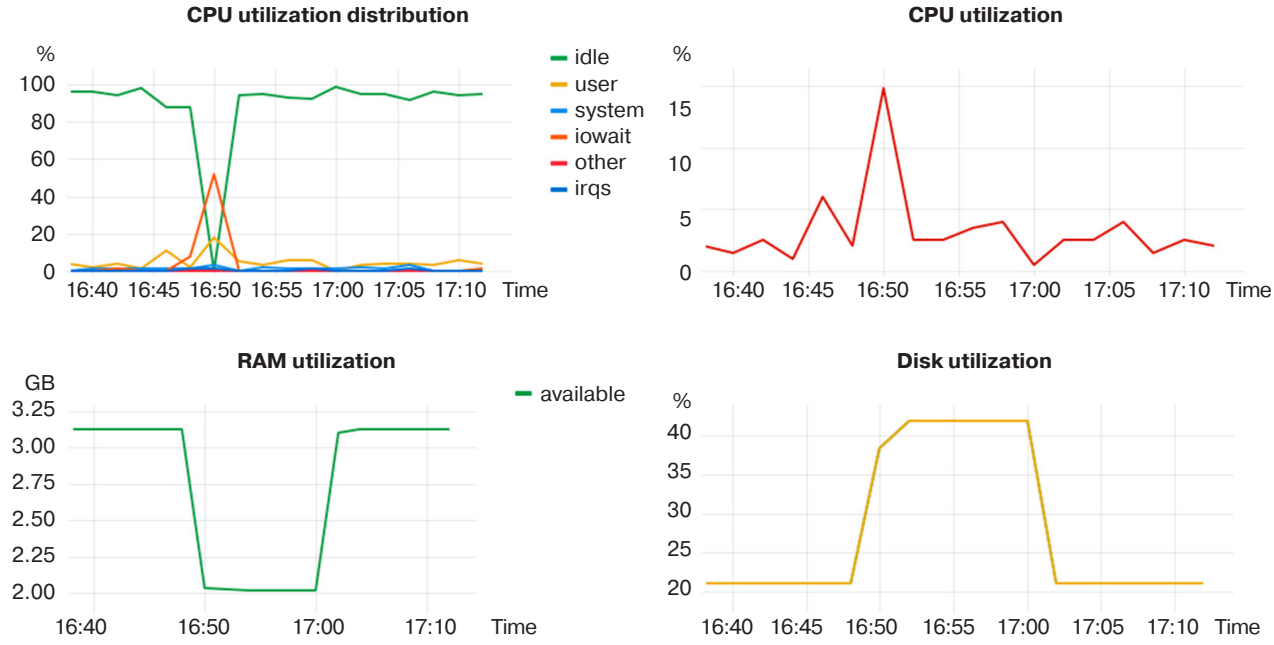

Fig. 10. Load testing with complicated queries using temporary tables and the number of 100 connections to the DB filled with test data

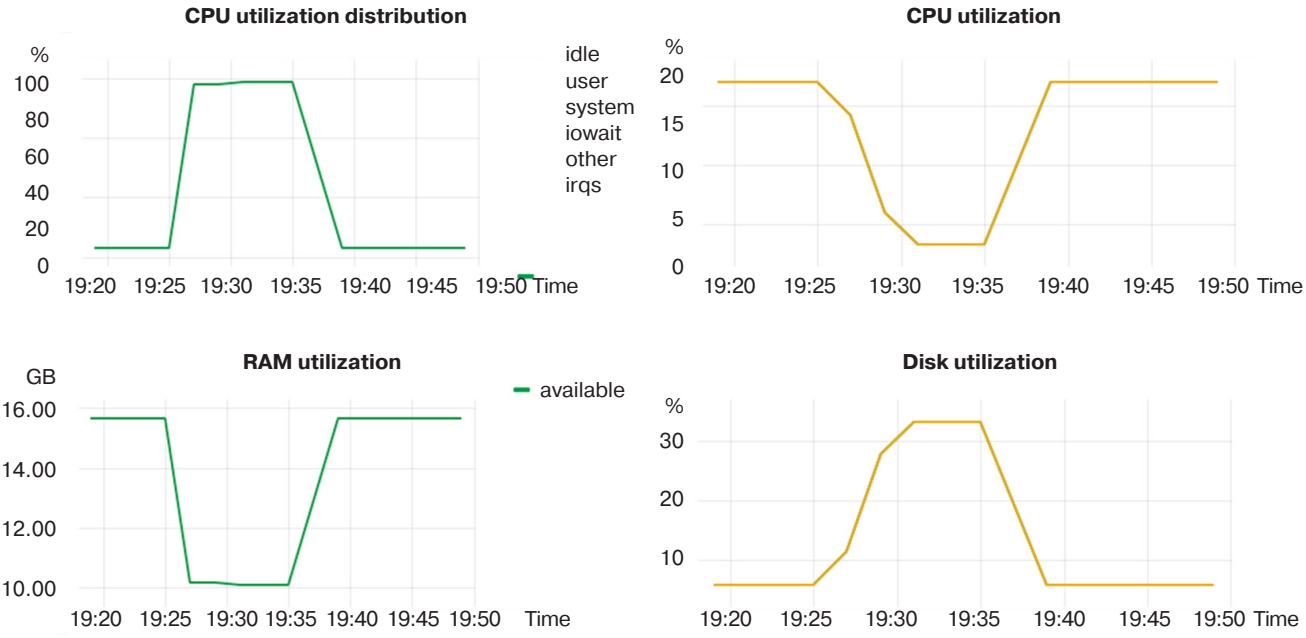

Fig. 11. Load testing with complex queries using temporary tables and 500 connections to the DB filled with test data

Testing demonstrated a significant influence of parallel operations on DB resources along with the possibility to minimize them by means of pool tools.

Let us examine RAM utilization at different number of direct connections to the DB:

1) 100 connections, 1125 MB (11.25 MB/connection);
2) 500 connections, 5900 MB (11.8 MB/connection);
3) 1000 connections, 10250 MB (10.25 MB/connection).

RAM utilization rates when tested via the pooler were extremely low and did not fluctuate depending on the number of connections, remaining at an extremely low level (~250 MB on all tests).

As compared to the previous test, utilization jumps can be observed for all the monitored metrics. The 500-connection test also shows the highest memory utilization per single connection, just like in the previous case. The test for 1000 connections shows

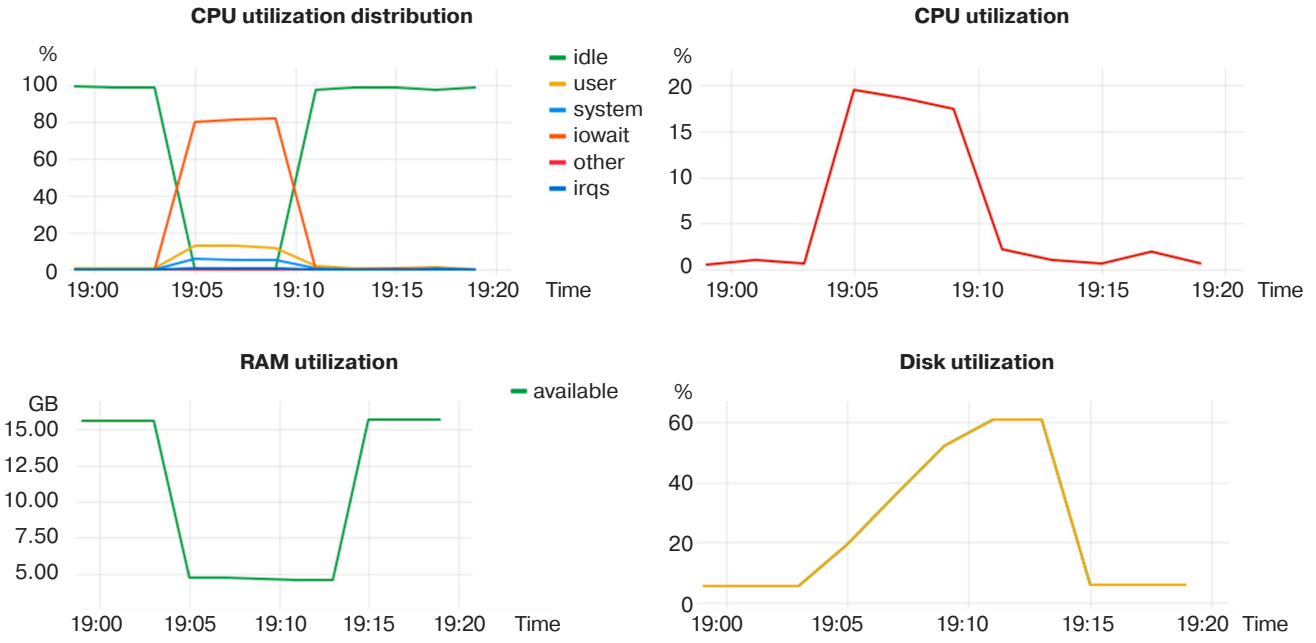

Fig. 12. Load testing with complex queries using temporary tables and 1000 connections to the DB filled with test data

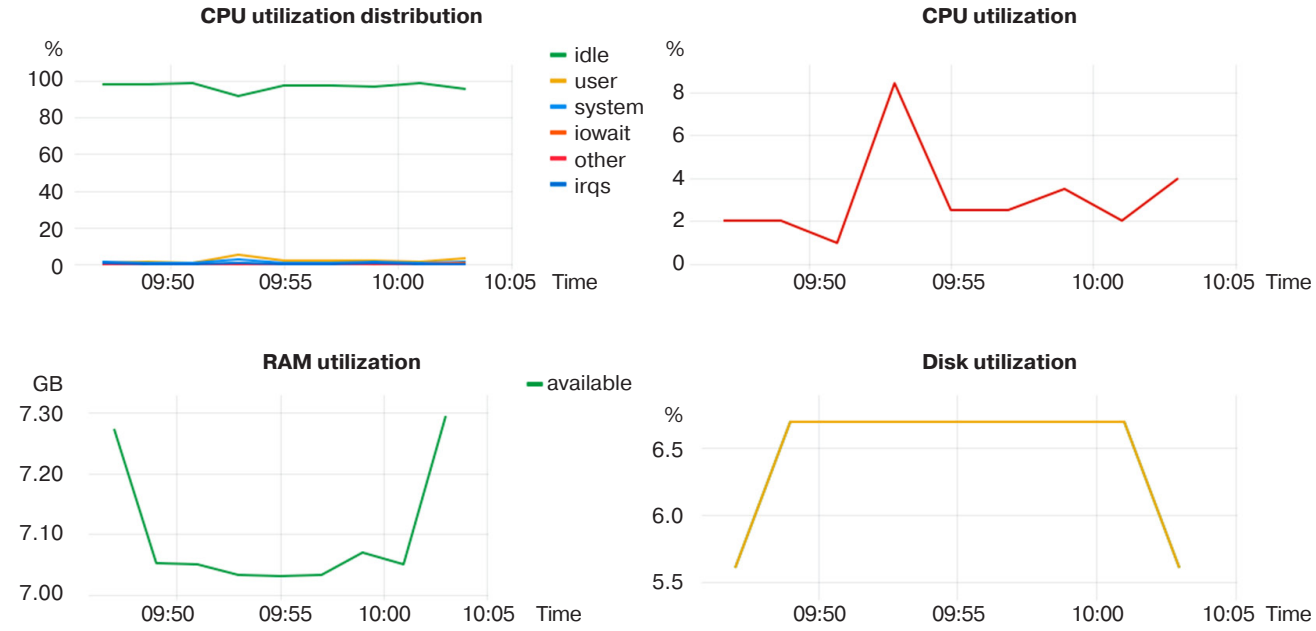

Fig. 13. Load testing with complex queries using temporary tables and 100 connections through the pooler to the DB filled with test data

that the DBMS is not oriented for such a number of connections, since the time of increased CPU and disk system utilization is comparatively higher than the other cases.

Optimization of disk subsystem utilization can also be observed. This is due to the possibility of transferring the processing of operations with temporary tables to the power of the pooler (since it knows the result of all queries in advance).

Reduced CPU load when testing through the pooler is due to the fact that it takes over session management (the most expensive process in terms of CPU resources).

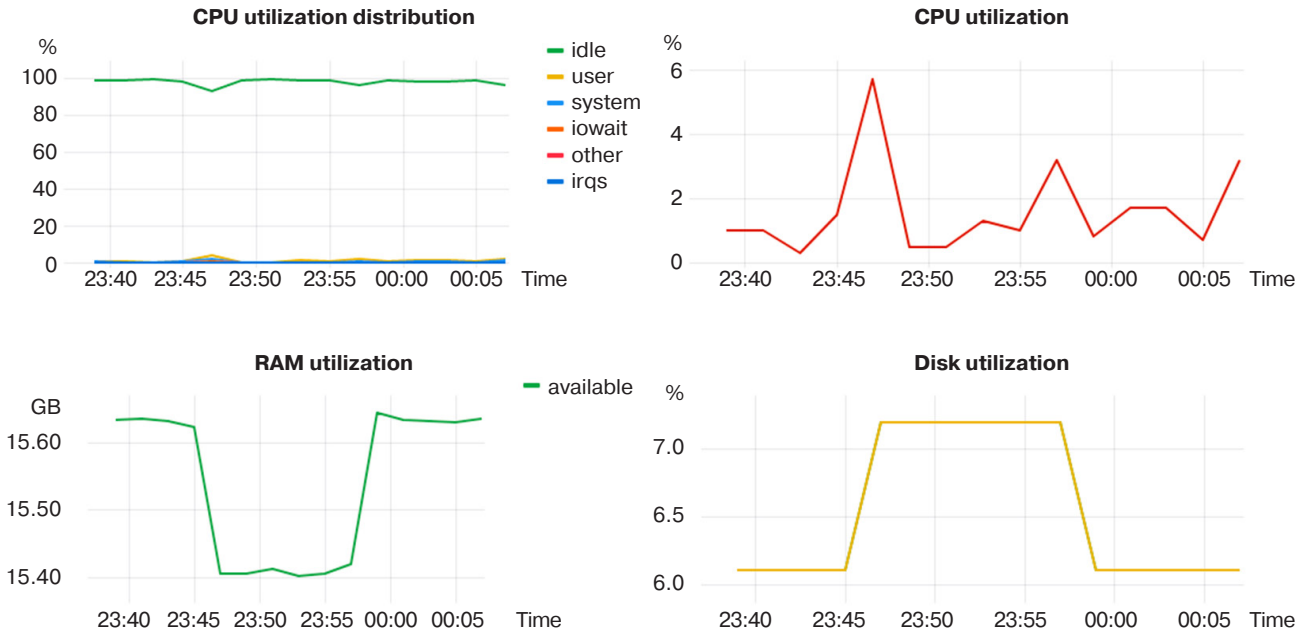

Fig. 14. Performing load testing with complex queries using temporary tables and 500 connections through a pooler to the DB filled with test data

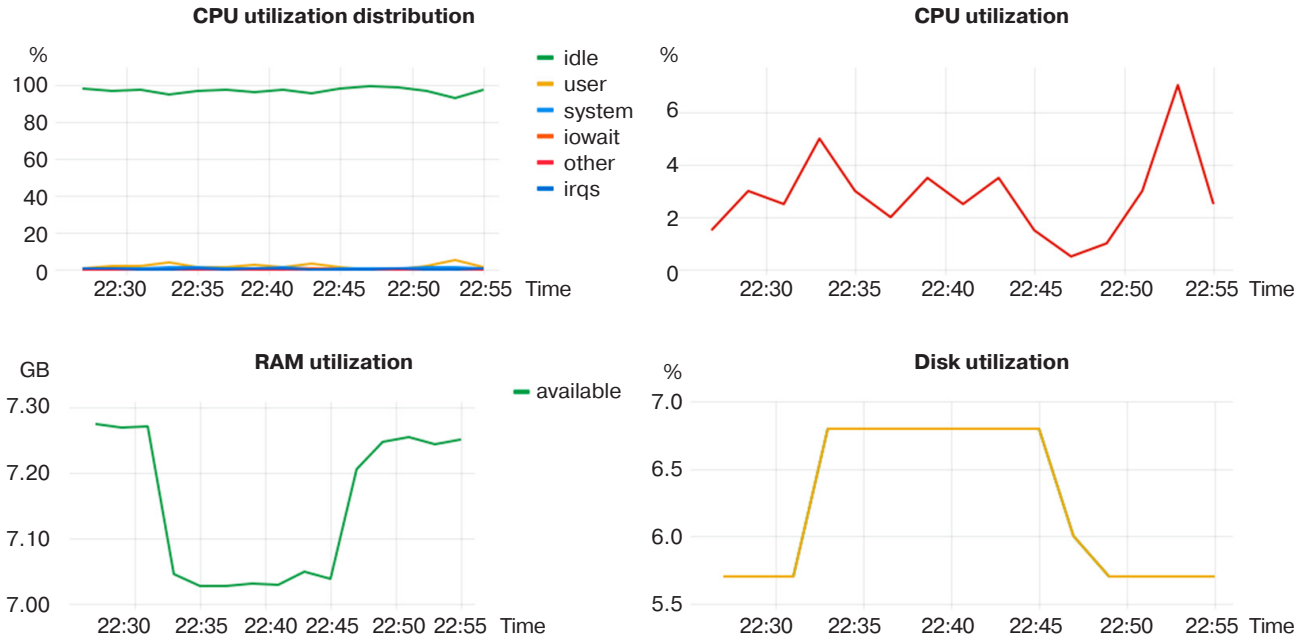

Fig. 15. Load testing with complex queries using temporary tables and 1000 connections through the pooler to the DB filled with test data

3.3. Combined queries

This test, which is a combination of the two previous ones, is aimed at evaluating a more general case of DB usage (parallel writing and reading).

Metrics for direct connections by combined queries are depicted in Fig. 16 (100 connections), Fig. 17 (500 connections), Fig. 18 (1000 connections), where the time segments shown in the graph represent the change in metrics during the testing period in real time in *hours:minutes* format.

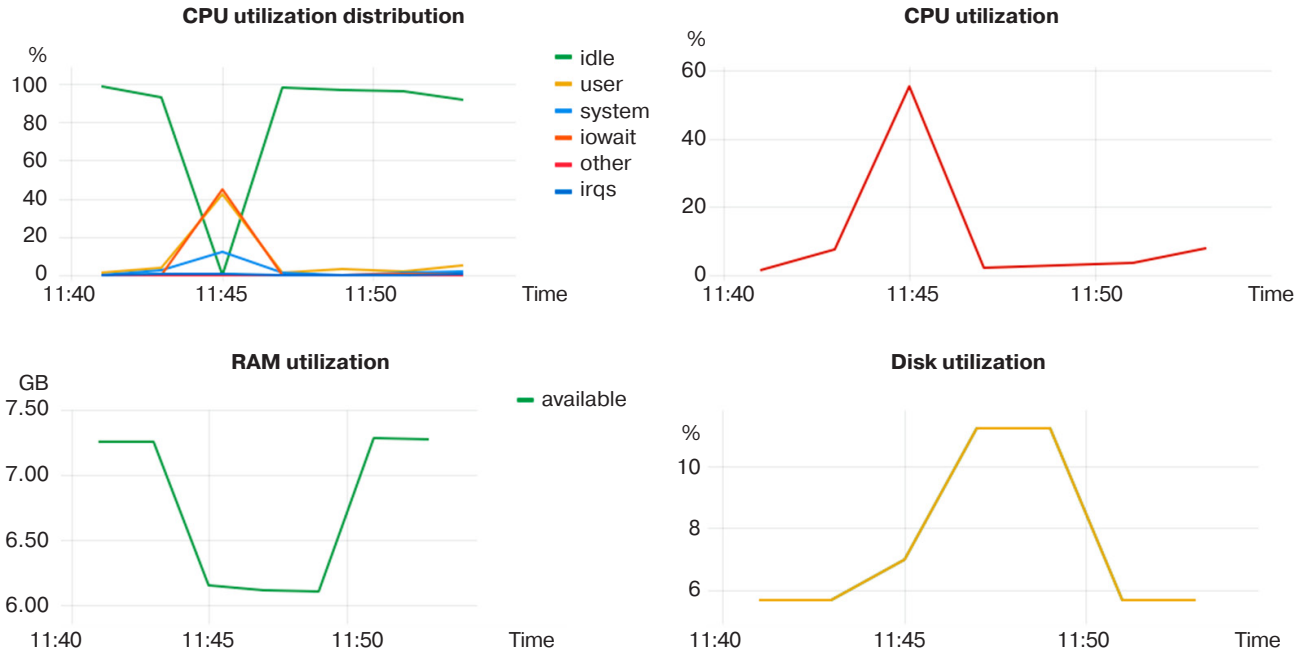

Fig. 16. Performing load testing with combined queries using temporary tables and 100 connections directly to the DB

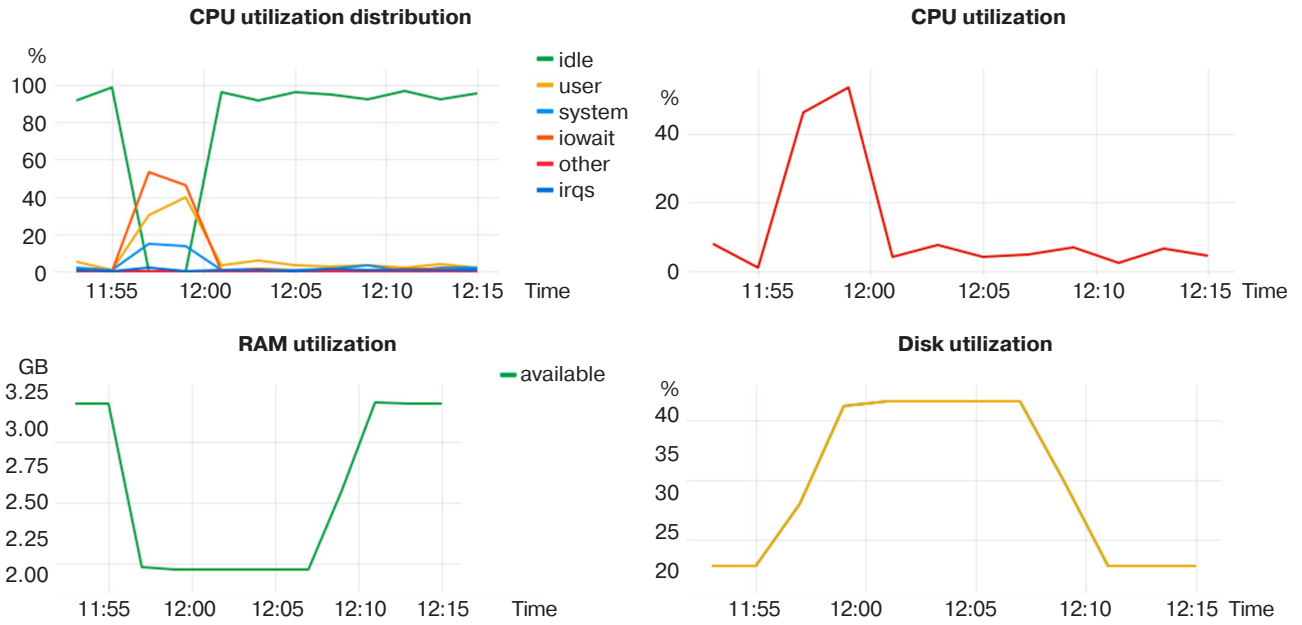

Fig. 17. Performing load testing with combined queries using temporary tables and 500 connections directly to the DB

Metrics for connections via pooler by combined queries are shown in Fig. 19 (100 connections), Fig. 20 (500 connections), and Fig. 21 (1000 connections).

Testing did not show any anomalies when running simultaneous read and write tests. This shows that testing with more real-world cases does not conflict in any way with using the Connection Balancer.

Let us examine RAM utilization at different number of direct connections to the DB:

1) 100 connections, 1200 MB (12.0 MB/connection);
2) 500 connections, 6050 MB (12.1 MB/connection);
3) 1000 connections, 11150 MB (11.15 MB/connection).

RAM utilization rates when tested via pooler were extremely low and did not fluctuate depending on the

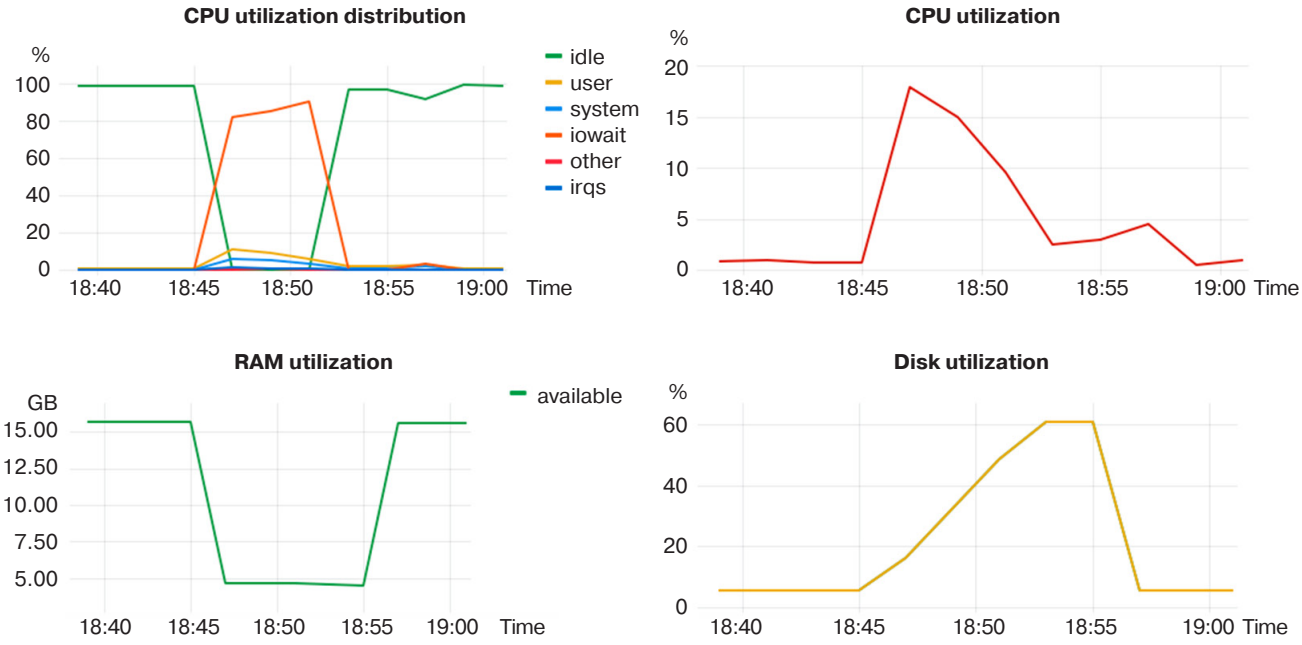

Fig. 18. Performing load testing with combined queries using temporary tables and 1000 connections directly to the DB

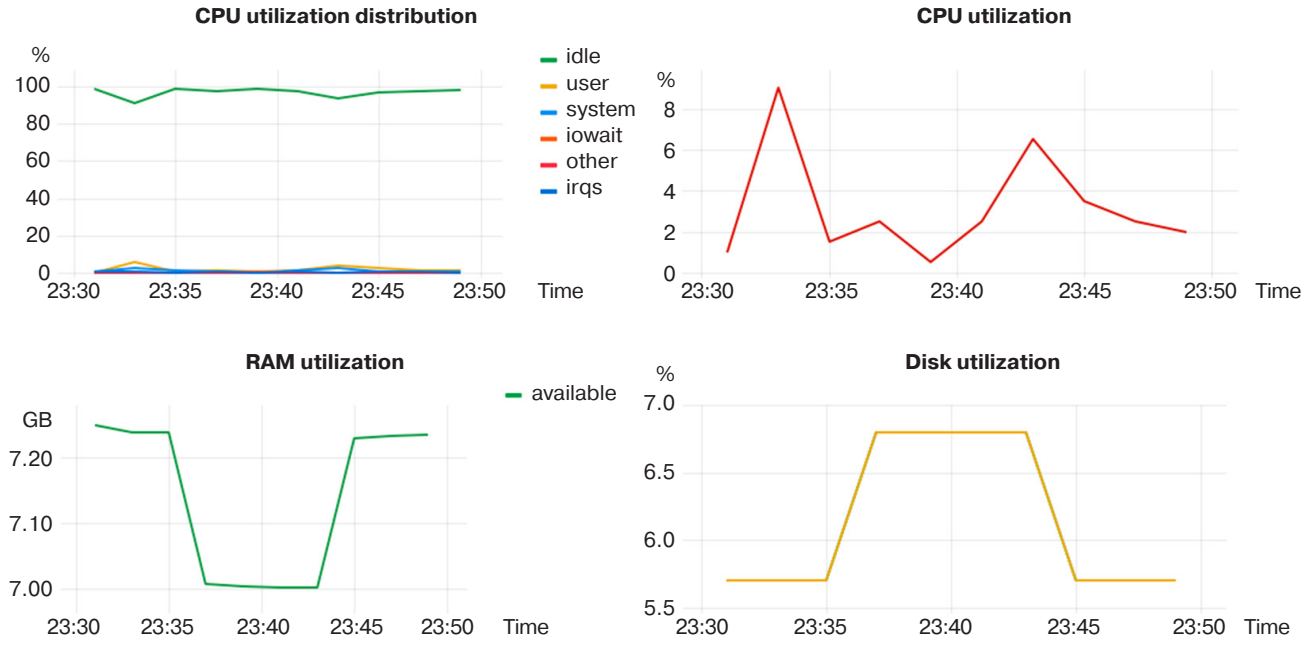

Fig. 19. Performing load testing with combined queries using temporary tables and 100 connections through the pooler to the DB

number of connections, remaining at an extremely low level (~250 MB on all tests).

3.4. Overall assessment of the results

In general, the testing showed the expected results, namely the reduction of the load on the system. Thus, using the balancer will not only reduce infrastructure costs, but also greatly optimize the system itself, especially in terms of avoiding "huge" VM solutions involving several hundred gigabytes of RAM and CPU cores for DBMS. Testing has shown that on average, connection optimization freed 25–50% of RAM that was intended for the DBMS itself, taking into account

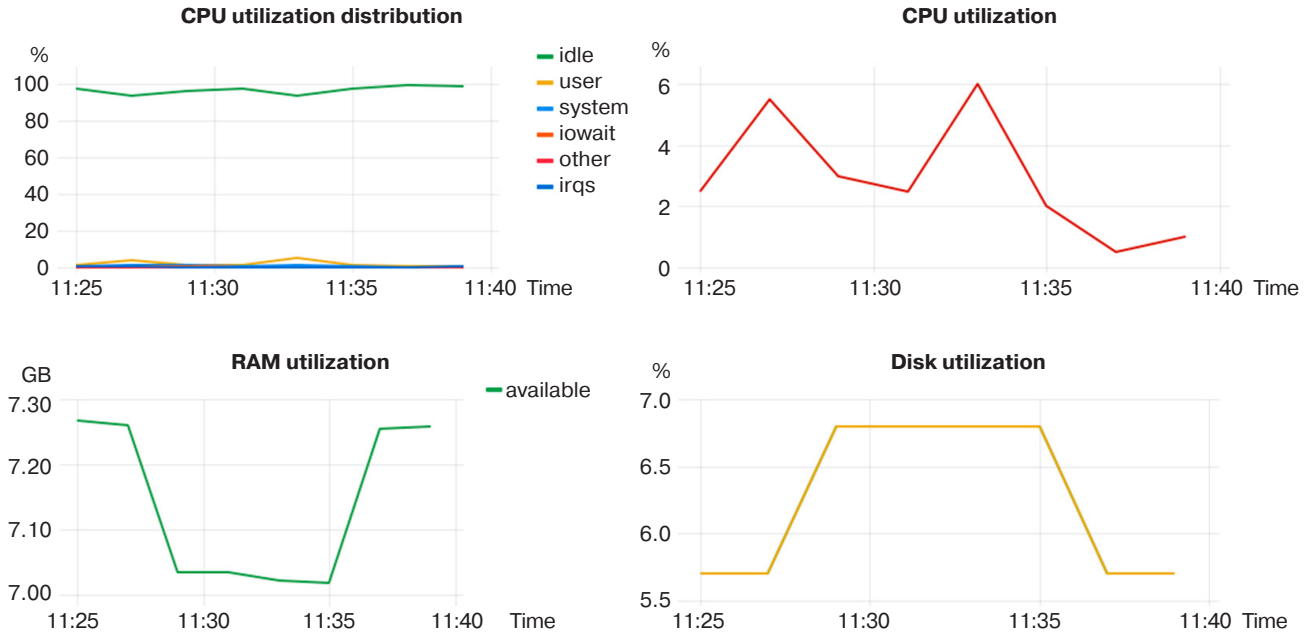

Fig. 20. Performing load testing with combined queries using temporary tables and 500 connections through the pooler to the DB

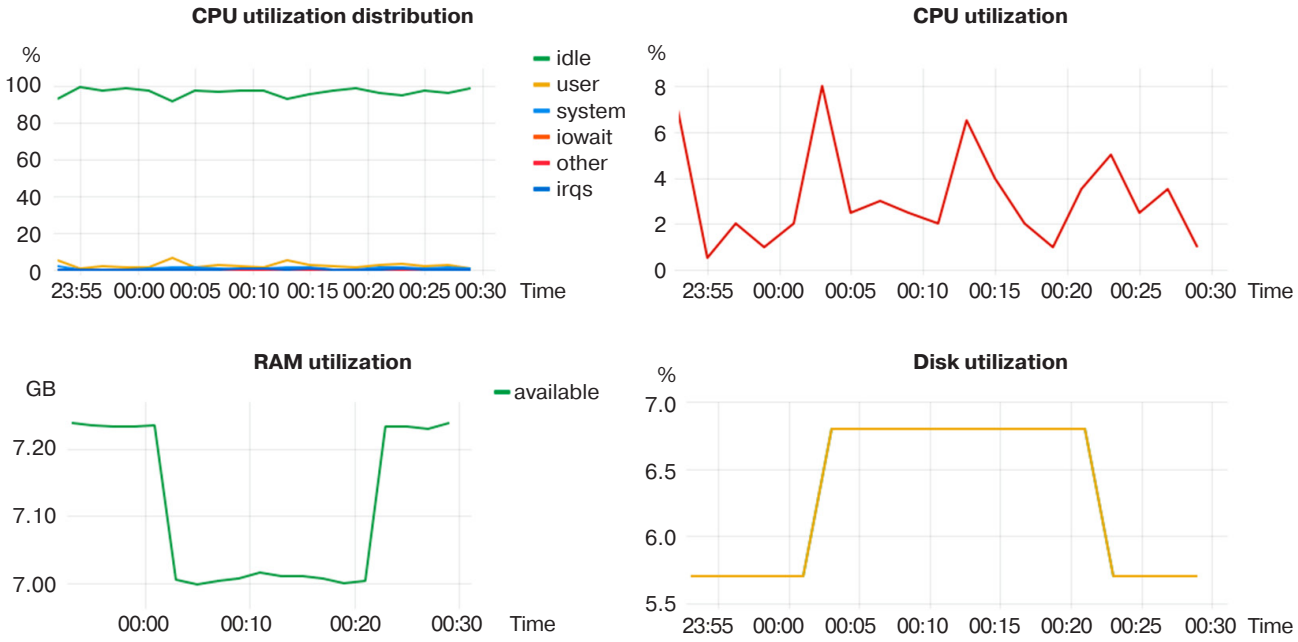

Fig. 21. Performing load testing with combined queries using temporary tables and 1000 connections through the pooler to the DB

Table 2. Results of load testing with simple queries

Number of queries	Method of sending queries to the DB	CPU utilization, %	RAM utilization, MB	Disk utilization, %
100 queries	Directly to the DB	7	230	0
	Through the pooler to the DB	14	30	0
500 queries	Directly to the DB	11	1100	0
	Through the pooler to the DB	8	30	0
1000 queries	Directly to the DB	8	1800	0
	Through the pooler to the DB	11	20	1.4

Table 3. Results of load testing with complex queries

Number of queries	Method of sending queries to the DB	CPU utilization, %	RAM utilization, MB	Disk utilization, %
100 queries	Directly to the DB	25	1125	20
	Through the pooler to the DB	8	260	1.5
500 queries	Directly to the DB	16	5900	30
	Through the pooler to the DB	6	250	1.5
1000 queries	Directly to the DB	19	10250	55
	Through the pooler to the DB	6	250	1.1

Table 4. Results of load testing with combined requests

Number of queries	Method of sending queries to the DB	CPU utilization, %	RAM utilization, MB	Disk utilization, %
100 queries	Directly to the DB	53	1200	7
	Through the pooler to the DB	8	250	1
500 queries	Directly to the DB	58	6050	32
	Through the pooler to the DB	4	260	1
1000 queries	Directly to the DB	18	11150	55
	Through the pooler to the DB	7	250	1

the size of VMs allocated for the pooler itself. If we take pure calculations without taking into account the resources for the balancer itself, the difference amounted to ~30 times. At the same time, *PgBouncer* demonstrated approximately the same values on different tests, which indicates some universality of this solution as opposed to adjusting the DBMS parameters itself.

The reduction of disk subsystem resources utilization when using query balancers should be noted. This optimization will help to reduce costs and decrease the parameters of the disk intended for the DB.

We have also noticed a decrease in CPU utilization when using the pooler. The average fluctuation was 15–20%, which can hardly be called an optimization, since the CPU load has an instantaneous, peak character, and the monitoring system collects data once a minute. For this reason, there can be sharp jumps in readings. The obtained results can be taken into account when designing the system.

"CPU usage distribution" graphs shown in the figures during testing display the information that the resources are directly spent for the *PostgreSQL* DBMS operation and not for other processes, for example, iowait, which occurs at the maximum load on the disk subsystem.

Summarized data of the conducted testing are presented in Tables 2–4.

CONCLUSIONS

The study has demonstrated the effectiveness of *PgBouncer* software for managing a *PostgreSQL* DB connection pool. The testing revealed an improvement in system performance by reducing the resources spent on *PostgreSQL* DBMS, namely, the load on the CPU decreased by 15%, RAM—by 25–50%, and disk subsystem—by 20%.

This balancer has a flexible and easy system of customization of operation modes, allowing the most

suitable option to be selected depending on the specific needs of applications and DB settings.

Using of *PgBouncer* increases DB reliability and reduces query processing time. This is especially important for applications working with a large amount of data that process many queries simultaneously.

Thus, *PgBouncer* can be concluded to represent a useful tool for *PostgreSQL* DB management. It can be successfully applied in many applications and infrastructures where high performance, scalability and security are required.

In the future, it is planned to study ways of deploying this architectural solution on the basis of the Russian platform and to conduct load testing to determine the feasibility of migrating systems, as well as to conduct testing as part of a high-availability cluster.

Authors' contributions

A.S. Boronnikov—the research idea, conducting research, writing the text of the article, interpretation and generalization of the results of the research, scientific editing of the article.

P.S. Tsyngalev—consultations on research issues, writing the text of the article.

V.G. Ilyin—consultations on research issues, writing the text of the article.

T.A. Demenkova—the research idea, research planning, scientific editing of the article.

REFERENCES

1. Sharaev E.V. Using Algorithmic Compositions in PostgreSQL Optimization with Machine Learning Methods. *Nauchnomu Progressu – Tvorchestvo Molodykh*. 2019;3:135–137 (in Russ.).
2. Borodin A., Mirvoda S., Porshnev S., Kulikov I. Optimization of Memory Operations in Generalized Search Trees of PostgreSQL. In: Kozielski S., Mrozek D., Kasprowski P., Małysiak-Mrozek B., Kostrzewa D. (Eds.). Beyond Databases, Architectures and Structures. Towards Efficient Solutions for Data Analysis and Knowledge Representation. BDAS 2017. *Communications in Computer and Information Science*. 2017;716:224–232. https://doi.org/10.1007/978-3-319-58274-0_19
3. Varakuta P.S., Kozlov R.K. Simulation of the capacity of connection pools to the PostgreSQL database. *Tribuna uchenogo = Tribune of the Scientist*. 2022;5:48–53 (in Russ.).
4. Mukhamedina A., Aidarov A.K. Modern load balancing tools. *Nauchnye issledovaniya 21 veka = Scientific Research of the 21st Century*. 2021;2:105–109 (in Russ.).
5. Gudilin D.S., Zvonarev A.E., Goryachkin B.S., Lychagin D.A. Relational Database Performance Comparation. In: *Proc. 5th International Youth Conference on Radio Electronics, Electrical and Power Engineering* (*REEPE*). March 16–18, 2023. Moscow. https://doi.org/10.1109/REEPE57272.2023.10086872
6. Tupikina M.A. Comparison of database management systems SQLite, MySQL and PostgreSQL. In: *Student Science for the Development of the Information Society: collection of materials of the 8th All-Russian Scientific and Technical Conference. Part 2*; May 22–23, 2018. Stavropol: North Caucasian Federal University; 2018. P. 345–347 (in Russ.).
7. Vinogradova M.V., Barashkova E.S., Berezin I.S., Orelikov M.G., Luzin D.S. An overview of the full-text search system in PostgreSQL post-relational database. *E-SCIO*. 2020;5(44):754–778 (in Russ.).
8. Pantilimonov M.V., Buchatskiy R.A., Zhuykov R.A. Machine code caching in PostgreSQL query JIT-compiler. *Trudy Instituta sistemnogo programmirovaniya RAN = Proceedings of the Institute for System Programming of the RAS* (*Proceedings of ISP RAS*). 2020;32(1):205–220 (in Russ.).
9. Portretov V.S. Comparison of PostgreSQL and MySQL. *Molodezhnaya Nauka v Razvitii Regionov*. 2017;1:136–139 (in Russ.).
10. Chauhan C., Kumar D. *PostgreSQL High Performance Cookbook*. 2nd ed. Birmingham: Packt Publishing; 2017. 360 p.
11. Rogov E.V. *PostgreSQL 15 iznutri* (*PostgreSQL 15 from the Inside*). Moscow: DMK Press; 2023. 662 p. (in Russ.).
12. Novikov B.A., Gorshkova E.A., Grafeeva N.G. *Osnovy tekhnologii baz dannykh* (*Bases of Technologies of Databases*). 2nd ed. Moscow: DMK Press; 2020. 582 p. (in Russ.).
13. Boichenko A.V., Rogojin D.K., Korneev D.G. Algorithm for dynamic scaling relational database in clouds. *Statistika i Ekonomika = Statistics and Economics.* 2014;6–2:461–465 (in Russ.).
14. Afanas'ev G.I., Abulkasimov M.M., Belonogov I.B. How to create a PostgreSQL Docker image on Ubuntu Linux. *Alleya nauki = Alley of Science*. 2018;2(1–17):913–918 (in Russ.).
15. Smolinski M. Impact of storage space configuration on transaction processing performance for relational database in PostgreSQL. In: Kozielski S., Mrozek D., Kasprowski P., Małysiak-Mrozek B., Kostrzewa D. (Eds.). Beyond Databases, Architectures and Structures. Towards Efficient Solutions for Data Analysis and Knowledge Representation. BDAS 2017. *Communications in Computer and Information Science*. 2018;928:157–167. https://doi.org/10.1007/978-3-319-99987-6_12

СПИСОК ЛИТЕРАТУРЫ

1. Шараев Е.В. Использование алгоритмических композиций при оптимизации PostgreSQL методами машинного обучения. *Научному Прогрессу – Творчество Молодых*. 2019;3:135–137.
2. Borodin A., Mirvoda S., Porshnev S., Kulikov I. Optimization of Memory Operations in Generalized Search Trees of PostgreSQL. In: Kozielski S., Mrozek D., Kasprowski P., Małysiak-Mrozek B., Kostrzewa D. (Eds.). Beyond Databases, Architectures and Structures. Towards Efficient Solutions for Data Analysis and Knowledge Representation. BDAS 2017. *Communications in Computer and Information Science*. 2017;716:224–232. https://doi.org/10.1007/978-3-319-58274-0_19

3. Варакута П.С., Козлов Р.К. Имитационное моделирование пропускной способности пулов соединений к базе данных PostgreSQL. *Трибуна ученого*. 2022;5:48–53.
4. Мухамедина А., Айдаров А.К. Современные средства балансировки перегрузки. *Научные исследования XXI века*. 2021;2:105–109.
5. Gudilin D.S., Zvonarev A.E., Goryachkin B.S., Lychagin D.A. Relational Database Performance Comparation. In: *Proc. 5th International Youth Conference on Radio Electronics, Electrical and Power Engineering* (*REEPE*). March, 16–18, 2023. Moscow. https://doi.org/10.1109/REEPE57272.2023.10086872
6. Тупикина М.А. Сравнение систем управления базами данных SQLite, MySQL и PostgreSQL. В сб.: *Студенческая наука для развития информационного общества: сборник материалов VIII Всероссийской научно-технической конференции*. Часть 2; 22–23 мая 2018 г. Ставрополь: Северо-Кавказский федеральный университет; 2018. С. 345–347.
7. Виноградова М.В., Барашкова Е.С., Березин И.С., Ореликов М.Г., Лузин Д.С. Обзор системы полнотекстового поиска в постреляционной базе данных PostgreSQL. *E-SCIO*. 2020;5(44):754–778.
8. Пантилимонов М.В., Бучацкий Р.А., Жуйков Р.А. Кэширование машинного кода в динамическом компиляторе SQL-запросов для СУБД PostgreSQL. *Труды Института системного программирования РАН*. 2020;32(1):205–220. https://doi.org/10.15514/ISPRAS-2020-32(1)-11
9. Портретов В.С. Сравнение PostgreSQL и MySQL. *Молодежная наука в развитии регионов*. 2017;1:136–139.
10. Chauhan C., Kumar D. *PostgreSQL High Performance Cookbook*. 2nd ed. Birmingham: Packt Publishing; 2017. 360 p.
11. Рогов Е.В. *PostgreSQL 15 изнутри*. М.: ДМК Пресс; 2023. 662 с.
12. Новиков Б.А., Горшкова Е.А., Графеева Н.Г. *Основы технологий баз данных*. 2-е изд. М.: ДМК Пресс; 2020. 582 с.
13. Бойченко А.В., Рогожин Д.К, Корнеев Д.Г. Алгоритм динамического масштабирования реляционных баз данных в облачных средах. *Статистика и Экономика.* 2014;6–2:461–465.
14. Афанасьев Г.И., Абулкасимов М.М., Белоногов И.Б. Методика создания Docker-образа PostgreSQL в среде Ubuntu Linux. *Аллея науки.* 2018;2(1–17):913–918.
15. Smolinski M. Impact of storage space configuration on transaction processing performance for relational database in PostgreSQL. In: Kozielski S., Mrozek D., Kasprowski P., Małysiak-Mrozek B., Kostrzewa D. (Eds.). Beyond Databases, Architectures and Structures. Towards Efficient Solutions for Data Analysis and Knowledge Representation. BDAS 2017. *Communications in Computer and Information Science*. 2018;928:157–167. https://doi.org/10.1007/978-3-319-99987-6_12

About the authors

Anton S. Boronnikov, Postgraduate Student, Senior Lecture, Computer Engineering Department, Institute of Information Technologies, MIREA – Russian Technological University (78, Vernadskogo pr., Moscow, 119454 Russia). E-mail: boronnikov-anton@mail.ru. RSCI SPIN-code 8232-6328, https://orcid.org/0009-0008-4911-6609

Pavel S. Tsyngalev, Student, MIREA – Russian Technological University (78, Vernadskogo pr., Moscow, 119454 Russia). E-mail: pstsyngalev@mail.ru. https://orcid.org/0009-0007-6354-1364

Victor G. Ilyin, Student, MIREA – Russian Technological University (78, Vernadskogo pr., Moscow, 119454 Russia). E-mail: vgilyin@yahoo.com. https://orcid.org/0009-0001-0304-3052

Tatiana A. Demenkova, Cand. Sci. (Eng.), Associate Professor, Computer Engineering Department, Institute of Information Technologies, MIREA – Russian Technological University (78, Vernadskogo pr., Moscow, 119454 Russia). E-mail: demenkova@mirea.ru. Scopus Author ID 57192958412, ResearcherID AAB-3937-2020, RSCI SPIN-code 3424-7489, https://orcid.org/0000-0003-3519-6683

Об авторах

Боронников Антон Сергеевич, аспирант, старший преподаватель, кафедра вычислительной техники, Институт информационных технологий, ФГБОУ ВО «МИРЭА – Российский технологический университет» (119454, Россия, Москва, пр-т Вернадского, д. 78). E-mail: boronnikov-anton@mail.ru. SPIN-код РИНЦ 8232-6328, https://orcid.org/0009-0008-4911-6609

Цынгалёв Павел Сергеевич, студент, ФГБОУ ВО «МИРЭА – Российский технологический университет» (119454, Россия, Москва, пр-т Вернадского, д. 78). E-mail: pstsyngalev@mail.ru. https://orcid.org/0009-0007-6354-1364

Ильин Виктор Георгиевич, студент, ФГБОУ ВО «МИРЭА – Российский технологический университет» (119454, Россия, Москва, пр-т Вернадского, д. 78). E-mail: vgilyin@yahoo.com. https://orcid.org/0009-0001-0304-3052

Деменкова Татьяна Александровна, к.т.н., доцент, кафедра вычислительной техники, Институт информационных технологий, ФГБОУ ВО «МИРЭА – Российский технологический университет» (119454, Россия, Москва, пр-т Вернадского, д. 78). E-mail: demenkova@mirea.ru. Scopus Author ID 57192958412, ResearcherID AAB-3937-2020, SPIN-код РИНЦ 3424-7489, https://orcid.org/0000-0003-3519-6683

Translated from Russian into English by Lyudmila O. Bychkova
Edited for English language and spelling by Thomas A. Beavitt

Information systems. Computer sciences. Issues of information security

Информационные системы. Информатика. Проблемы информационной безопасности

UDC 004.056
https://doi.org/10.32362/2500-316X-2024-12-3-25-36
EDN LNWLOK

RESEARCH ARTICLE

Criteria and indicators for assessing the quality of the investigation of an information security incident as part of a targeted cyberattack

Stanislav I. Smirnov @, Mikhail A. Eremeev, Shamil G. Magomedov, Dmitry A. Izergin

MIREA – Russian Technological University, Moscow, 119454 Russia
@ Corresponding author, e-mail: smirnov_si@mirea.ru

Abstract

Objectives. The currently increasing number of targeted cyberattacks raises the importance of investigating information security incidents. Depending on the available means of protection, computer forensic experts use software and hardware tools for analyzing digital artifacts of various operating systems and network traffic to create an event chronology (timeline) of the incident. However, to date, there is no formal approach for assessing the effectiveness of expert activities when investigating an information security incident within the framework of a targeted cyberattack. The present study aims to develop partial indicators of promptness, effectiveness, and resource intensity as part of the suitability criterion for investigating an information security incident.

Methods. Methods informed by purposeful process efficiency and set theory are used along with expert evaluation approaches.

Results. An analysis of works in the field of investigation of computer incidents is presented. The terminology and main guiding documents on specifics of conducting information security incident investigations are described along with examples of digital artifacts defined in the form of classification. The expediency of forming criteria and indicators for assessing the quality of an information security incident investigation is substantiated. The suitability criterion and subsequent indicators for assessing the quality of the investigation are selected: the effectiveness (completeness) indicator for detecting digital artifacts by a computer criminologist is based on the conducted activities, resource intensity indicator, and promptness indicator for investigating an information security incident.

Conclusions. The obtained results can be used not only by heads of departments but also by rank-and-file information security professionals for objective analysis of the available software and human resources, the time spent on these activities, and the identified digital artifacts as part of a cyber incident investigation.

Keywords: information security incident, targeted cyberattack, cyber incident investigation, MITRE ATT&CK matrix, digital artifact, information security threat assessment, targeted process, quality assessment criteria and indicators

• **Submitted:** 02.05.2023 • **Revised:** 22.11.2023 • **Accepted:** 05.04.2024

For citation: Smirnov S.I., Eremeev M.A., Magomedov Sh.G., Izergin D.A. Criteria and indicators for assessing the quality of the investigation of an information security incident as part of a targeted cyberattack. *Russ. Technol. J.* 2024;12(3):25–36. https://doi.org/10.32362/2500-316X-2024-12-3-25-36

Financial disclosure: The authors have no a financial or property interest in any material or method mentioned.

The authors declare no conflicts of interest.

НАУЧНАЯ СТАТЬЯ

Критерии и показатели оценивания качества проведения расследования инцидента информационной безопасности при целевой кибератаке

С.И. Смирнов [@], М.А. Еремеев, Ш.Г. Магомедов, Д.А. Изергин

МИРЭА – Российский технологический университет, Москва, 119454 Россия
[@] Автор для переписки, e-mail: smirnov_si@mirea.ru

Резюме

Цели. В настоящее время при нарастающем числе целевых атак задача расследования инцидента информационной безопасности (ИБ) приобретает важное значение. Компьютерные криминалисты, в зависимости от имеющихся средств защиты, применяют программные и программно-аппаратные средства форензики, проводят анализ цифровых артефактов различных операционных систем и сетевого трафика с построением хронологии событий (таймлайна) инцидента. На сегодняшний день отсутствует какой-либо формальный подход к оцениванию эффективности действий специалистов при проведении расследования инцидента ИБ в рамках целевой кибератаки. Целью работы является формирование частных показателей оперативности, результативности и ресурсоемкости в рамках критерия пригодности при расследовании инцидента ИБ.

Методы. Использованы методы теории эффективности целенаправленных процессов, методы экспертных оценок и теории множеств.

Результаты. Проведен анализ актуальных работ в области расследования компьютерных инцидентов. Представлены терминология и основные руководящие документы спецификации проведения расследования инцидента ИБ. Определены примеры цифровых артефактов в виде классификации. Обоснована целесообразность формирования критериев и показателей оценки качества проведения расследования инцидента ИБ. Выбраны критерий пригодности и следующие показатели оценивания качества проведения расследования: показатель результативности (полноты) выявления цифровых артефактов компьютерным криминалистом на основе проведенных мероприятий, показатель ресурсоемкости и показатель оперативности расследования инцидента ИБ.

Выводы. Полученные результаты могут быть использованы не только руководителями подразделений, но и рядовыми специалистами по ИБ для объективного анализа имеющихся программных и человеческих ресурсов, времени, затраченного на эти мероприятия, и выявленных цифровых артефактов в рамках расследования киберинцидента.

Ключевые слова: инцидент информационной безопасности, целевая кибератака, расследование киберинцидента, матрица MITRE ATT&CK, цифровой артефакт, оценка угроз безопасности информации, целенаправленный процесс, критерий и показатели оценки качества

• **Поступила:** 02.05.2023 • **Доработана:** 22.11.2023 • **Принята к опубликованию:** 05.04.2024

Для цитирования: Смирнов С.И., Еремеев М.А., Магомедов Ш.Г., Изергин Д.А. Критерии и показатели оценивания качества проведения расследования инцидента информационной безопасности при целевой кибератаке. *Russ. Technol. J*. 2024;12(3):25–36. https://doi.org/10.32362/2500-316X-2024-12-3-25-36

Прозрачность финансовой деятельности: Авторы не имеют финансовой заинтересованности в представленных материалах или методах.

Авторы заявляют об отсутствии конфликта интересов.

INTRODUCTION

In recent years, geopolitical events around the world have substantially influenced the increased activity of hacker groups. According to the Positive Technologies[1] company final report for 2022, the number of information security (InfoSec) incidents increased by 20.8% over the past year, among which the volume of successful targeted attacks using ransomware (encryptors) amounted to 51%. The practice of responding to modern InfoSec incidents shows that, over the last decade, the number of techniques and tools used by attackers in targeted attacks on information and telecommunications networks of organizations has been increasing daily [1].

As a result, the organization of an integrated approach when investigating an InfoSec incident acquires increased importance. Such an integrated approach consists in aggregating identified digital artifacts from various security systems (e.g., security information and event management (SIEM), intrusion detection/prevention system (IDS/IPS), data loss prevention (DPL), next generation firewall (NGFW), etc.) to create cyberattack timelines. In case this information is not available in the organization, it becomes much more difficult for experts to search for forensically significant data, thus increasing the investigation timeframe. An important role in this process is played by the availability of live systems by means of which computer forensic experts can capture random access memory (RAM) dumps.

Thus, one of the most urgent scientific directions within the InfoSec incident investigation consists in the creation of a theoretical framework for calculating the effectiveness of computer forensics activities depending on the availability of forensic software and protection systems in the organization. The present work aims to develop partial indicators of promptness, effectiveness, and resource intensity in terms of suitability criterion for investigating an InfoSec incident from targeted attacks.

The paper continues studies [2, 3] aimed at developing a theoretical basis for assessing the effectiveness of targeted processes.

TERMINOLOGY AND KEY GUIDANCE DOCUMENTS ON THE SPECIFICS OF CONDUCTING AN INFOSEC INCIDENT INVESTIGATION

A number of regulatory documents and instructions issued by commercial organizations describe professional activities when investigating and responding to computer attacks. At the same time, state standards do not define criteria and indicators for assessing the quality of cyber incident investigation. For example, the guidance document GOST R 59709-2022[2] defines only terms and definitions, as well as their interconnections within these processes, while the GOST R 59712-2022[3] standard is limited to an organizational description of the actions of cyber incident management units.

The methodological document of the Federal Service for Technical and Export Control "Methodology for Assessing Information Security Threats" lists ten basic tactics and corresponding techniques used to build scenarios for implementing InfoSec threats.[4] The MITRE ATT&CK[5] matrix serves as a basis for developing this list. According to GOST R ISO/IEC TO 18044-2007[6], when the first signs of an InfoSec incident are detected, computer forensic experts are faced with the task of determining their causes. In this regard, digital artifacts are collected whose main sources include hard disk copies, RAM dumps, security event logs, and network device traffic.

The basic terminology of the InfoSec incident investigation is summarized below, which is essential for further research.

- *Computer attack* is a purposeful unauthorized network computer impact (or sequence thereof) on an information resource carried out by an intruder using software and/or hardware and information technologies with the aim of disrupting and/or stopping the functioning of an information resource or to implement a threat to the security of information processed by this resource.[7]
- *Targeted cyberattack* is a continuous process of unauthorized activity in the infrastructure of the information system (IS) under attack, remotely hand-operated in real time.[8]

[1] https://www.ptsecurity.com/ru-ru/research/analytics/cybersecurity-threatscape-2022/ (in Russ.). Accessed March 30, 2023.

[2] GOST R 59709-2022. National Standard of the Russian Federation. *Information protection. Detection, prevention and liquidation of the consequences of computer attacks and response to computer incidents. Terms and Definitions*. Moscow: Rosstandart; 2022 (in Russ.).

[3] GOST R 59712-2022. National Standard of the Russian Federation. *Guide to Planning and Prepare for Incident Response ISO/IEC 27035-2*. Moscow: Rosstandart; 2022 (in Russ.).

[4] https://fstec.ru/dokumenty/vse-dokumenty/spetsialnye-normativnye-dokumenty/metodicheskij-dokument-ot-5-fevralya-2021-g (in Russ.). Accessed April 06, 2023.

[5] https://attack.mitre.org/. Accessed April 06, 2023.

[6] GOST R ISO/IEC TO 18044-2007. National Standard of the Russian Federation. *Information technologies. Methods and means of ensuring security. Information security incident management*. Moscow: Standartinform; 2007 (in Russ.).

[7] GOST R 59709-2022. National Standard of the Russian Federation. *Information protection. Detection, prevention and liquidation of the consequences of computer attacks and response to computer incidents. Terms and Definitions*. Moscow: Rosstandart; 2022 (in Russ.).

[8] https://www.kaspersky.ru/blog/targeted-attack-anatomy/4388/ (in Russ.). Accessed March 14, 2023.

- *InfoSec incident* is the occurrence of one or more undesirable InfoSec events that may cause IS failure or disruption[9]. According to GOST R ISO/IEC 13335-1-2006[10], examples of cyber incidents may include loss of equipment (devices), system user errors, failure to comply with InfoSec policy or recommendations, violation of physical protection measures, software failures, technical failures, system failures or overloads, and violation of access rules.
- *InfoSec incident investigation* is a set of actions by InfoSec experts aimed at identifying the vector of a targeted cyberattack for minimizing the damage and developing recommendations to prevent an InfoSec incident in the future [2].
- *Computer incident response* is the process (procedure, function) of automatic (automated) processing of a computer incident.[11]
- *Digital artifact* is potential evidence found on a target device (e.g., personal computer, mobile device, and network device) that can be used in forensic practice [3].
- *Forensically significant data* is computerized information used to substantiate the conclusions of forensic investigations and solve the tasks set for forensic investigation.[12]

A classification of digital artifacts that can be used by experts in investigating an InfoSec incident is presented in Figure. In the classification, significant evidence of common operating systems (OS) and network traffic is specified.

By establishing criteria and indicators for assessing the quality of a cyber incident investigation, the effectiveness of the process can be improved, as well as the consequent process of responding to a computer attack for minimizing financial and reputational damage to the organization. Thus, the better a cyber incident investigation is conducted by experts, the more quickly they are able to respond to and stop the malicious process.

REVIEW OF RELEVANT STUDIES IN THE FIELD OF INFOSEC INCIDENT INVESTIGATION

Practical issues of investigating InfoSec incidents are discussed in the works of S.I. Makarenko [4], M.A. Eremeev [5], P.D. Zegrzda, D.P. Zegzhda [6], A.G. Lomako [7], V.A. Ovcharov [8], S.A. Petrenko [9], I.B. Saenko [10], I.V. Kotenko [11], I.A. Pribylov [12], V.S. Avramenko [13], and D.S. Levshun [14].

While there are a number of existing instructions for Russian commercial organizations to describe the actions of experts in responding to a cyber incident, these instructions have a number of disadvantages.

The experts from F.A.C.C.T (formerly Group-IB in Russia) have developed an instruction[13] for responding to incidents related to remote banking systems. The main disadvantage of this document is its use only in IS of financial institutions.

In the manual[14] published by Kaspersky Lab, employees describe the actions of experts in responding to InfoSec incidents. However, this document is not a universal instruction, but only describes the use of basic tools for data collection as well as analysis of potential threats and their removal. This guide requires modifications based on knowledge of modern techniques and methods used by attackers.

In an earlier thesis[15], the present author introduced a generalized indicator of malicious authentication activity of the attacker based on the completeness indicator of detecting authentication actions performed by the attacker during "horizontal movement" in the domain, and the promptness indicator of investigating a cyber incident. This indicator can be considered only in the case of a cyberattack on the organization's domain.

The above analysis of existing studies pertaining to cyber incident investigation demonstrates that existing documents adopted at state and commercial levels describe only approximate actions of experts and fail to define timeframes for assessing the quality of cyber incident investigation.

[9] https://normative_reference_dictionary.academic.ru/23474/ (in Russ.). Accessed March 15, 2023.

[10] GOST R ISO/IEC 13335-1-2006. National Standard of the Russian Federation. *Information technology. Methods and means of ensuring security*. Part 1. Concept and models of security management of information and telecommunication technologies. Moscow: Standartinform; 2006 (in Russ.).

[11] GOST R 59709-2022. National Standard of the Russian Federation. *Information protection. Detection, prevention and liquidation of the consequences of computer attacks and response to computer incidents. Terms and Definitions*. Moscow: Rosstandart; 2022 (in Russ.).

[12] https://www.group-ib.com/wp-content/uploads/media/2016/02/Group-IB_dbo_instruction.pdf (in Russ.). Accessed March 13, 2023.

[13] https://www.group-ib.com/wp-content/uploads/media/2016/02/Group-IB_dbo_instruction.pdf (in Russ.). Accessed March 13, 2023.

[14] https://media.kasperskycontenthub.com/wp-content/uploads/sites/43/2018/03/07172131/Incident_Response_Guide_rus.pdf (in Russ.). Accessed March 15, 2023.

[15] Smirnov S.I. *A methodology for conducting a cyber incident investigation based on an automated analysis of domain security events*: Cand. Sci. Thesis. St. Petersburg, 2022. 124 p. https://www.elibrary.ru/item.asp?id=54428705 (in Russ.). Accessed March 25, 2023.

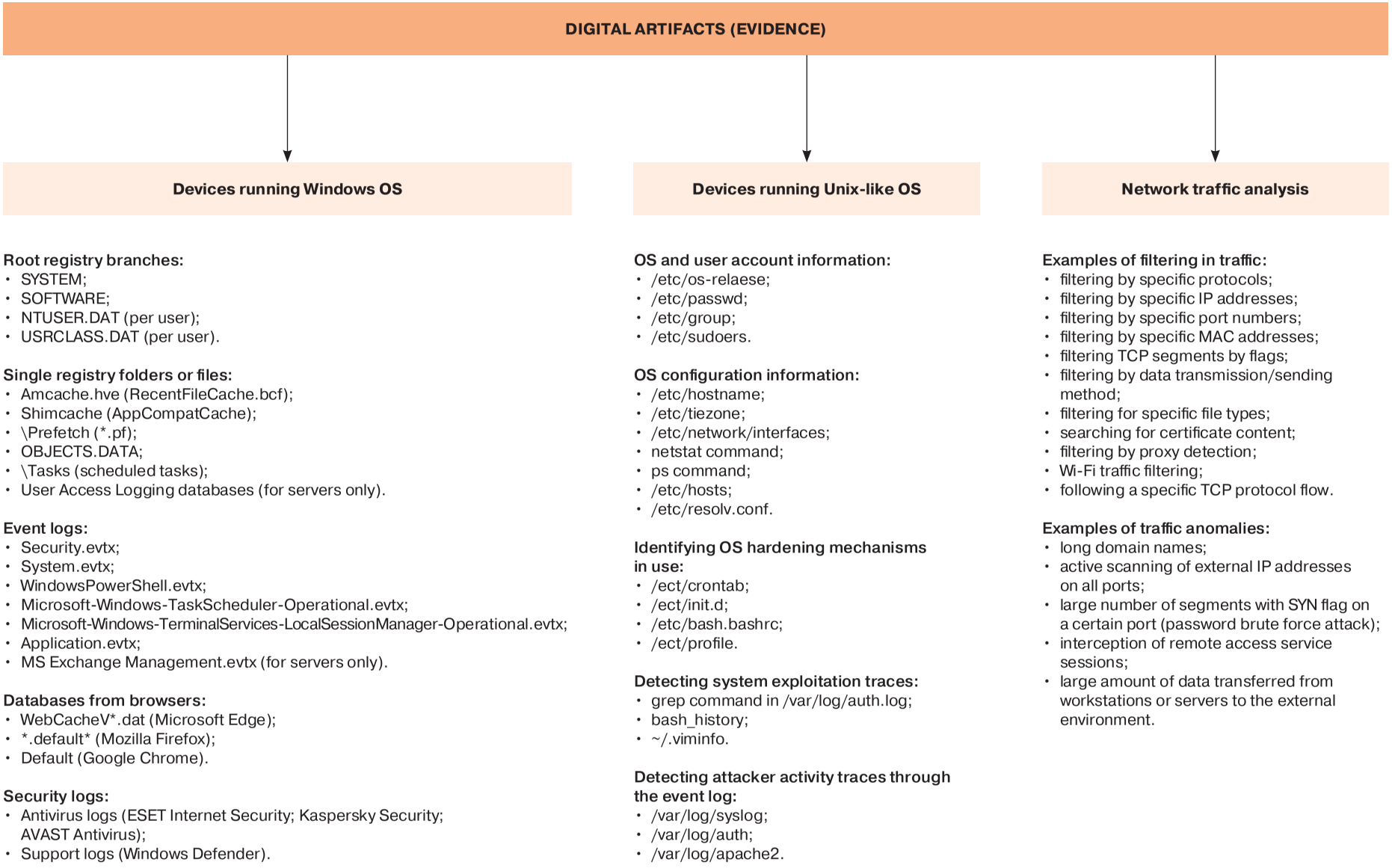

Figure. Classification of digital artifacts. TCP—Transmission Control Protocol

DESCRIPTION OF CRITERIA AND INDICATORS FOR ASSESSING THE QUALITY OF CONDUCTING THE CYBER INCIDENT INVESTIGATION WITHIN TARGETED CYBERATTACK

The theory of efficiency of purposeful processes defines the following concept: *efficiency* is a complex operational property of a purposeful functioning process that characterizes its adaptability to perform the task facing the system [15].

The concept of efficiency is directly related to the concept of quality. *Quality* is a property or a set of properties of an object that determine its suitability for intended use. Each of the properties of an object can be described quantitatively using some variable, whose value characterizes the measure (intensity) of its quality in relation to this property. This measure is called the *property indicator* or single, *partial indicator of quality* of the object [15].

When assessing the quality of any object described by an n-dimensional vector index, a set of criteria is implemented, each of which can belong to one of three classes in general case:

- class $\{G\}$ of suitability criteria;
- class $\{O\}$ of optimality;
- class $\{S\}$ of superiority [15].

Criteria can be represented either in vector or scalar form.

The effectiveness assessment criterion comprises a set of conditions defining operation objectives (InfoSec incident investigation) and the suitability, optimality, or superiority of the investigated operation based on it [15].

In the paper, *the suitability criterion G* is selected for the study.

For assessing the quality of InfoSec incident investigation within the targeted cyberattack (including an ongoing one), the following indicators are proposed:

- effectiveness (completeness) indicator for detecting digital artifacts by a computer forensic investigator based on the conducted activities, r;
- resource intensity indicator (availability of forensics software products and expenditure of human resources), p;
- promptness indicator of the InfoSec incident investigation, t.

DESCRIPTION OF EFFECTIVENESS INDICATOR

The effectiveness indicator, which is determined by the degree of completeness of detecting digital artifacts r, directly depends on nine main activities implemented during the investigation:

1) collecting and analyzing event logs of the domain controller and workstations or servers;
2) analyzing processes from the RAM dump of workstations or servers;
3) analyzing browser history of workstations;
4) analyzing mail messages of workstations;
5) analyzing logs of antivirus systems available in the organization;
6) analyzing hard disk copies from workstations or servers;
7) analyzing traffic from available network devices (routers, firewalls) and intrusion detection/prevention systems (if any);
8) analyzing SIEM-system events (if any);
9) building a timeline of the target attack.

The main activities are determined on the basis of practical recommendations of experts from Division "K" of the Ministry of Internal Affairs of the Russian Federation[16]. Using the collected numerical evidence, an expert should form a report on the conducted activities, providing recommendations for the prompt elimination of the abnormal situation.

Based on the activities described above, a table has been compiled to present the notation of the *effectiveness (completeness) indicator r* in s activities and, accordingly, the required values with its description (Table 1).

Table 1. Description of the required effectiveness when investigating an InfoSec incident

Event No.	Notation of the effectiveness indicator for event s	Description of typical results for each activity
1	r_1	Detecting non-standard methods of attacker authentication (e.g., Pass-the-Hash, Kerberoasting techniques), password brute force methods, and authentication of domain users after hours
2	r_2	Detecting malicious processes from RAM dump of "infected" machines or servers
3	r_3	Detecting the web resource through which the workstation is infected
4	r_4	Detecting the phishing email infected the workstation
5	r_5	Detecting warnings or malware in antivirus logs
6	r_6	Detecting malicious files or software in hard disk copies
7	r_7	Detecting malicious files or software as well as the presence of network connections to the attacker's command and control server from traffic

[16] Department of Information Technologies, Communications and Information Protection of the Ministry of Internal Affairs of the Russian Federation. https://xn--b1aew.xn--p1ai/mvd/structure1/Upravlenija/%D1%83%D0%B1%D0%BA/%D0%BF%D0%BE%D0%BB%D0%BE%D0%B6%D0%B5%D0%BD%D0%B8%D0%B5 (in Russ.). Accessed March 30, 2023.

Table 1. Continued

Event No.	Notation of the effectiveness indicator for event *s*	Description of typical results for each activity
8	r_8	Detecting SIEM system warnings about a cyberattack through correlation rules and normalization of security events
9	r_9	Creating a chronology of the target attack specifying the attacker's penetration vector

Thus, the effectiveness (completeness) indicator of detection of digital artifacts r is equal to the sum of success rates of activities from the set $\{r_s\}$ described in binary form (completed/not completed). The formula for calculating the effectiveness indicator is as follows:

$$r = r_1 + r_2 + (r_3 \vee r_4) + r_5 + r_6 + r_7 + r_8 + r_9. \quad (1)$$

The suitability criterion for the effectiveness (completeness) indicator of digital artifact detection can be represented as the inequality $r > r_{req}$. The value of the required effectiveness indicator ($r_{req} = 7$) is determined based on the method of expert assessments excluding the following measures: #3 or #4 depending on the vector of the target cyberattack (logical addition is applied).

DESCRIPTION OF RESOURCE INTENSITY INDICATOR

The resource intensity indicator p is determined by the availability of forensic software tools in cyber incident investigation along with human resources. It is proposed that the software tools be divided into three subsets. Since these OSs are most common in organizations when building information and communication networks, it is necessary to conduct the analysis of network traffic from network equipment for a complete picture of the InfoSec incident:

- for analyzing Windows-like systems $\{p_{win}\}$;
- for analyzing Unix-like systems $\{p_{unix}\}$;
- for analyzing network traffic $\{p_{traf}\}$.

The proposed subsets are calculated based on available InfoSec incident investigation software tools (available/not available). Examples of these programs are presented below.

For analyzing *Windows-like systems*, computer forensic investigators should possess the necessary set of software tools such as *UserAssist*[17], *ESEDatabaseView*[18], *wmi-parser*[19], *RegRipper*[20], *NirSoft*[21] utilities (e.g., *winprefetchview*, *fulleventlogview*), Eric Zimmerman's toolkit[22] (e.g., *AmcacheParser*, *Registry Explorer*, *MFTECmd*, *AppCompatCacheParser*, and *PECmd*), and Microsoft's *Sysinternals Suite*[23] (e.g., *PSLoglist*, *Process Monitor*, *Process Explorer*, *Autoruns*, *Autologon*, etc.).

For studying *Unix-like systems*, the built-in utilities such as *dc3dd*, *ddrescue*, *Autopsy*, *LiME*, *Bulk Extractor*, *Dumpzilla*, and others should be used.

For analyzing traffic, the *wireshark*, *NetworkMiner*[24], *tcpdump*[25], *Kismet*[26], *SolarWinds Network Bandwidth Analyzer*[27], *Xplico*[28], and others are used.

The *FTK Imager*[29], *volatility3*[30], *artifactcollector*[31], *osquery*[32], and *ir-rescue*[33] utilities are cross-platform and suitable for studying popular OSs.

When investigating an InfoSec incident, department heads should understand the number of experts available for promptly conducting the event. In the study, the maximum number of computer forensic experts is defined as the staffing of the department.

Human resource (HR) costs of investigating an InfoSec incident are roughly categorized into three subsets:

- Up to 2 specialists $\{p_{two}\}$;
- Group of experts (3–5 persons) $\{p_{group}\}$;
- In-house department (10–12 persons) $\{p_{dep}\}$.

Mathematically, the relation of these sets is represented by disjunction. The coefficient k demonstrating a direct

[17] https://www.nirsoft.net/utils/userassist_view.html. Accessed April 30, 2023.

[18] https://www.nirsoft.net/utils/ese_database_view.html. Accessed April 30, 2023.

[19] https://github.com/woanware/wmi-parser/releases. Accessed April 30, 2023.

[20] https://github.com/keydet89/RegRipper3.0. Accessed April 30, 2023.

[21] https://nirsoft.net/. Accessed April 30, 2023.

[22] https://github.com/EricZimmerman/. Accessed April 30, 2023.

[23] https://learn.microsoft.com/ru-ru/sysinternals/downloads/sysinternals-suite/ (in Russ.). Accessed April 30, 2023.

[24] https://networkminer.softonic.ru/ (in Russ.). Accessed April 30, 2023.

[25] https://www.microolap.ru/products/tcpdump-for-windows/ (in Russ.). Accessed April 30, 2023.

[26] https://ru.freedownloadmanager.org/Windows-PC/Kismet-FREE.html (in Russ.). Accessed April 30, 2023.

[27] https://softradar.com/solarwinds-network-bandwidth-analyzer-pack/. Accessed April 30, 2023.

[28] https://www.xplico.org/download. Accessed April 30, 2023.

[29] https://accessdata-ftk-imager.software.informer.com/3.1/. Accessed April 30, 2023.

[30] https://github.com/volatilityfoundation/volatility3. Accessed April 30, 2023.

[31] https://github.com/forensicanalysis/artifactcollector. Accessed April 30, 2023.

[32] https://github.com/osquery/osquery. Accessed April 30, 2023.

[33] https://github.com/diogo-fernan/ir-rescue. Accessed April 30, 2023.

dependence on the number of computer forensic specialists involved in the investigation is introduced: $k_{two} = 0.8$, $k_{group} = 1$, $k_{dep} = 1.2$. These coefficients are determined on the basis of the expert evaluation method for investigating modern cyber incidents. For successfully solving the task assigned to computer forensic experts, a group of experts is required; therefore, a coefficient equal to one is assigned to this subset.

Thus, the resource intensity indicator p is equal to the product of the resource intensity indicators of three types of software described in binary form (available/not available) by the sum of the logical addition of HR availability using k factor.

Mathematically, calculation of the resource intensity indicator is represented by the following formula:

$$p = (\{p_{win}\} + \{p_{unix}\} + \{p_{traf}\}) \cdot (k_{two}\{p_{two}\} \vee \vee k_{group}\{p_{group}\} \vee k_{dep}\{p_{dep}\}). \quad (2)$$

The suitability criterion in terms of resource intensity (availability of software and HR) can be represented as inequality $p > p_{req}$. Since, in targeted cyberattacks, attackers primarily target the organization's domain in order to encrypt all data, the value of the required resource intensity indicator ($p_{req} = 3$) is determined based on the expert evaluation method excluding software tools for Unix-like systems. This also includes the value of the required resource intensity of HR availability.

DESCRIPTION OF PROMPTNESS INDICATOR

The InfoSec incident investigation timeliness indicator t is calculated based on timeframes of events ($s = 9$) conducted by the computer forensic investigator. It defines time aspects of the investigation.

The InfoSec incident investigation timeliness indicator t is calculated using the following formula:

$$t = \sum_{i=1}^{s} t_i, \quad (3)$$

where t_i is the time spent on one event.

The required timeframes for 9 events in investigating the incident given in Table 2 are calculated on the basis of the expert evaluation method in past Russian investigations. The total required investigation time t_{req} should not exceed 2 h.

The suitability criterion for the promptness indicator in conducting the InfoSec incident investigation can be represented as inequality $t < t_{req}$. The value of the required effectiveness indicator is $t_{req} = 2$.

Thus, suitability criterion G is mathematically represented based on three indicators described earlier, as follows:

$$G : \bigcap_{i=1}^{n}((r_j^i > \{r_j^{req}\}),(p_j^i > \{p_j^{req}\}),(t_j^i > \{t_j^{req}\})) \cong \cong U, [j = 1(1)m)], \quad (4)$$

Table 2. Timeframes required for nine events in InfoSec incident investigation

Event No.	Notation of the promptness indicator for event s	Required value of the event timeframe when investigating InfoSec incident, h
1	t_{1_req}	0.25
2	t_{2_req}	0.15
3	t_{3_req}	0.25
4	t_{4_req}	0.25
5	t_{5_req}	0.1
6	t_{6_req}	0.3
7	t_{7_req}	0.2
8	t_{8_req}	0.15
9	t_{9_req}	0.35
10	t_{req}	2

where U is a valid event (true statement); ∩ is a Boolean intersection symbol for events; $j = 1(1)m$ is an ordered set of variables at which the linear objective function reaches the extreme value with all constraints in the form of equalities or inequalities satisfied.

CONCLUSIONS

The paper describes indicators for assessing the quality of an investigation on the basis of the suitability criterion. An attempt has been undertaken to provide a scientific basis for the process of InfoSec incident investigation into a targeted attack, namely, to form indicators and criteria for assessing the quality of the investigation at the qualitative and quantitative level based on purposeful process efficiency theory. Since the scientific results presented in the paper more deliberative than definitive, the authors hope that they will represent a useful starting point for managers and computer forensic experts when developing scientific approaches in their professional activities.

Further planned studies will develop the mathematical apparatus for this research area to increase the number of indicators/criteria for assessing the process of investigating an InfoSec incident from modern targeted attacks.

Authors' contributions

S.I. Smirnov—description of criteria and indicators for assessing the quality of an information security investigation.

M.A. Eremeev—the idea of research, the development of aims and objectives, the formulation of conclusions.

Sh.G. Magomedov—study of digital evidence and software tools in the investigation of an information security incident.

D.A. Izergin—justification of the expediency of forming criteria and indicators for assessing the quality of the investigation of an information security incident.

REFERENCES

1. Smirnov S.I., Eremeev M.A., Gorbachev I.E., Nefedov V.S., Izergin D.A. Analysis of techniques and tools used by an attacker when moving horizontally in the corporate network. *Zashchita Informatsii. Insaid*. 2021;1(97):58–61 (in Russ.). https://www.elibrary.ru/pltlpq
2. Smirnov S.I. Cyber incident investigation methodology based on intelligent analysis of domain security events. *Zashchita Informatsii. Insaid*. 2022;4(106):60–69 (in Russ.). https://www.elibrary.ru/mefhpc
3. Smirnov S.I., Kiselev A.N., Azerskii V.D., Karel'skii D.V., Kumurzhi G.M. Comprehensive methodology for conducting an information security incident investigation. *Zashchita Informatsii. Insaid*. 2023;2(110):14–26 (in Russ.). https://www.elibrary.ru/fdhgzq
4. Makarenko S.I. Criteria and parameters for estimating quality of penetration testing. *Voprosy kiberbezopasnosti = Cybersecurity Issues J*. 2021;3(43):43–57 (in Russ.). https://www.elibrary.ru/udlknn
5. Smirnov S.I., Eremeev M.A., Pribylov I.A. Approach to Recognition of Malicious Behavior Based on Autoregression Model upon Investigation into Cyberincident. *Aut. Control Comp. Sci*. 2021;55(8):1099–1103. http://doi.org/10.3103/S0146411621080290, https://www.elibrary.ru/ubwpai
6. Zegzhda D.P., Lavrova D.S., Pavlenko E.Y. Management of a Dynamic Infrastructure of Complex Systems Under Conditions of Directed Cyber Attacks. *J. Comput. Syst. Sci. Int.* 2020;59(3):358–370. https://doi.org/10.1134/S1064230720020124 [Original Russian Text: Zegzhda D.P., Lavrova D.S., Pavlenko E.Y. Management of a Dynamic Infrastructure of Complex Systems Under Conditions of Directed Cyber Attacks. *Izvestiya Rossiiskoi akademii nauk. Teoriya i sistemy upravleniya*. 2020;3:50–63 (in Russ.). https://doi.org/10.31857/S0002338820020134]
7. Kalinin V.N., Lomako A.G., Ovcharov V.A., Petrenko S.A. Investigation of information security incidents using the behavior profiling of dynamic network objects. *Zashchita Informatsii. Insaid*. 2018;3(81):58–67 (in Russ.). https://www.elibrary.ru/xqlamp
8. Ovcharov V.A., Romanov P.A. Investigation of computer incidents based on the identification of discrete IS events and reverse analysis by final outcomes. *Trudy Voenno-kosmicheskoi akademii imeni A.F. Mozhaiskogo = Proceedings of the Mozhaisky Military Aerospace Academy*. 2015;648:84–89 (in Russ.). https://www.elibrary.ru/uzmkox
9. Lomako A.G., Ovcharov V.A., Petrenko S.A. Method for investigating security incidents based on behavior profiles of network objects. In: *Distance Educational Technologies: Materials of the Third All-Russian Scientific and Practical Conference*, September 17–22, 2018. Yalta: Arial; 2018. P. 366–373 (in Russ.). https://www.elibrary.ru/uzzdah
10. Saenko I.B., Lauta O.S., Karpov M.A., Kribel A.M. Model of threats to information and telecommunication network resources as a key asset of critical infrastructure. *Elektrosvyaz*. 2021;1:36–44 (in Russ.). https://doi.org/10.34832/ELSV.2021.14.1.004

11. Bystrov I.S., Kotenko I.V. Analysis of user behavior models for the task of detecting cyber insiders. In: *Actual Problems of Infotelecommunications in Science and Education: collection of scientific articles*: in 4 v. V. 1. St. Petersburg: Bonch-Bruevich St. Petersburg State University of Telecommunications; 2021. P. 139–143 (in Russ.). https://www.elibrary.ru/sqzvma
12. Eremeev M.A., Smirnov S.I., Pribylov I.A. Detection of malicious actions of an attacker based on event logs when investigating an ongoing cyber incident. In: *Innovative Aspects of the Development of Science and Technologies: Collection of articles of the 7th International Scientific and Practical Conference*. Saratov: Tsifrovaya nauka; 2021. P. 22–28 (in Russ.). https://www.elibrary.ru/ygoyfz
13. Avramenko V.S., Malikov A.V. Neural network model for diagnosing computer incidents in special purpose infocommunication systems. In: *Problems of Technical Support of Troops in Modern Conditions: Proceedings of the Forth Interuniversity Scientific and Practical Conference*. St. Petersburg; 2019. P. 41–45 (in Russ.). https://www.elibrary.ru/flomvh
14. Levshun D.S. Building an attacker model for a modern cyberphysical system. In: *Actual Problems of Infotelecommunications in Science and Education* (*APINO 2020*). *The 9th International Scientific-Technical and Scientific-Methodological Conference: collection of scientific articles*. V. 1. St. Petersburg: Bonch-Bruevich St. Petersburg State University of Telecommunications; 2020. P. 679–682 (in Russ.). https://www.elibrary.ru/krafgr
15. Petukhov G.B., Yakunin V.I. *Metodologicheskie osnovy vneshnego proektirovaniya tselenapravlennykh protsessov i tseleustremlennykh system* (*Methodological Foundations of External Design of Purposeful Processes and Purposeful Systems*). Moscow: AST; 2006. 504 p. (in Russ.).

СПИСОК ЛИТЕРАТУРЫ

1. Смирнов С.И., Еремеев М.А., Горбачев И.Е., Нефедов В.С., Изергин Д.А. Анализ техник и инструментов, используемых злоумышленником при горизонтальном перемещении в корпоративной сети. *Защита информации. Инсайд*. 2021;1(97):58–61. https://www.elibrary.ru/pltlpq
2. Смирнов С.И. Методика расследования киберинцидента, основанная на интеллектуальном анализе событий безопасности домена. *Защита информации. Инсайд.* 2022;4(106):60–69. https://www.elibrary.ru/mefhpc
3. Смирнов С.И., Киселев А.Н., Азерский В.Д., Карельский Д.В., Кумуржи Г.М. Комплексная методика проведения расследования инцидента информационной безопасности. *Защита информации. Инсайд*. 2023;2(110):14–26. https://www.elibrary.ru/fdhgzq
4. Макаренко С.И. Критерии и показатели оценки качества тестирования на проникновение. *Вопросы кибербезопасности*. 2021;3(43):43–57. https://www.elibrary.ru/udlknn
5. Smirnov S.I., Eremeev M.A., Pribylov I.A. Approach to Recognition of Malicious Behavior Based on Autoregression Model upon Investigation into Cyberincident. *Aut. Control Comp. Sci*. 2021;55(8):1099–1103. http://doi.org/10.3103/S0146411621080290, https://www.elibrary.ru/ubwpai
6. Зегжда Д.П., Лаврова Д.С., Павленко Е.Ю. Управление динамической инфраструктурой сложных систем в условиях целенаправленных кибератак. *Известия РАН. Теория и системы управления*. 2020;4(3):50–63. https://doi.org/10.31857/S0002338820020134
7. Калинин В.Н., Ломако А.Г., Овчаров В.А., Петренко С.А. Расследование ИБ-инцидентов с использованием профилирования поведения динамических сетевых объектов. *Защита информации. Инсайд*. 2018;3(81):58–67. https://www.elibrary.ru/xqlamp
8. Овчаров В.А., Романов П.А. Расследование компьютерных инцидентов на основе идентификации дискретных событий информационной безопасности и обратного анализа по конечным исходам. *Труды Военно-космической академии имени А.Ф. Можайского*. 2015;648:84–89. https://www.elibrary.ru/uzmkox
9. Ломако А.Г., Овчаров В.А., Петренко С.А. Метод расследования инцидентов безопасности на основе профилей поведения сетевых объектов. В сб.: *Дистанционные образовательные технологии: Материалы III Всероссийской научно-практической конференции*, 17–22 сентября 2018 г. Ялта: ООО «Издательство Типография «Ариал»; 2018. С. 366–373. https://www.elibrary.ru/uzzdah
10. Саенко И.Б., Лаута О.С., Карпов М.А., Крибель А.М. Модель угроз ресурсам ИТКС как ключевому активу критически важного объекта инфраструктуры. *Электросвязь*. 2021;1:36–44. https://doi.org/10.34832/ELSV.2021.14.1.004
11. Быстров И.С., Котенко И.В. Анализ моделей поведения пользователей для задачи обнаружения кибер-инсайдеров. В сб.: *Актуальные проблемы инфотелекоммуникаций в науке и образовании: сборник научных статей*: в 4 т. Т. 1. СПб.: Санкт-Петербургский государственный университет телекоммуникаций им. проф. М.А. Бонч-Бруевича; 2021. С. 139–143. https://www.elibrary.ru/sqzvma
12. Eremeev M.A., Smirnov S.I., Pribylov I.A. Detection of malicious actions of an attacker based on event logs when investigating an ongoing cyber incident. В сб.: *Инновационные аспекты развития науки и техники: Сборник статей VII Международной научно-практической конференции.* Саратов: НОО «Цифровая наука»; 2021. С. 22–28. https://www.elibrary.ru/ygoyfz
13. Авраменко В.С., Маликов А.В. Нейросетевая модель диагностирования компьютерных инцидентов в инфокоммуникационных системах специального назначения. В сб.: *Проблемы технического обеспечения войск в современных условиях: Труды IV Межвузовской научно-практической конференции*. Т. 1. СПб.; 2019. С. 41–45. https://www.elibrary.ru/flomvh

14. Левшун Д.С. Построение модели атакующего для современной киберфизической системы. В сб.: *Актуальные проблемы инфотелекоммуникаций в науке и образовании* (*АПИНО 2020*). *IX Международная научно-техническая и научно-методическая конференция: сборник научных статей*. Т. 1. СПб.: Санкт-Петербургский государственный университет телекоммуникаций им. проф. М.А. Бонч-Бруевича; 2020. С. 679–682. https://www.elibrary.ru/krafgr
15. Петухов Г.Б., Якунин В.И. *Методологические основы внешнего проектирования целенаправленных процессов и целеустремленных систем*. М.: АСТ; 2006. 504 с.

About the authors

Stanislav I. Smirnov, Cand. Sci. (Eng.), Assistant Professor, Department of Intelligent Information Security Systems, Institute of Cybersecurity and Digital Technologies, MIREA – Russian Technological University (78, Vernadskogo pr., Moscow, 119454 Russia). E-mail: smirnov_si@mirea.ru. Scopus Author ID 57475289100, ResearcherID HZM-3994-2023, RSCI SPIN-code 1472-6572, https://orcid.org/0000-0003-4387-0850

Mikhail A. Eremeev, Dr. Sci. (Eng.), Professor, Department of Information and Analytical Cybersecurity Systems, Institute of Cybersecurity and Digital Technologies, MIREA – Russian Technological University (78, Vernadskogo pr., Moscow, 119454 Russia). E-mail: eremeev_m@mirea.ru. Scopus Author ID 57188205500, RSCI SPIN-code 3609-5733, https://orcid.org/0000-0002-5511-4000

Shamil G. Magomedov, Cand. Sci. (Eng.), Associate Professor, Head of the Department of Intelligent Information Security Systems, Institute of Cyber Security and Digital Technologies, MIREA – Russian Technological University (78, Vernadskogo pr., Moscow, 119454 Russia). msgg@list.ru. Scopus Author ID 57204759220, ResearcherID M-5782-2016, RSCI SPIN-code 5029-8310, https://orcid.org/0000-0001-8560-1937

Dmitry A. Izergin, Cand. Sci. (Eng.), Assistant Professor, Department of Digital Data Processing Technologies, Institute of Cybersecurity and Digital Technologies, MIREA – Russian Technological University (78, Vernadskogo pr., Moscow, 119454 Russia). E-mail: izergin@mirea.ru. Scopus Author ID 57224822181, RSCI SPIN-code 2318-9152, https://orcid.org/0000-0002-3174-4550

Об авторах

Смирнов Станислав Игоревич, к.т.н., доцент, кафедра интеллектуальных систем информационной безопасности, Институт кибербезопасности и цифровых технологий, ФГБОУ ВО «МИРЭА – Российский технологический университет» (119454, Россия, Москва, пр-т Вернадского, д. 78). E-mail: smirnov_si@mirea.ru. Scopus Author ID 57475289100, ResearcherID HZM-3994-2023, SPIN-код РИНЦ 1472-6572, https://orcid.org/0000-0003-4387-0850

Еремеев Михаил Алексеевич, д.т.н., профессор, кафедра информационно-аналитических систем кибербезопасности, Институт кибербезопасности и цифровых технологий, ФГБОУ ВО «МИРЭА – Российский технологический университет» (119454, Россия, Москва, пр-т Вернадского, д. 78). E-mail: eremeev_m@mirea.ru. Scopus Author ID 57188205500, SPIN-код РИНЦ 3609-5733, https://orcid.org/0000-0002-5511-4000

Магомедов Шамиль Гасангусейнович, к.т.н., доцент, заведующий кафедрой интеллектуальных систем информационной безопасности, Институт кибербезопасности и цифровых технологий, ФГБОУ ВО «МИРЭА – Российский технологический университет» (119454, Россия, Москва, пр-т Вернадского, д. 78). E-mail: msgg@list.ru. Scopus Author ID 57204759220, ResearcherID M-5782-2016, SPIN-код РИНЦ 5029-8310, https://orcid.org/0000-0001-8560-1937

Изергин Дмитрий Андреевич, к.т.н., доцент, кафедра цифровых технологий обработки данных, Институт кибербезопасности и цифровых технологий, ФГБОУ ВО «МИРЭА – Российский технологический университет» (119454, Россия, Москва, пр-т Вернадского, д. 78). E-mail: izergin@mirea.ru. Scopus Author ID 57224822181, SPIN-код РИНЦ 2318-9152, https://orcid.org/0000-0002-3174-4550

Translated from Russian into English by Kirill V. Nazarov
Edited for English language and spelling by Thomas A. Beavitt

Information systems. Computer sciences. Issues of information security

Информационные системы. Информатика. Проблемы информационной безопасности

UDC 004.2
https://doi.org/10.32362/2500-316X-2024-12-3-37-45
EDN PXKDKR

RESEARCH ARTICLE

Method for designing specialized computing systems based on hardware and software co-optimization

Ilya E. Tarasov @, Peter N. Sovietov, Daniil V. Lulyava, Dmitry I. Mirzoyan

MIREA – Russian Technological University, Moscow, 119454 Russia
@ Corresponding author, e-mail: tarasov_i@mirea.ru

Abstract

Objectives. Following the completion of development stages due to transistor scaling (Dennard's law) and an increased number of general-purpose processor cores (limited by Amdahl's law), further improvements in the performance of computing systems naturally proceeds to the stage of developing specialized computing subsystems for performing specific tasks within a limited computational subclass. The development of such systems requires both the selection of the relevant high-demand tasks and the application of design techniques for achieving desired indicators within the developed specializations at very large scales of integration. The purpose of the present work is to develop a methodology for designing specialized computing systems based on the joint optimization of hardware and software in relation to a selected subclass of problems.

Methods. The research is based on various methods for designing digital systems.

Results. Approaches to the analysis of computational problems involving the construction of a computational graph abstracted from the computing platform, but limited by a set of architectural solutions, are considered. The proposed design methodology based on a register transfer level (RTL) representation synthesizer of a computing device is limited to individual computing architectures for which the relevant circuit is synthesized and optimized based on a high-level input description of the algorithm. Among computing node architectures, a synchronous pipeline and a processor core with a tree-like arithmetic-logical unit are considered. The efficiency of a computing system can be increased by balancing the pipeline based on estimates of the technological basis, and for the processor—based on optimizing the set of operations, which is performed based on the analysis of the abstract syntax tree graph with its optimal coverage by subgraphs corresponding to the structure of the arithmetic logic unit.

Conclusions. The considered development approaches are suitable for accelerating the process of designing specialized computing systems with a massively parallel architecture based on pipeline or processor computing nodes.

Keywords: processor, RTL, synthesis, translator

• **Submitted:** 18.10.2023 • **Revised:** 04.12.2023 • **Accepted:** 22.03.2024

For citation: Tarasov I.E., Sovietov P.N., Lulyava D.V., Mirzoyan D.I. Method for designing specialized computing systems based on hardware and software co-optimization. *Russ. Technol. J*. 2024;12(3):37–45. https://doi.org/10.32362/2500-316X-2024-12-3-37-45

Financial disclosure: The authors have no a financial or property interest in any material or method mentioned.

The authors declare no conflicts of interest.

НАУЧНАЯ СТАТЬЯ

Методика проектирования специализированных вычислительных систем на основе совместной оптимизации аппаратного и программного обеспечения

И.Е. Тарасов [@], П.Н. Советов, Д.В. Люлява, Д.И. Мирзоян

МИРЭА – Российский технологический университет, Москва, 119454 Россия
[@] Автор для переписки, e-mail: tarasov_i@mirea.ru

Резюме

Цели. Следующим этапом повышения производительности вычислительных систем после завершения этапов роста за счет масштабирования транзисторов (закон Деннарда) и за счет увеличения количества процессорных ядер общего назначения (ограничиваемого законом Амдала) является переход к разработке специализированных вычислительных подсистем для работы в ограниченном подклассе задач. Создание таких систем требует как выбора соответствующих массово востребованных задач, так и применения методик проектирования, обеспечивающих достижение высоких технико-экономических показателей разрабатываемых специализированных сверхбольших интегральных схем. Цель работы – разработка методики проектирования специализированных вычислительных систем на основе совместной оптимизации аппаратного и программного обеспечения применительно к выбранному подклассу задач.

Методы. Использованы методы проектирования цифровых систем.

Результаты. Рассмотрены подходы к анализу вычислительных задач путем построения графа вычислений, абстрагированного от вычислительной платформы, однако ограниченного набором архитектурных решений. Предложена методика проектирования, использующая маршрут, основанный на применении синтезатора представления уровня регистровых передач (RTL-представления) вычислительного устройства, ограниченного отдельными вычислительными архитектурами, для которых производятся синтез и оптимизация схемы на основе высокоуровневого входного описания алгоритма. Среди архитектур вычислительных узлов рассмотрены синхронный конвейер и процессорное ядро с древовидным арифметико-логическим устройством. Повышение эффективности вычислительной системы осуществляется путем балансировки конвейера на основе оценок технологического базиса, а для процессора – путем оптимизации набора операций на основе анализа графа абстрактного синтаксического дерева с его оптимальным покрытием подграфами, соответствующим структуре арифметико-логического устройства.

Выводы. Рассмотренные подходы к разработке позволяют ускорить процесс проектирования специализированных вычислительных систем с массово-параллельной архитектурой, основанных на конвейерных вычислительных узлах.

Ключевые слова: процессор, RTL, синтез, транслятор

• **Поступила:** 18.10.2023 • **Доработана:** 04.12.2023 • **Принята к опубликованию:** 22.03.2024

Для цитирования: Тарасов И.Е., Советов П.Н., Люлява Д.В., Мирзоян Д.И. Методика проектирования специализированных вычислительных систем на основе совместной оптимизации аппаратного и программного обеспечения. *Russ. Technol. J*. 2024;12(3):37–45. https://doi.org/10.32362/2500-316X-2024-12-3-37-45

Прозрачность финансовой деятельности: Авторы не имеют финансовой заинтересованности в представленных материалах или методах.

Авторы заявляют об отсутствии конфликта интересов.

INTRODUCTION

The field of element base design for high-performance computing in Russia is characterized by trends corresponding to objective technical limitations and the need to intensify import substitution processes to ensure technological sovereignty. Analysis of the desired technical characteristics should take into account production capacity limitations, as well as the need to reduce technical and economic risks.

Analysis of architectural trends in the field of computing is presented by Patterson and Hennessy in [1]. The authors draw attention to a number of major milestones in the development of processor architectures since the 1970s. The first of these concerns the replacement of the CISC (complex instruction set computer) concept with the RISC (reduced instruction set computer) approach. Due to the ensuing reduction in combinational logic complexity, it became possible to increase the clock frequency of processor devices.

Further increases in clock frequency, however, turned out to be limited according to Dennard's Law, which describes an inherent limit to the possibility of increasing processor performance by scaling transistor sizes. The response to this limitation was the transition to multi-core processors, which took place in the mass segment of personal computers during the mid-2000s.

Improved performance by increasing the number of processor cores is in turn limited by Amdahl's law, which defines the potential performance improvement of a multiprocessor complex by defining the fraction of computations that can be performed in parallel. A related problem is the so-called *wall of interfaces* [2], which takes into account the fact that performance increases quadratically with decreasing process standards, while the bandwidth of memory and peripheral interfaces increases linearly. Therefore, the construction of multicore systems entails the problem of organizing inter-processor data exchange, which cannot be effectively implemented due to the outstripping growth of the volume of received data compared to the possibility of their transmission through existing communication channels designed according to comparable technological standards.

In [1], in connection with the above problems, a transition to domain-specific architectures is proposed by analogy with domain-specific languages (DSL). In this case, the specialization of a processor for performing certain classes of computations implies its reduced efficiency in other classes, necessitating the selection of specialized computational tasks corresponding to current technical needs. Such an approach can find wide application due to considerations of reducing design and production unit costs, as well as corresponding to technically feasible approaches to the design of digital devices.

ANALYSIS OF COMPUTATIONAL TASKS FOR IMPLEMENTATION AS A PART OF SPECIALIZED COMPUTING SYSTEMS

Important areas for the application of high-performance computing systems include video processing systems, virtual and augmented reality, robotics, industrial automation, digital radio communications, measurement technology [3, 4]. Among the implemented areas of signal processing are digital filtering [5], spectral analysis [6], machine learning algorithms [7], including those based on specialized neural processors [8], or reconfigurable gas pedals based on field-programmable gate array (FPGA).

Computational tasks that can be accelerated by specialized computing systems include the following subclasses:

1) solving differential equation systems by numerical methods;
2) operations with three-dimensional images;
3) digital signal processing based on mass application of "multiply and accumulate" operations;
4) computation of hash functions in information protection tasks;
5) implementation of neural networks in terms of calculating neural function values (neural net inference), not including neural net training tasks.

Types of operations characteristic of the above tasks are given in the Table. The columns of the table are placed in such a way that the complexity of realization of the corresponding types of operations increases from left to right. Although significant difficulties are associated with high-complexity memory operations based on increasing the throughput capacity of a memory subsystem, some memory operations themselves do not have high complexity.

The Table uses the following scores to characterize use intensity of certain types of operations. The assessment *no*, which corresponds to the situation when the operation is not used in algorithms, does not require support. While the assessment *possibly* characterizes situations when such operations take place, these do not have a noticeable impact on the efficiency of the computing device due to their rare use. For such operations, it is possible to use non-optimized solutions or ready-made components having functional redundancy. The assessment *massively*, which corresponds to operations forming the basis of algorithms, determines the intended implementation efficiency of the computing device to the greatest extent.

According to the preliminary estimates, the implementation of hash functions and digital signal processing operations demonstrates the advantages of pipelined architectures to a greater extent, since it provides for streaming data processing without intensive exchange with external memory.

Table. Intensity of use of operations characteristic of a number of tasks requiring the use of high-performance computing systems

Task type	Shifts, addition, bitwise operations	Multiplication	Floating point operations	Transcendental functions	Memory operations
Hash functions	Massively	No	No	No	Possibly
Neural networks implementation	No	Massively	Possibly	Possibly	Possibly
Digital signals processing (filtration)	Massively	Massively	Possibly	Possibly	Possibly
Differential equation systems	No	Possibly	Massively	Possibly	Massively
3D graphics processing	No	Often	Massively	Often	Massively

COMPUTING NODE ARCHITECTURES

Architectural approaches to the realization of individual computational nodes in modern digital electronics are quite diverse. For their effective practical use, however, it is necessary to limit ourselves to a set of possible solutions for using computer-aided design methods at the level of mathematical and software models. Further transformations in the representation of the register transfer level circuit (RTL-representation) do not make significant changes in the characteristics of such a system. It can be noted, for example, that the use of means of description of high-level language (HLL) class implies automated construction of control diagrams (flow control) designed for a wide class of realized architectural approaches. This leads to excessive complication of synthesized control diagrams.

The following architectural approaches to the construction of computational nodes are considered for the practically realizable design methodology:

1) processor unit;
2) synchronous pipeline;
3) modification of synchronous pipeline with the possibility of reusing of individual stages.

Structural diagrams of the main computing nodes are shown in Fig. 1.

Given variants of nodes are considered as architectural templates for realization of selected subclasses of computations. In this case, the required set of operations for the processor is realized as part of the arithmetic-logic unit (ALU), while for the pipeline, it is realized in successive stages. To use a pipeline, it is necessary for the order of operations for the realization of the algorithm to remain unchanged, otherwise the adjustment will require complication of control diagrams. Provided that the frequency of receiving input data is significantly less than the clock frequency of the pipeline, repetition of operations can be used in algorithms such as computation of hash functions and realization of filters with finite impulse response. When this condition is fulfilled, the same stage of the pipeline can be used repeatedly until the arrival of a new input value.

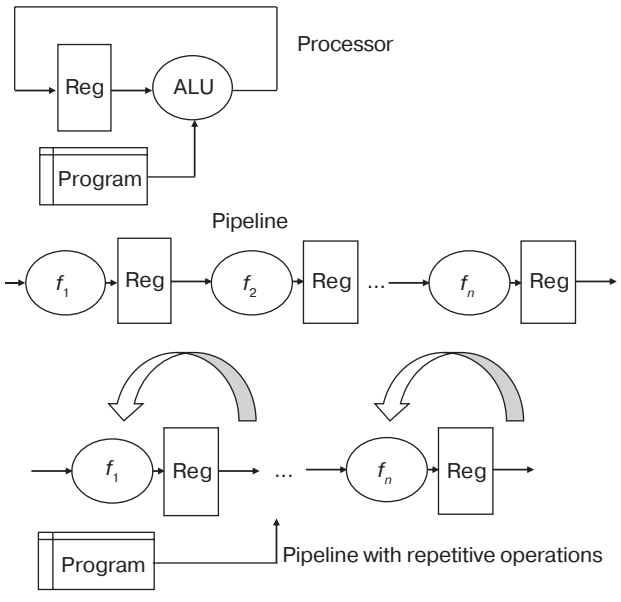

Fig. 1. Diagrams of the main computing nodes (architectural templates). f_1, f_2, ..., f_n are the functional devices

Since operations involving RTL-representation synthesis and optimization depends on the choice of a particular architectural pattern, the present work article

considers the application of the technique for pipelined computational structures. The addition of processor and pipeline architectural templates with operational repetition is provided for subsequent stages of the project.

Design route according to the proposed methodology of designing computing modules of a specialized computing system is shown in Fig. 2.

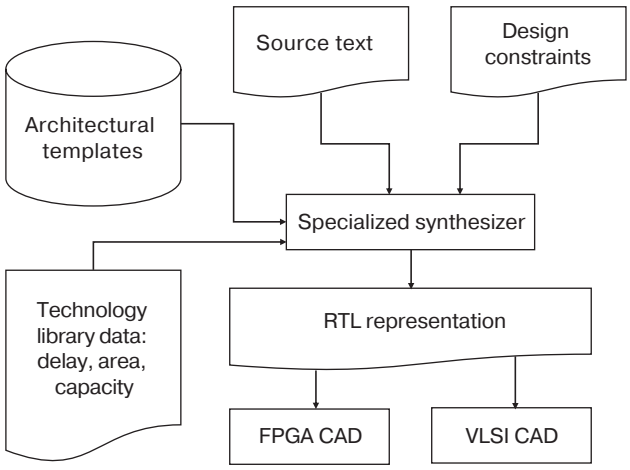

Fig. 2. Route for designing modules of a specialized computer system

According to the presented route, it can be seen that the input data are the source code of the algorithm to be implemented, while design constraints are presented in the form of the limiting characteristics of the required solution. The specialized synthesizer developed by P.N. Sovetov [9] based on architectural templates generates the RTL representation of a module using the data on the technological library for preliminary evaluation of its characteristics. The resulting RTL representation is further used in FPGA or very large-scale integration (VLSI) design paths, where the corresponding computer-aided design systems (CAD) are used to estimate the module characteristics following synthesis or after performing placement and tracing (which gives a more accurate estimation of characteristics compared to the estimation after synthesis).

For example, the values of signal propagation delays become the basis for re-synthesis of RTL representation with additional pipelining of the identified critical circuits. In addition, the synthesizer provides additional information about the interconnections of the synthesized nodes to generate design constraints specifying the coordinates of individual nodes of the synthesized circuit (stages of the pipeline). While such capabilities are also partially provided by such design tools as *Vitis HLS*[1], the characteristics of the technological platform are set out in the form of libraries. Using the route developed as part of the present work, these characteristics can to be refined during the process of project optimization.

OPTIMIZATION OF COMPUTATIONAL NODE BASED ON SOFTWARE MODEL OF COMPUTATIONS

The development of compilers for new processor architectures is an important element in the provision of tools for designing systems based on them [10]. Translators of DSL into RTL representation represent a promising approach to fast design of hardware gas pedals for some narrow class of architectures [11]. Let us briefly outline the design steps of a tool system consisting of an embedded DSL based on a subset of the Python language and a translator for synthesizing hardware gas pedals based on pipelining of a linear program section.

The user program, representing a behavioral description of the hardware gas pedal being synthesized, is input to the translator. This program is automatically converted into the form of an abstract syntax tree (AST) using the ast module from the Python standard library. The AST checks and propagates information about the types used in the input program based on Python's type annotation mechanism.

In addition, the user provides a table of delays and operation combination rules for the selected chip type, as well as one of the selected pipeline control templates in the Verilog language. The result of the translator is the code of the synthesized pipelined gas pedal in the Verilog language.

After all functions in the input program are embedded in the main function, the loops are fully unrolled. Then the program is transformed into an acyclic data dependency graph (DDG), where the convolution and promotion of constants, removal of matching expressions, and removal of dead code are performed based on the numbering of values. In order to achieve a potentially greater parallelism of calculations, balancing of expression tree heights is carried out.

Prior to the direct synthesis of the pipeline, auxiliary steps are performed: a step of partial coverage of the DDG using multiple input single output (MISO) subgraphs, as well as a step of calculating the maximum delays between pairs of nodes in the DDG.

The target chip type may use resources that enable combination, i.e., combining the execution of several operations in time, for example, using a look-up table (LUT). The translator uses partial DDG coverage of combined operations using a variant of the MAXMISO algorithm for instruction synthesis.

[1] https://www.xilinx.com/products/design-tools/vitis/vitis-hls.html. Accessed October 10, 2023.

This algorithm allows us to enumerate in DDG non-intersecting subgraphs having the number of inputs not more than a given number and one output.

The result of the pipeline synthesis is DDG with added nodes representing pipelining registers. By realizing the pipeline synthesis mainly using third-party constraint programming and linear programming solvers, the implementation of the code generator is simplified. The pipeline synthesis is implemented in one of the following ways: with minimization of the pipeline depth, with minimization of the total size of the pipeline registers, or with minimization of the pipeline depth followed by minimization of the total size of the pipeline registers. The pipeline is synthesized using information about the end-user nodes that takes the DDG representation of the program into account. This simplifies the algorithm synthesis process by reducing the number of generated constraints. A similar approach was used to create a compiler for a specialized controller based on a field-programmable gate array (FPGA) [12]. Here, the presence of similar approaches to the translation of high-level program representation [13, 14] can be noted; however, these do not involve feedback from CAD, which determines the actually achieved time delays by tracing the project. At the same time, attention is paid to pipelined architectures for FPGA [15].

METHODOLOGY FOR EVALUATING THE TOPOLOGICAL IMPLEMENTATION OF A COMPUTATIONAL NODE

The synthesized RTL representation discussed above uses the estimated delays introduced by individual operations as input information. For the selected technological basis, it is therefore necessary to:

1) determine the delays of individual elements that implement the computations supported by the synthesizer;
2) identify the possibility of using an additive delay model or determine a way to determine the total delay of a combinational node taking into account the interaction of individual elements.

Verification of the topological realization of the example of the pipeline calculator was carried out in *AMD/Xilinx Vivado*[2] FPGA CAD. The pipeline calculator implements the COordinate Rotational DIgital Computer (CORDIC) vector rotation algorithm, forming the basis for the computation of transcendental functions. This choice is related to the inclusion of the CORDIC IP core in the library components of *AMD/Xilinx Vivado* CAD; thus, its characteristics can be compared with the obtained results. The calculation of the steps of the CORDIC algorithm is combined with the sequential calculation of the result of multiplication with accumulation. In this way, an excess of functionality with respect to the CORDIC IP core is ensured. A quantitative criterion for assessing the quality of preliminary delay modeling is the histogram of time delay stocks (slack histogram)[3]. In static timing analysis, the slack value is the difference between the value of the clock signal period and the maximum signal propagation delay between synchronous nodes of the circuit. Depending on the complexity of expressions and mutual arrangement of nodes, the delay will be individual for each circuit. On this basis, a histogram is constructed showing the number of circuits that have appropriate time reserves before the arrival of the next edge of the clock signal. Such a histogram, which is referred to here as a stock histogram, is generated in *Vivado* CAD at the operator's request based on the static time analysis performed in CAD.

Based on the considerations of balancing the stages of the pipeline in the ideal case, we can assume that the stocks will be grouped around the minimum values to indicate the absence of circuits having an excessively short delay and consequent inefficient use of hardware resources. An example of a histogram of time delay stocks is shown in Fig. 3.

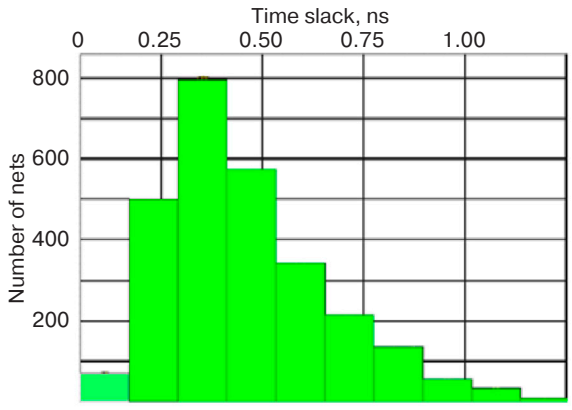

Fig. 3. Histogram of time delay stocks for the pipeline example

The grouping of circuits on the histogram shows that balancing of the pipeline stages is performed correctly: the main proportion of circuits falls in the left part of the histogram, which corresponds to small values of time reserve.

[2] https://docs.xilinx.com/r/en-US/ug910-vivado-getting-started. Accessed October 10, 2023.

[3] https://docs.xilinx.com/r/en-US/ug906-vivado-design-analysis/Timing-Analysis. Accessed October 10, 2023.

EXAMPLES OF PRACTICAL TESTING OF THE METHODOLOGY

Practical approbation of the method was carried out on the basis of a number of computational nodes of pipeline type. A configurable pipeline with the combination of calculations of the result of multiplication with accumulation and vector rotation based on the CORDIC algorithm was realized. The synthesized pipeline can be used to calculate a pair of values of sine, cosine or multiply independent 32-bit operands in the mode of switching functional nodes.

When estimating the achievable clock speed of FPGA-based digital circuits, the concept of logic levels is used to refer to the number of nodes connected in series in a circuit of maximum length. This circuit is a limiting factor where the achievable clock frequency is preliminarily estimated as the system clock frequency divided by the logic levels figure. With a system clock frequency on the order of 700–750 MHz for a modern FPGA architecture, achieving logic levels equal to 1 is quite a challenging technical task. Nevertheless, the balancing of the pipeline allowed us to obtain a clock signal period of 1.6–1.7 ns, which corresponds to a clock frequency of 600–625 MHz for the *AMD/Xilinx Kria* platform constructed according to 16 nm FinFET[4] technological standards.

CONCLUSIONS

Approaches considered in the article enable the optimization of pipeline calculators designed to work as part of VLSI. The obtained positive results can be used to extend the methodology for designing processor nodes and pipelines with repetition of operations, whose architectural templates were considered in the introductory part of the article. The calculator is optimized in accordance with the selected quality criteria by means of joint analysis of the design at several levels (software model, circuit, and topological representations), including controlled increase of clock frequency for high-performance computing systems due to balancing delays of functional nodes of the pipeline.

ACKNOWLEDGMENTS

The work was performed within the framework of the State assignment of the Ministry of Science and Higher Education of the Russian Federation (theme No. FSFZ-2022-0004 “Architectures of specialized computing complexes, methods, algorithms, and tools for designing digital computing devices”).

Authors’ contribution. All authors equally contributed to the research work

REFERENCES

1. Hennessy J.L., Patterson D.A. A new golden age for computer architecture: Domain-specific hardware/software co-design, enhanced security, open instruction sets, and agile chip development. In: *Proceedings of the 2018 ACM/IEEE 45th Annual International Symposium on Computer Architecture* (*ISCA*). IEEE; 2018. https://doi.org/10.1109/ISCA.2018.00011
2. Hennessy J.L, Patterson D.A. *Computer Architecture*: *A Quantitative Approach*. 6th ed. The Morgan Kaufmann Series in Computer Architecture and Design. Morgan Kaufmann; 2017. 936 p.
3. Sesin I.Yu., Bolbakov R.G. Comparative analysis of software optimization methods in context of branch predication on GPUs. *Russ. Technol. J.* 2021;9(6):7–15 (in Russ.). https://doi.org/10.32362/2500-316X-2021-9-6-7-15
4. Sleptsov V.V., Afonin V.L., Ablaeva A.E., Dinh B. Development of an information measuring and control system for a quadrocopter. *Russ. Technol. J*. 2021;9(6):26–36 (in Russ.). https://doi.org/10.32362/2500-316X-2021-9-6-26-36
5. Smirnov A.V. Optimization of digital filters performances simultaneously in frequency and time domains. *Russ. Technol. J*. 2020;8(6):63–77 (in Russ.). https://doi.org/10.32362/2500-316X-2020-8-6-63-77
6. Umnyashkin S.V. *Osnovy teorii tsifrovoi obrabotki signalov* (*Fundamentals of the Theory of Digital Signal Processing*). 3rd ed. Moscow: Litres; 2022. 551 p. (in Russ.). ISBN 978-5-4576-1810-7
7. Abadi M., Barham P., Chen J., et al. TensorFlow: A system for Large-Scale Machine Learning. In: *Proceedings of the 12th USENIX Symposium on Operating Systems Design and Implementation* (*OSDI ’16*). USENIX Association; 2016. P. 265–283.
8. Nurvitadhi E., Sheffield D., Sim J., et al. Accelerating Binarized Neural Networks: Comparison of FPGA, CPU, GPU, and ASIC. In: *2016 International Conference on Field-Programmable Technology* (*FPT*). IEEE; 2016. P. 77–84. https://doi.org/10.1109/FPT.2016.7929192
9. Sovetov P.N. Synthesis of linear programs for a stack machine. *Vysokoproizvoditel’nye vychislitel’nye sistemy i tekhnologii = High-Performance Computing Systems and Technologies*. 2019;3(1):17–22 (in Russ.).
10. Aho A.V., Lam M.S., Sethi R., Ullman J.D. *Kompilyatory: printsipy, tekhnologii i instrumentarii* (*Compilers: Principles, Techniques, & Tools*): transl. from Engl. Moscow: Vil’yams; 2018. 1184 p. ISBN 978-5-8459-1932-8 (in Russ.).
[Aho A.V., Lam M.S., Sethi R., Ullman J.D. *Compilers: Principles, Techniques, & Tools*. Pearson Addison Wesley; 2007. 1035 p.]

[4] https://www.xilinx.com/products/som/kria/k26c-commercial.html. Accessed October 10, 2023.

11. Pratt T.W., Zelkowitz M.V. *Yazyki programmirovaniya: razrabotka i realizatsiya* (*Programming Languages. Design and Implementation*): transl. from Engl. St. Petersburg: Piter; 2002. 688 p. (in Russ.).
[Pratt T.W., Zelkowitz M.V. *Programming Languages. Design and Implementation*. Prentice Hall; 2001. 649 p.]
12. Tarasov I.E., Potekhin D.S., Khrenov M.A., Sovetov P.N. Computer-aided design of multicore system for embedded applications. *Ekonomika i Menedzhment Sistem Upravleniya*. 2017;25(3–1):179–185 (in Russ.).
13. Huang S., Wu K., Jeong H., Wang C., Chen D., Hwu W.M. PyLog: An Algorithm-Centric Python-Based FPGA Programming and Synthesis Flow. *IEEE Trans. Comput*. 2021;70(12):2015–2028. https://doi.org/10.1109/TC.2021.3123465
14. Jiang S., Pan P., Ou Y., Batten C. PyMTL3: A Python Framework for Open-Source Hardware Modeling, Generation, Simulation, and Verification. *IEEE Micro*. 2020;40(4):58–66. https://doi.org/10.1109/MM.2020.2997638
15. Oishi R., Kadomoto J., Irie H., Sakai S. FPGA-based Garbling Accelerator with Parallel Pipeline Processing. *IEICE Transactions on Information and Systems*. 2023;E106-D(12):1988–1996. https://doi.org/10.1587/transinf.2023PAP0002

СПИСОК ЛИТЕРАТУРЫ

1. Hennessy J.L., Patterson D.A. A new golden age for computer architecture: Domain-specific hardware/software co-design, enhanced security, open instruction sets, and agile chip development. In: *Proceedings of the 2018 ACM/IEEE 45th Annual International Symposium on Computer Architecture* (*ISCA*). IEEE; 2018. https://doi.org/10.1109/ISCA.2018.00011
2. Hennessy J.L, Patterson D.A. *Computer Architecture*: *A Quantitative Approach*. 6th ed. The Morgan Kaufmann Series in Computer Architecture and Design. Morgan Kaufmann; 2017. 936 p.
3. Сесин И.Ю., Болбаков Р.Г. Сравнительный анализ методов оптимизации программного обеспечения для борьбы с предикацией ветвлений на графических процессорах. *Russian Technological Journal*. 2021;9(6):7–15. https://doi.org/10.32362/2500-316X-2021-9-6-7-15
4. Слепцов В.В., Афонин В.Л., Аблаева А.Е., Динь Б. Разработка информационно-измерительной и управляющей системы квадрокоптера. *Russian Technological Journal*. 2021;9(6):26–36. https://doi.org/10.32362/2500-316X-2021-9-6-26-36
5. Смирнов А.В. Оптимизация характеристик цифровых фильтров одновременно в частотной и временной областях. *Russian Technological Journal*. 2020;8(6):63–77. https://doi.org/10.32362/2500-316X-2020-8-6-63-77
6. Умняшкин С.В. *Основы теории цифровой обработки сигналов*. 6-е изд. М.: Litres; 2022. 551 с. ISBN 978-5-4576-1810-7
7. Abadi M., Barham P., Chen J., et al. TensorFlow: A system for Large-Scale Machine Learning. In: *Proceedings of the 12th USENIX Symposium on Operating Systems Design and Implementation* (*OSDI '16*). USENIX Association; 2016. P. 265–283.
8. Nurvitadhi E., Sheffield D., Sim J., et al. Accelerating Binarized Neural Networks: Comparison of FPGA, CPU, GPU, and ASIC. In: *2016 International Conference on Field-Programmable Technology* (*FPT*). IEEE; 2016. P. 77–84. https://doi.org/10.1109/FPT.2016.7929192
9. Советов П.Н. Синтез линейных программ для стековой машины. *Высокопроизводительные вычислительные системы и технологии*. 2019;3(1):17–22.
10. Ахо А.В., Лам М.С., Сети Р., Ульман Д.Д. *Компиляторы: принципы, технологии и инструментарий*: пер. с англ. М.: Вильямс; 2018. ISBN 978-5-8459-1332-8
11. Пратт Т., Зелковиц М. *Языки программирования: разработка и реализация*: пер. с англ. СПб.: Питер; 2002. 688 с.
12. Тарасов И.Е., Потехин Д.С., Хренов М.А., Советов П.Н. Автоматизация проектирования многопроцессорной системы на базе ПЛИС для управления во встраиваемых приложениях. *Экономика и менеджмент систем управления*. 2017;25(3–1):179–185.
13. Huang S., Wu K., Jeong H., Wang C., Chen D., Hwu W.M. PyLog: An Algorithm-Centric Python-Based FPGA Programming and Synthesis Flow. *IEEE Trans. Comput*. 2021;70(12):2015–2028. https://doi.org/10.1109/TC.2021.3123465
14. Jiang S., Pan P., Ou Y., Batten C. PyMTL3: A Python Framework for Open-Source Hardware Modeling, Generation, Simulation, and Verification. *IEEE Micro*. 2020;40(4):58–66. https://doi.org/10.1109/MM.2020.2997638
15. Oishi R., Kadomoto J., Irie H., Sakai S. FPGA-based Garbling Accelerator with Parallel Pipeline Processing. *IEICE Transactions on Information and Systems*. 2023;E106-D(12):1988–1996. https://doi.org/10.1587/transinf.2023PAP0002

About the authors

Ilya E. Tarasov, Dr. Sci. (Eng.), Associated Professor, Head of the Laboratory of Specialized Computing Systems, MIREA – Russian Technological University (78, Vernadskogo pr., Moscow, 119454 Russia). E-mail: tarasov_i@mirea.ru. Scopus Author ID 57213354150, RSCI SPIN-code 4628-7514, http://orcid.org/0000-0001-6456-4794

Peter N. Sovietov, Cand. Sci. (Eng.), Senior Researcher, Laboratory of Specialized Computing Systems, MIREA – Russian Technological University (78, Vernadskogo pr., Moscow, 119454 Russia). E-mail: sovetov@mirea.ru. Scopus Author ID 57221375427, RSCI SPIN-code 9999-1460. http://orcid.org/0000-0002-1039-2429

Daniil V. Lulyava, Junior Researcher, Laboratory of Specialized Computing Systems, MIREA – Russian Technological University (78, Vernadskogo pr., Moscow, 119454 Russia). E-mail: lyulyava@mirea.ru. Scopus Author ID 58811698000, RSCI SPIN-code 1882-0989, http://orcid.org/0009-0009-9623-7777

Dmitry I. Mirzoyan, Senior Researcher, Laboratory of Specialized Computing Systems, MIREA – Russian Technological University (78, Vernadskogo pr., Moscow, 119454 Russia). E-mail: mirzoyan@mirea.ru. Scopus Author ID 57432027000, ResearcherID JJE-7844-2023, RSCI SPIN-code 8135-9802, http://orcid.org/0009-0002-4703-8340

Об авторах

Тарасов Илья Евгеньевич, д.т.н., доцент, заведующий лабораторией специализированных вычислительных систем, ФГБОУ ВО «МИРЭА – Российский технологический университет» (119454, Россия, Москва, пр-т Вернадского, д. 78). E-mail: tarasov_i@mirea.ru. Scopus Author ID 57213354150, SPIN-код РИНЦ 4628-7514, http://orcid.org/0000-0001-6456-4794

Советов Петр Николаевич, к.т.н., старший научный сотрудник, лаборатория специализированных вычислительных систем, ФГБОУ ВО «МИРЭА – Российский технологический университет» (119454, Россия, Москва, пр-т Вернадского, д. 78). E-mail: sovetov@mirea.ru. Scopus Author ID 57221375427, SPIN-код РИНЦ 9999-1460. http://orcid.org/0000-0002-1039-2429

Люлява Даниил Вячеславович, младший научный сотрудник, лаборатория специализированных вычислительных систем, ФГБОУ ВО «МИРЭА – Российский технологический университет» (119454, Россия, Москва, пр-т Вернадского, д. 78). E-mail: lyulyava@mirea.ru. Scopus Author ID 58811698000, SPIN-код РИНЦ 1882-0989, http://orcid.org/0009-0009-9623-7777

Мирзоян Дмитрий Ильич, старший научный сотрудник, лаборатория специализированных вычислительных систем, ФГБОУ ВО «МИРЭА – Российский технологический университет» (119454, Россия, Москва, пр-т Вернадского, д. 78). E-mail: mirzoyan@mirea.ru. Scopus Author ID 57432027000, ResearcherID JJE-7844-2023, SPIN-код РИНЦ 8135-9802, http://orcid.org/0009-0002-4703-8340

Translated from Russian into English by Lyudmila O. Bychkova
Edited for English language and spelling by Thomas A. Beavitt

Modern radio engineering and telecommunication systems

Современные радиотехнические и телекоммуникационные системы

UDC 621.396, 621.371, 621.372
https://doi.org/10.32362/2500-316X-2024-12-3-46-54
EDN QREZGM

RESEARCH ARTICLE

Impacts of noise and interference on the bit error rate of the FBMC-OQAM modulation scheme in 5G systems

Abed Androon [@], Olga V. Tikhonova

MIREA – Russian Technological University, Moscow, 119454 Russia
[@] Corresponding author, e-mail: abed.androon@yandex.com

Abstract

Objectives. The work sets out to evaluate the noise immunity of the signal modulation method in 5G networks using a filter bank multicarrier with offset quadrature amplitude modulation (FBMC-OQAM) and to analyze the bit error rate (BER).

Methods. In the work, probability theory and mathematical statistics methods are applied according to computer modeling approaches.

Results. An analysis of BER for the signal modulation method in 5G networks, which uses a bank of filters with multiple carriers with offset quadrature amplitude modulation under noise conditions, is presented. The resistance of the method to intra-cell, inter-cell, and inter-beam types of interference in the 5G channel, as well as additive white Gaussian noise, is investigated. The graphical and numerical data obtained through computer modeling demonstrates improved BER in 5G networks using FBMC-OQAM. The presented comparative analysis of error probability in the FBMC-OQAM system under various types of noise and interference emphasizes the impact of these factors on the quality of information transmission.

Conclusions. The FBMC-OQAM method is characterized by the low impact on the error probability of the data transmission system in 5G networks of various types of interference including intra-cell and inter-cell interference, inter-beam interference, and nonlinear distortions. However, it will be necessary to further optimize the method and develop algorithms for enhancing error probability in the FBMC-OQAM system under real conditions in 5G networks. The research results can be used in the development of 5G networks.

Keywords: 5G network, FBMC-OQAM method, white gaussian noise, BER, SNR, inter-cell interference, nonlinear distortion

• **Submitted:** 04.05.2023 • **Revised:** 18.11.2023 • **Accepted:** 12.03.2024

For citation: Androon A., Tikhonova O.V. Impacts of noise and interference on the bit error rate of the FBMC-OQAM modulation scheme in 5G systems. *Russ. Technol. J*. 2024;12(3):46–54. https://doi.org/10.32362/2500-316X-2024-12-3-46-54

Financial disclosure: The authors have no a financial or property interest in any material or method mentioned.

The authors declare no conflicts of interest.

НАУЧНАЯ СТАТЬЯ

Влияние шумов и помех на вероятность битовых ошибок в системах 5G, использующих банк фильтров с несколькими несущими со смещенной квадратурной амплитудной модуляцией

А. Андрун [@], **О.В. Тихонова**

МИРЭА – Российский технологический университет, Москва, 119454 Россия
[@] *Автор для переписки, e-mail: abed.androon@yandex.com*

Резюме

Цели. Целью работы являются оценка помехоустойчивости метода модуляции сигналов в сетях 5G с использованием банка фильтров с несколькими несущими со смещенной квадратурной амплитудной модуляцией (FBMC-OQAM) и анализ вероятности битовых ошибок.

Методы. В работе применяются методы теории вероятностей и математической статистики, а также методы компьютерного моделирования.

Результаты. Представлен анализ вероятности битовых ошибок метода модуляции сигналов в сетях 5G с использованием банка фильтров с несколькими несущими со смещенной квадратурной амплитудной модуляцией в условиях шумов и исследована устойчивость метода к различным типам помех, таких как внутрисотовые и межсотовые помехи, межлучевые помехи в канале 5G, а также аддитивный белый гауссов шум. Представлены графические и численные данные, полученные компьютерным моделированием, показывающие улучшение вероятности битовых ошибок в сетях 5G, использующих FBMC-OQAM. Проведен сравнительный анализ вероятности ошибки в системе FBMC-OQAM при различных типах шумов и помех, подчеркивающий влияние этих факторов на качество передачи информации.

Выводы. Метод FBMC-OQAM характеризуется малым влиянием на вероятность ошибки системы передачи данных в сетях 5G таких типов помех, как внутрисотовые и межсотовые помехи, межлучевые помехи и нелинейные искажения. В статье подчеркивается необходимость дальнейшей оптимизации и разработки алгоритмов для улучшения вероятность ошибки в системе FBMC-OQAM в реальных условиях сетей 5G. Результаты исследования могут быть использованы при разработке сетей 5G.

Ключевые слова: сеть 5G, метод FBMC-OQAM, белый гауссов шум, вероятность битовой ошибки, отношение сигнал/шум, межсотовые помехи, нелинейные искажения

• **Поступила:** 04.05.2023 • **Доработана:** 18.11.2023 • **Принята к опубликованию:** 12.03.2024

Для цитирования: Андрун А., Тихонова О.В. Влияние шумов и помех на вероятность битовых ошибок в системах 5G, использующих банк фильтров с несколькими несущими со смещенной квадратурной амплитудной модуляцией. *Russ. Technol. J.* 2024;12(3):46–54. https://doi.org/10.32362/2500-316X-2024-12-3-46-54

Прозрачность финансовой деятельности: Авторы не имеют финансовой заинтересованности в представленных материалах или методах.

Авторы заявляют об отсутствии конфликта интересов.

INTRODUCTION

It is widely anticipated that the fifth generation of wireless communication systems, commonly known as 5G, will revolutionize the ways in which people interact. Promising higher data rates, lower latency, and greater bandwidth, the 5G system has the potential to transform a wide range of industries including healthcare, transportation, and manufacturing. However, the success of 5G depends on its ability to operate reliably in different environments including various types of interference and noise. One of the key technologies used in 5G networks to address these challenges is Filter Bank Multicarrier Modulation Offset Quadrature Amplitude Modulation (FBMC-OQAM) [1]. Offset Quadrature Amplitude Modulation (OQAM) represents an approach according to which the in-phase and quadrature components of the signal are staggered, i.e., offset relative to each other. Such offsetting permits more efficient utilization of the available frequency bandwidth, as well as reducing inter-symbol interference and improving robustness to frequency selective fading. FBMC-OQAM offers several advantages over the traditional orthogonal frequency-division channelization method widely used in 4G networks and earlier wireless communication systems. For example, the higher spectral efficiency of the FBMC-OQAM method increases tolerance to interference and noise. However, the error probability of a system using FBMC-OQAM under different types of interference and noise has yet to be fully investigated. Such research should be urgently conducted in order to inform the design of more efficient 5G networks.

In this connection, the present paper aims to analyze the bit error rate (BER) in 5G systems using the FBMC-OQAM method under different types of interference and noise. The analysis results provide information on the error probability of the FBMC-OQAM system in real communication environments to inform the future development of 5G systems.

1. TYPES OF NOISE AND INTERFERENCE IN THE 5G CELLULAR NETWORK

As compared to previous generations of cellular networks, the fifth-generation New Radio (5GNR)[1] system proposed by the 3rd Generation Partnership Project (3GPP) promises improved spectral efficiency, higher bandwidth, increased data rates, and communication reliability [1]. The spectrum resources used in 5G systems and defined in the 3GPP protocol are divided into two frequency bands (FBs): FB1 < 6 GHz and FB2 > 24 GHz (millimeter band) [2].

[1] https://www.3gpp.org/technologies/5g-system-overview. Accessed January 20, 2023.

The FB1 frequency band, which is almost fully occupied, has limited resources for use in 5G networks, while FB2, representing a portion of the available spectrum where the majority of frequencies are not yet occupied, can be easily applied to future cellular networks [3].

Defined as undesirable impacts on the transmitted signal, interference, which typically results in signal modification or distortion, can arise from a variety of sources including neighboring signals, electromagnetic fields, overlapping signals, and obstacles in the signal propagation path [4]. Noise interference refers to a wideband impact on a signal that acts over an extended period of time. In 5G systems, noise (noise interference) can arise from a variety of sources including electronic components and thermal effects. Interference, which degrades the signal quality to reduce bandwidth and cause errors in data transmission [5], is proving to be a major problem in developing new spectral regions and exploiting the existing spectra in modern 5G systems [6].

In a wireless cellular network based around small cells, multi-level interference, which is determined by the specific characteristics of each low-power node, continuously generates and receives unwanted signals from various nearby sources [7]. The most common kinds of interference associated with wireless networks are self-interference, adjacent channel interference, as well as intra-and inter-cell interference. However, the mobile network is not limited to these interferences only. Each network is susceptible to interference that arises depending on the specific scenario of its deployment.

1.1. Intra-cell and inter-cell interference

Inter-cell interference is a significant cause of network degradation. Such interference occurs when users of two neighboring cells are trying to use the same frequency band simultaneously [8]. Moreover, inter-cell interference has a significant impact on user communication quality at cell edges since the user receives signals both from the macro base station of his cell and from the neighboring cell due to frequency reuse (Fig. 1). Distortions caused by additional equipment within the same cell are called inter-cell interference.

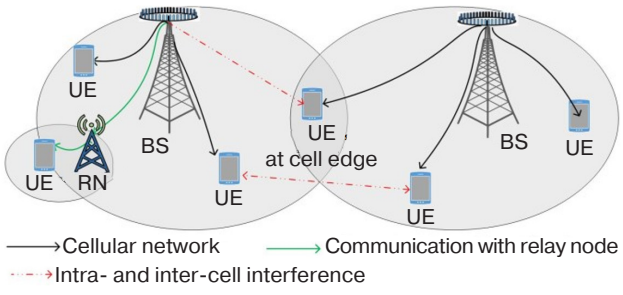

Fig. 1. Intra-cellular and inter-cellular interference. BS is base station, UE is user equipment, RN is relay node

As shown in Fig. 2, inter-channel interference occurs when signals from two or more separate channels interfere with each other (the horizontal axis shows frequency f (Hz), while the vertical axis represents signal strength (dB); f_1 is the center frequency of channel 1; f_2 is the center frequency of channel 2) due to multiple wireless communication devices operating at close range. As a consequence, the stronger signal transmitter interferes with the weaker signal receiver.

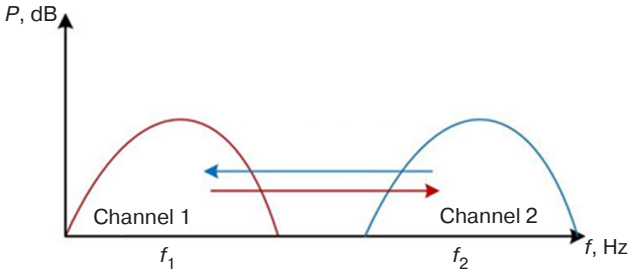

Fig. 2. Inter-channel interference

1.2. Inter-beam interference

Representing a novel technology used in modern cellular communications systems, beamforming defines the best route for providing optimal bandwidth to a certain user in a particular direction. This approach is necessary to compensate for attenuation losses in signal transmission, especially in millimeter wave communications. The base station (BS) generates multiple narrow beams of radio frequency (RF) signals in all directions of the coverage area. The BS and/or mobile terminal antennas are tuned to focus the transmitted signal in a particular direction, forming the so-called "beam" or directional signal [9]. However, the spatial separation of multiple beams results in inter-beam interference [10]. As shown in Fig. 3, this is caused by neighboring BS beams of the same or neighboring cell.

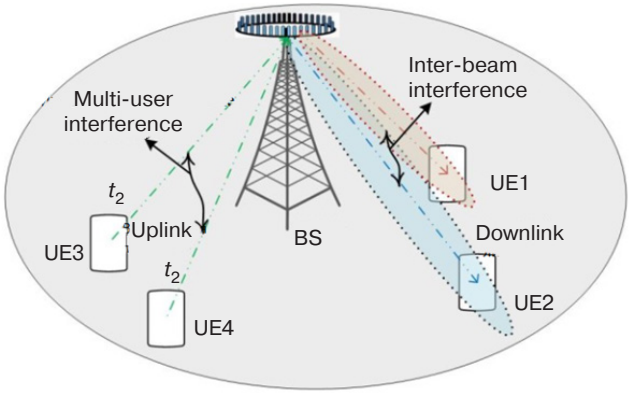

Fig. 3. Inter-beam and multi-user interference; t_2 is data transmission path

1.3. Nonlinear distortion in 5G networks

A common problem in wireless communication systems, including 5G networks, Nonlinear distortion occurs when the transmitted signal is significantly amplified and its power becomes too high, resulting in the amplifier going into nonlinear mode [11]. In this case, the signal is distorted, and information is incorrectly decoded in the receiver.

In 5G networks, nonlinear distortion can occur in transmitter or receiver circuits as a result of multiple factors to affect the characteristics of the transmitted signal [12]. In the frame of FBMC, nonlinear distortion can cause intermodulation distortion. This occurs when transmitted signals mix with each other to generate additional undesired frequencies, resulting in increased interference between subcarriers and leading to increased bit error rates and reduced data transmission efficiency.

The output signal $y(t)$ passed through the nonlinear distortion amplifier can be represented using the Taylor expansion:

$$y(t) = a_0x(t) + a_1x^2(t) + a_2x^3(t), \quad (1)$$

where $x(t)$ is the input signal; a_0 is the linear gain of the power amplifier; a_1 and a_2 are coefficients at the nonlinear terms of the expansion.

1.4. Noise interference

The error probability in the communication channel depends on the noise level. Additive white Gaussian noise (AWGN) comes from many natural sources ranging from the motion of atoms in a conductor to radiation emitted by the earth and space objects. The linear and time independent AWGN channel, which is well suited for wireless communication, allows modulated signals to pass through it without any amplitude loss or phase distortion [13]. The output signal of the channel may be defined as follows:

$$y(t) = x(t) + n(t), \quad (2)$$

where summand $n(t)$ is the noise having the Gaussian distribution with zero mean and variance as the noise power; $x(t)$ is the transmitted signal.

The AWGN channel can be used by designers to evaluate the impact of various factors on the error probability in the system, in particular, to evaluate the impact of modulation schemes, channel coding techniques, and error correction algorithms [14], as well as physical layer parameters such as carrier frequency, bandwidth, and transmitted power.

2. BER AND SIGNAL-TO-NOISE RATIO

Representing the accuracy of digital data transmission in a communication system, the bit error rate is defined as the ratio of the number of bits received with an error to the total number of bits transmitted over the communication channel. It can be expressed as a percentage or decimal. Meanwhile, the bit error rate defines the probability that a bit in the transmitted signal will be received with an error. The BER value can be affected by various factors such as noise, interference, modulation scheme, and transmission range.

An important parameter determining the performance of a communication system is the signal-to-noise ratio (SNR), typically expressed in decibels, as follows:

$$\mathrm{SNR} = 10 \lg \frac{P_\mathrm{s}}{P_\mathrm{n}}, \quad (3)$$

where P_s is the signal power; P_n is the noise power.

In practical terms, a high SNR value is preferable for any communication system due to providing higher accuracy and reliability of information transmission. On the other hand, a low SNR value may cause errors in the transmitted data, thus resulting in the reduced quality of the communication system.

3. SIMULATION AND ANALYSIS RESULTS

The present paper continues analysis of the model presented in previously published research [15, 16].

The model consists of a transmitter and a receiver of FBMC-OQAM signal, according to which the signal itself is simulated along with various perturbances: white Gaussian noise, spurious components of adjacent channels, intra-cell and inter-cell interference, inter-beam interference, and nonlinear distortion. By simulating the division of the signal into multiple subcarriers, each with its own narrowband filter, the model promotes efficient frequency utilization and high spectral efficiency. The offset quadrature modulation is used, where each subcarrier is split into two parallel streams: in-phase (I) and quadrature (Q). This permits a reduction in the inter-symbol interference caused by overlapping neighboring subcarriers. Using this model, numerical estimates for BER as a function of SNR can be obtained for different conditions.

New results obtained using the described model and its further analysis—in particular, investigating the impact of different noise and interference in 5G networks—are hereby presented.

The system is capable of processing I-data and Q-data of different sizes and different lengths of Fast Fourier Transform (FFT). Experiments are conducted using different combinations of parameters to demonstrate the adaptability of the system to different conditions.

For model verification, the experimentally obtained BER are compared with the known BER derived theoretically under identical AWGN channel conditions. The BER dependence on SNR for FBMC-OQAM system, obtained via a simulation for verifying the model's efficiency, is shown in Fig. 4 [17].

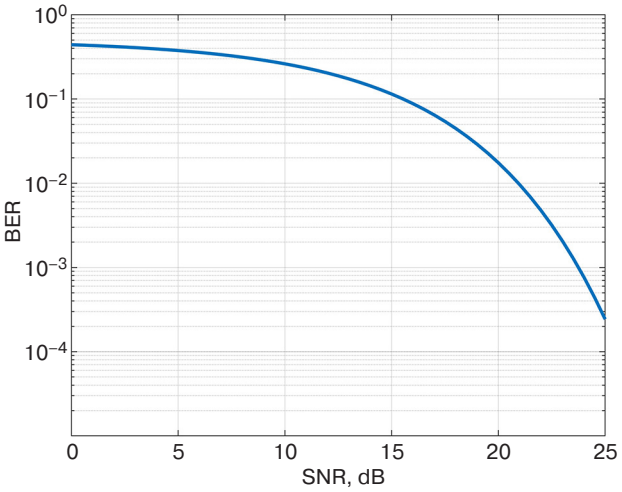

Fig. 4. BER on SNR dependence obtained through simulation

Simulation results are obtained at parameters given in the Table below.

Table. Model parameters

Number of subcarriers	2048
I/Q data size	$N = 64, 32, 16$
Data frame length	1
FFT size	8192, 4096, 2048, 512
Filter type	Prototype filter used in FBMC-OQAM
Overlap coefficient	$K = 4$
Channel model	Randomized initial sequence
Noise type	AWGN
Interference type	Interference from other cellular communication systems, nonlinear distortion, inter-cell interference
SNR range	From −10 dB to 30 dB

The error probability of the system is studied for a 512-point, 2048-point, 4096-point, and 8192-point FFT. The system uses matched filtering with overlapping coefficient K representing the number of multicarrier symbols overlapped on the time interval. The impact of changing the symbol length is analyzed for a 512-point, 1024-point, and 2048-point FFT. The results show that changing the symbol length has almost no impact on the error probability in FBMC-OQAM system.

From the results (Fig. 5) for $N = 64$, it can be seen that when the FFT length is reduced, the SNR required to achieve BER value equal to 10^{-6} increases. In particular, for an 8192-point FFT, SNR = 6 dB is required to achieve the desired BER value, while for 4096-point, 2048-point, and 512-point FFTs, the required SNR values are 7.8, 12, and 20 dB, respectively. This means that longer FFT length provides better BER at lower SNR values. Thus, increasing FFT length may be a useful strategy for reducing error probability.

Simulation results for $N = 32$ with different FFT lengths are shown in Fig. 6. It can be seen that, upon reduction of FFT length, the SNR required to achieve a BER value equal to 10^{-6} increases. In particular, for an 8192-point FFT, SNR = 1.5 dB is required for the system to achieve the desired BER value, while for 4096-point,

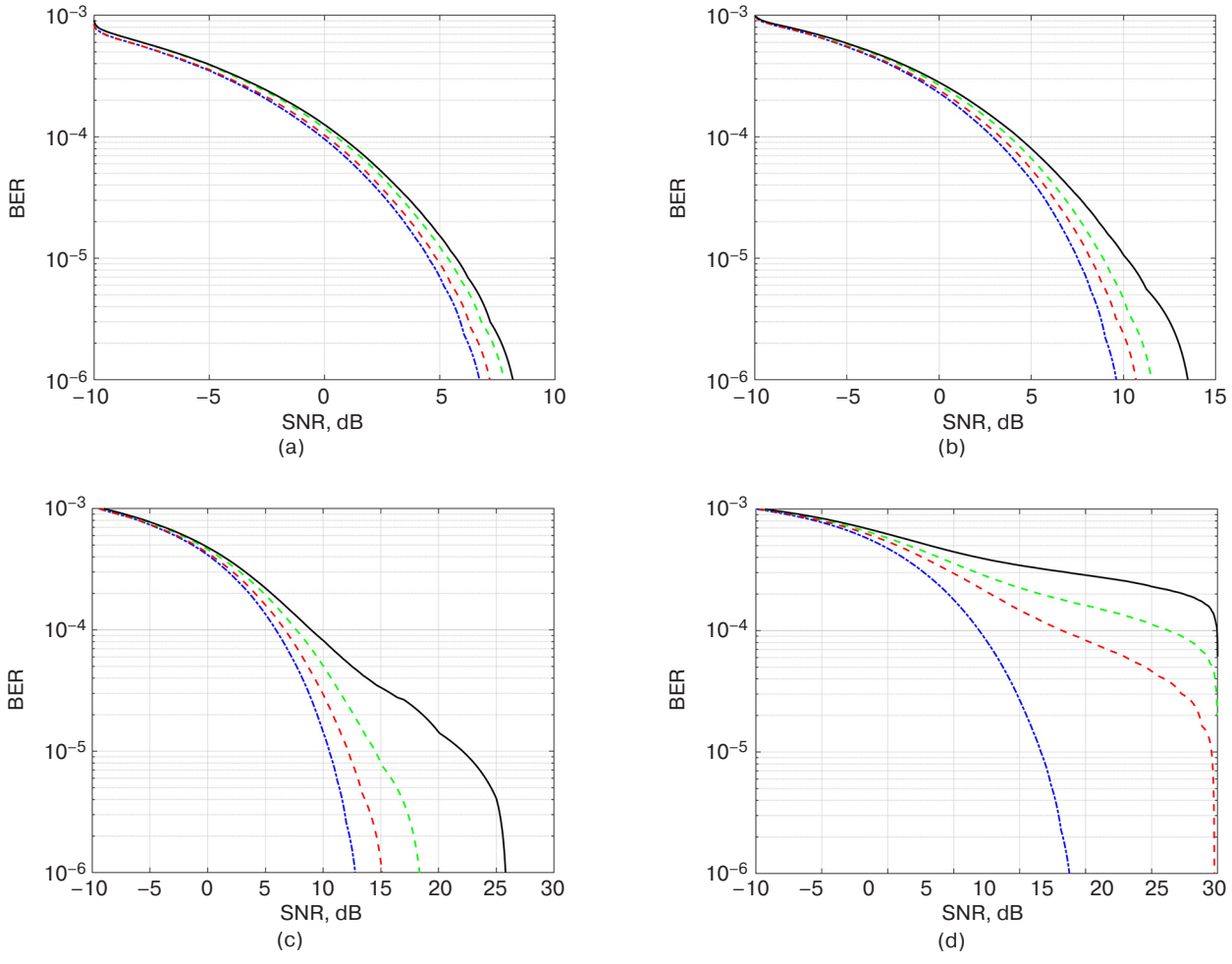

Fig. 5. Simulation results for $N = 64$ and FFT length:
(a) 8192,
(b) 4096,
(c) 2048,
and (d) 512

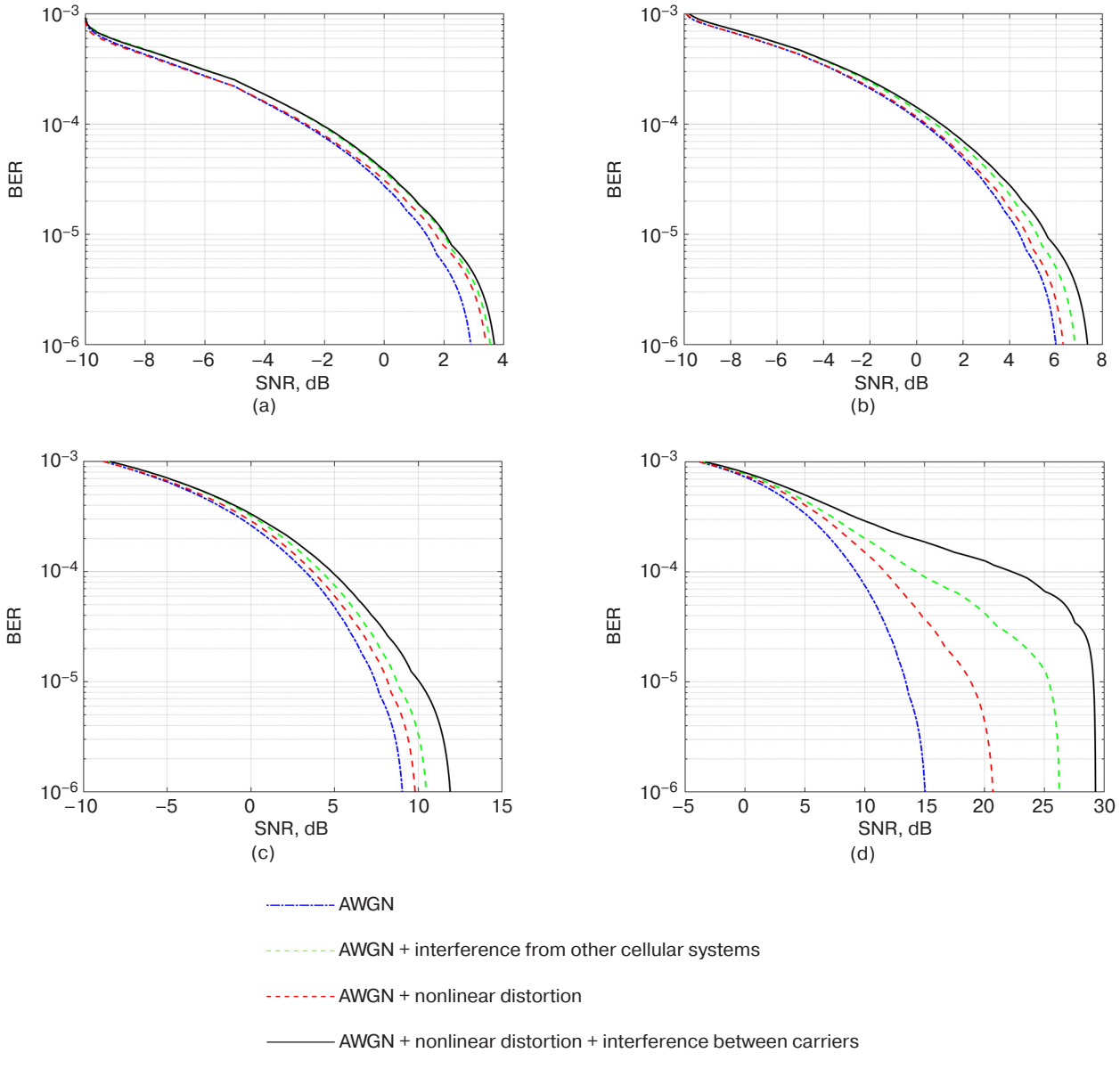

Fig. 6. Simulation results for $N = 32$ and FFT length:
(a) 8192,
(b) 4096,
(c) 2048,
and (d) 512

2048-point, and 512-point FFTs, the required SNR values are 5, 8, and 14 dB, respectively. Hence, even in this case, increasing the FFT length may be a useful strategy for reducing error probability.

It can be observed from Fig. 7 that the trend of increasing the required SNR to achieve the same BER level for $N = 16$ becomes even more noticeable as the FFT length decreases. The same dependence can be observed in Figs. 5 and 6. Here, it can be seen that BER decreases with SNR increasing for all FFT lengths. In addition, the system with the longest FFT length equal to 8192 has a low BER, requiring the highest SNR to achieve BER equal to 10^{-6}. On the other hand, the system with the minimal FFT length of 512 has the best BER, requiring the lowest SNR to achieve the same BER value. Systems with FFT lengths of 4096 and 2048 have similar error probabilities, the former requiring a slightly higher SNR to achieve the same BER. Hence, it can be concluded from these results that, for a system with fixed $N = 16$, smaller FFT lengths result in better BER at higher SNR levels, while greater FFT lengths require a higher SNR to achieve the same BER. This emphasizes the importance of selecting the appropriate FFT length in the system.

CONCLUSIONS

Simulation results verify high resistance of FBMC-OQAM modulation method in 5G networks

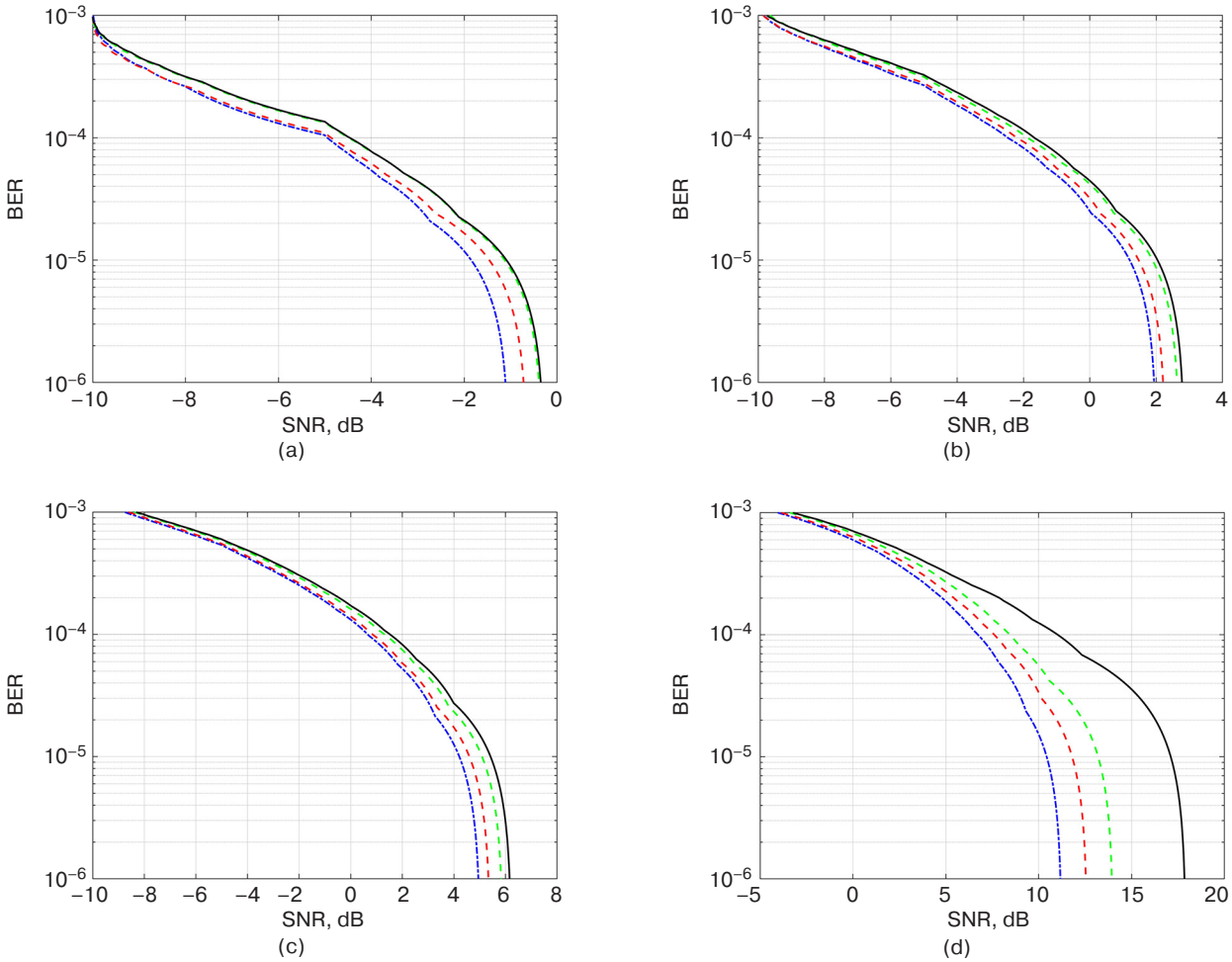

Fig. 7. Simulation results for $N = 16$ and FFT length:
(a) 8192,
(b) 4096,
(c) 2048,
and (d) 512

to various types of interference, thus significantly improving communication quality. Increasing the FFT length effectively reduces the probability of data transmission errors, while the optimal choice of the FFT length depends on specific conditions of 5G networks.

Authors' contribution. All authors equally contributed to the research work.

REFERENCES

1. Qamar F., Hindia M.N., Abbas T., Dimyati K.B., Amiri I.S. Investigation of QoS performance evaluation over 5G network for indoor environment at millimeter wave bands. *Int. J. Electron. Telecommun*. 2019;65(1):95–101.
2. Sanfilippo G., Galinina O., Andreev S., Pizzi S., Araniti G. A concise review of 5G new radio capabilities for directional access at mmWave frequencies. In: Galinina O., Andreev S., Balandin S., Koucheryavy Y. (Eds.). *Internet of Things, Smart Spaces, and Next Generation Networks and Systems. NEW2AN ruSMART 2018. Lecture Notes in Computer Science.* 2018. P. 340–354. Correction: https://doi.org/10.1007/978-3-030-01168-0_65

3. Dilli R. Analysis of 5G Wireless Systems in FR1 and FR2 Frequency Bands. In: *2020 2nd International Conference on Innovative Mechanisms for Industry Applications* (*ICIMIA*). 2020. IEEE. P. 767–772. https://doi.org/10.1109/ICIMIA48430.2020.9074973
4. Rebato M., Mezzavilla M., Rangan S., Boccardi F., Zorzi M. Understanding noise and interference regimes in 5G millimeter wave cellular networks. In: *European Wireless 2016; 22th European Wireless Conference*. 2016; VDE. P. 84–88. https://doi.org/10.48550/arXiv.1604.05622
5. Liu J., Sheng M., Liu L., Li J. Effect of densification on cellular network performance with bounded pathloss model. *IEEE Communications Letters*. 2016;21(2):346–349. https://doi.org/10.1109/LCOMM.2016.2615298
6. Liu J., Sheng M., Liu L., Li J. Interference management in ultra-dense networks: Challenges and approaches. *IEEE Network*. 2017;31(6):70–77. https://doi.org/10.1109/MNET.2017.1700052
7. Shende N., Gurbuz O., Erkip E. Half-duplex or full-duplex relaying: A capacity analysis under self-interference. In: *2013 47th Annual Conference on Information Sciences and Systems* (*CISS*). 2013; IEEE, 6 p. https://doi.org/10.1109/CISS.2013.6552276
8. Qamar F., Dimyati K.B., Hindia M.N., Noordin K.A.B., Al-Samman A.M. A comprehensive review on coordinated multipoint operation for LTE-A. *Computer Networks*. 2017;123:19–37. https://doi.org/10.1016/j.comnet.2017.05.003
9. Guo Z., Fei Y. On the Cross Link Interference of 5G with Flexible Duplex and Full Duplex. In: *2020 IEEE Wireless Communications and Networking Conference Workshops* (*WCNCW*). 2020; IEEE. 4 p. https://doi.org/10.1109/WCNCW48565.2020.9124866
10. Xue Q., Li B., Zuo X., Yan Z., Yang M. Cell capacity for 5G cellular network with inter-beam interference. In: *2016 IEEE International Conference on Signal Processing, Communications and Computing* (*ICSPCC*). 2016; IEEE. 5 p. https://doi.org/10.1109/ICSPCC.2016.7753608
11. El Ghzaoui M., Hmamou A., Foshi J., Mestoui J. Compensation of non-linear distortion effects in MIMO-OFDM systems using constant envelope OFDM for 5G applications. *J. Circuits, Syst. Comput.* 2020;29(16):2050257. https://doi.org/10.1142/S0218126620502576
12. Mathews A.B., Mathews A.B., Kumar C.A. A Non-Linear Improved CNN Equalizer with Batch Gradient Decent in 5G Wireless Optical Communication. *IETE Journal of Research.* 2023. P. 1–13. https://doi.org/10.1080/03772063.2022.2163930
13. Kaur N., Kansal L. Performance Comparison of MIMO Systems over AWGN and Rician Channels with Zero Forcing Receivers. *International Journal of Wireless & Mobile Networks* (*IJWMN*). 2013;5(1):73–84. http://doi.org/10.5121/ijwmn.2013.5106
14. Mezher M., AlAbbas A.R. BER performance of Reed-Solomon codes with 16 PSK modulation over *in-vivo* radio channel. In: *Proc. International Conference on Electrical, Computer and Energy Technologies* (*ICECET*). 2022; IEEE. 6 p. https://doi.org/10.1109/ICECET55527.2022.9873485
15. Androon A., Tikhonova O.V. Digital data conversion for transmission over 5G networks. In: *Actual Problems and Prospects for the Development of Radio Engineering and Infocommunication Systems Radioinfocom 2021: Collection of scientific articles of the 5th International Scientific and Practical Conference*. Moscow: RTU MIREA; 2021. P. 22–26 (in Russ.).
16. Androon A., Tikhonova O.V. Signal processing method in modern wireless networks 5G. *Voprosy elektromekhaniki. Trudy VNIIEM = Electromechanical Matters. VNIIEM Studies.* 2023;192(1):21–26 (in Russ.).
17. Kumar A., Bharti S. Design and performance analysis of OFDM and FBMC modulation techniques. *The Scientific Bulletin of Electrical Engineering Faculty*. 2017;17(2):30–34. https://doi.org/10.1515/sbeef-2017-0007

About the authors

Abed Androon, Postgraduate Student, Department of Radio Electronic Systems and Complexes, Institute of Radio Electronics and Informatics, MIREA – Russian Technological University (78, Vernadskogo pr., Moscow, 119454 Russia). E-mail: abed.androon@yandex.com. https://orcid.org/0000-0001-9624-2060

Olga V. Tikhonova, Dr. Sci. (Eng.), Senior Researcher, Professor, Department of Radio Electronic Systems and Complexes, Institute of Radio Electronics and Informatics, MIREA – Russian Technological University (78, Vernadskogo pr., Moscow, 119454 Russia). E-mail: o_tikhonova@inbox.ru. Scopus Author ID 57208923772, RSCI SPIN-code 3362-9924, https://orcid.org/0009-0009-4013-9182

Об авторах

Андрун Абед, аспирант, кафедра радиоэлектронных систем и комплексов, Институт радиоэлектроники и информатики ФГБОУ ВО «МИРЭА – Российский технологический университет» (119454, Россия, Москва, пр-т Вернадского, д. 78). E-mail: abed.androon@yandex.com. https://orcid.org/0000-0001-9624-2060

Тихонова Ольга Вадимовна, д.т.н., старший научный сотрудник, профессор, кафедра радиоэлектронных систем и комплексов, Институт радиоэлектроники и информатики ФГБОУ ВО «МИРЭА – Российский технологический университет» (119454, Россия, Москва, пр-т Вернадского, д. 78). E-mail: o_tikhonova@inbox.ru. Scopus Author ID 57208923772, SPIN-код РИНЦ 3362-9924, https://orcid.org/0009-0009-4013-9182

Translated from Russian into English by K. Nazarov
Edited for English language and spelling by Thomas A. Beavitt

Micro- and nanoelectronics. Condensed matter physics

Микро- и наноэлектроника. Физика конденсированного состояния

UDC 537.632
https://doi.org/10.32362/2500-316X-2024-12-3-55-64
EDN SWVVUI

RESEARCH ARTICLE

Modeling of the magnetorefractive effect in Co-Al_2O_3 nanocomposites in the framework of the Bruggeman approximation

Muza A. Mukhutdinova,
Alexey N. Yurasov @

MIREA – Russian Technological University, Moscow, 119454 Russia
@ *Corresponding author, e-mail: alexey_yurasov@mail.ru*

Abstract

Objectives. To investigate the magnetorefractive effect (MRE) in nanocomposites, which consists in changing the reflection, transmittance and light absorption coefficients of samples with large magnetoresistance (MR) upon their magnetization. Materials offering high magneto-optical activity and significant MR include magnetic nanocomposites. These materials are based on a polymer matrix, which includes inorganic magnetic particles, fibers or layered particles, whose nanometer sizes range from 1 to 100 nm in at least one dimension. The main purpose of creating such nanocomposites is to combine the special properties of several components in one material. The presence in such materials of gigantic, colossal and tunneling MR, as well as the giant anomalous Hall effect, is of practical interest. Uses range from magnetic recording, light modulation, and receivers for thermal radiation, while the MRE itself is a promising method for the non-destructive testing of any nanostructures, e.g., measuring MR.

Methods. The use of effective medium theory to describe the optics and magneto-optics of dispersed media provides a means to determine the complex permittivity of a medium through the permittivity of its constituent components or vice versa. The present work considers the example of a Co-Al_2O_3 nanocomposite with a concentration of ferromagnetic metal Co 0.4 near the percolation threshold. This particular case was considered for study, since all the properties of nanocomposites change dramatically near the percolation threshold.

Results. Using the Bruggeman effective medium approximation (EMA) to describe the optical and magneto-optical properties of nanocomposites on the example of Co-Al_2O_3, the characteristics of MRE are obtained, namely, the change in MRE for reflection and transmission of light at normal incidence and at the angle of incidence near the Brewster angle (below the percolation threshold) or the main angle of incidence for metals (above the percolation threshold), which enhances MRE. The advantage of the EMA is the ability to study magneto-optical spectra in the range of average volume concentrations of the metal component.

Conclusions. The obtained values correspond well to the known experimental data. Moreover, the described approach can be used to study any nanostructures.

Keywords: magnetorefractive effect, nanocomposites, magnetoresistance, dielectric permittivity tensor, Bruggeman approximation

• **Submitted:** 16.05.2023 • **Revised:** 16.10.2023 • **Accepted:** 08.04.2024

For citation: Mukhutdinova M.A., Yurasov A.N. Modeling of the magnetorefractive effect in Co-Al_2O_3 nanocomposites in the framework of the Bruggeman approximation. *Russ. Technol. J.* 2024;12(3):55–64. https://doi.org/10.32362/2500-316X-2024-12-3-55-64

Financial disclosure: The authors have no a financial or property interest in any material or method mentioned.

The authors declare no conflicts of interest.

НАУЧНАЯ СТАТЬЯ

Моделирование магниторефрактивного эффекта в нанокомпозитах Co-Al_2O_3 в рамках приближения Бруггемана

М.А. Мухутдинова,
А.Н. Юрасов @

МИРЭА – Российский технологический университет, Москва, 119454 Россия
@ *Автор для переписки, e-mail: alexey_yurasov@mail.ru*

Резюме

Цели. Цель работы – изучить магниторефрактивный эффект (МРЭ) в нанокомпозитах, заключающийся в изменении коэффициентов отражения, пропускания и поглощения света образцов с большим магнитосопротивлением (МС) при их намагничивании. Существует ряд материалов, обладающих большой магнитооптической активностью и значительным МС. К таким материалам относятся магнитные нанокомпозиты. Они представляют из себя материалы на основе полимерной матрицы, в которую включены неорганические магнитные частицы, волокна или слоистые частицы, с нанометровыми размерами от 1 до 100 нм хотя бы в одном измерении. Главной целью создания таких нанокомпозитов является совмещение нескольких компонентов с их особыми свойствами в одном материале. Наличие в таких материалах гигантского, колоссального и туннельного МС, гигантского аномального эффекта Холла представляет практический интерес. Данные материалы применяют для магнитной записи, модуляции света, как приемники теплового излучения, а сам МРЭ является перспективным методом неразрушающего контроля любых наноструктур, например, для измерения МС.

Методы. Для описания оптики и магнитооптики дисперсных сред рассмотрена теория эффективной среды, благодаря которой можно решить задачу определения комплексной диэлектрической проницаемости среды через диэлектрические проницаемости составляющих ее компонент или наоборот. В статье этот подход рассматривался на примере нанокомпозита Co-Al_2O_3 с концентрацией ферромагнитного металла Co, равной 0.4, вблизи порога перколяции. Для изучения рассмотрен именно этот случай, т.к. вблизи порога перколяции кардинально меняются все свойства нанокомпозитов.

Результаты. Используя приближение Бруггемана (effective medium approximation, EMA) для описания оптических и магнитооптических свойств нанокомпозитов на примере Co-Al_2O_3, авторы получили характеристики МРЭ, а именно: изменение МРЭ на отражение и пропускание света при нормальном падении и при угле падения вблизи угла Брюстера (ниже порога перколяции) или главного угла падения для металлов (выше порога перколяции), что усиливает МРЭ. Преимущество EMA заключается в возможности исследовать магнитооптические спектры в диапазоне средних объемных концентраций металлической компоненты.

Выводы. Полученные значения хорошо соответствуют известным экспериментальным данным. Важно отметить, что данный подход позволяет исследовать любые наноструктуры.

Ключевые слова: магниторефрактивный эффект, нанокомпозиты, магнитосопротивление, тензор диэлектрической проницаемости, приближение Бруггемана

• **Поступила:** 16.05.2023 • **Доработана:** 16.10.2023 • **Принята к опубликованию:** 08.04.2024

Для цитирования: Мухутдинова М.А., Юрасов А.Н. Моделирование магниторефрактивного эффекта в нанокомпозитах Co-Al_2O_3 в рамках приближения Бруггемана. *Russ. Technol. J.* 2024;12(3):55–64. https://doi.org/10.32362/2500-316X-2024-12-3-55-64

Прозрачность финансовой деятельности: Авторы не имеют финансовой заинтересованности в представленных материалах или методах.

Авторы заявляют об отсутствии конфликта интересов.

INTRODUCTION

The magnetorefractive effect (MRE) describes changes in the reflection $R\left(\frac{\Delta R}{R}\right)$, transmission $T\left(\frac{\Delta T}{T}\right)$ and absorption A coefficients of light in samples with large magnetoresistance (MR) when they are magnetized [1].

Nanocomposites are promising multiphase materials obtained by introducing nanoparticles having geometric particle sizes ranging from 1 to 100 nm into the matrix of a base material [1]. Nanocomposites have a significant MR $\frac{\Delta\rho}{\rho}$, where ρ is the electrical resistance. Significant opportunities are opened by the application of nanocomposites in the field of magneto-optics (MO), which studies the phenomena arising in the magnetic field as a result of the interaction of optical radiation with matter. For example, nanocomposites are used to measure MR. Magnetic nanocomposites, representing heterogeneous magnetics in which ferromagnetic particles are placed in a metal or dielectric matrix, are also used for magnetic recording, light modulation, and as receivers of thermal radiation [1–7]. In turn, MO methods are methods of nondestructive testing of any nanostructures [1, 2].

The purpose of the present work is to investigate MREs in nanocomposites near the percolation threshold.

CALCULATION METHODOLOGY

Under the influence of magnetic field, the dispersion curves of refractive index n and absorption coefficient k, leading to the appearance or change of optical anisotropy of the medium. When MR changes, the value of reflection and transmittance coefficients changes. The reflection coefficient (Fresnel formulae) at normal incidence has the form:

$$R = \frac{(1-n)^2 + k^2}{(1+n)^2 + k^2}, \quad (1)$$

where n is the refraction coefficient, and k is the extinction coefficient of the nanocomposite [1].

Formula (1) is used to calculate the value of $\frac{\Delta R}{R}$ [2]:

$$\frac{\Delta R}{R} = -(1-R)\cdot\frac{\Delta\rho}{\rho}\cdot k^2 \times \times \frac{3n^2 - k^2 - 1}{(n^2+k^2)((1-n)^2+k^2)}\cdot 100\%. \quad (2)$$

At an angle of incidence different from zero, the reflection coefficient for a semi-infinite medium is calculated by the following formulas:

$$R = |r_{12}|^2, \quad (3)$$

$$r_{12} = \frac{g_1\eta_2^2 - g_2 n_1^2}{g_1\eta_2^2 + g_2 n_1^2}, \quad (4)$$

where $g_1 = \sqrt{n_1 - n_1(\sin\varphi_0)^2}$, $g_2 = \sqrt{\eta_2 - n_2(\sin\varphi_0)^2}$, φ_0 is the angle of incidence of light on the nanocomposite surface, $\eta_2 = n_2 - k_2 i$ is the complex refractive index of the nanocomposite, and n_1 is the refractive index of the medium from which the light is incident [2].

For the transmittance at normal incidence of light we have [2]:

$$T = |t_{12}|^2, \quad (5)$$

$$t_{12} = \frac{g_1 2\eta_2}{g_1\eta_2^2 + g_2 n_1^2}, \quad (6)$$

$$\frac{\Delta T}{T} = \frac{1}{2}\cdot\frac{\Delta\rho}{\rho}\cdot Tk^2\cdot\left(\frac{2n^2+n}{n^2+k^2}\right)\cdot 100\%. \quad (7)$$

The effective dielectric permittivity tensor (DPT) is considered to describe the electrical, optical and magnetic properties of are complex nanocomposite materials:

$$\tilde{\varepsilon}^{\text{eff}} = \begin{pmatrix} \varepsilon_{xx}^{\text{eff}} & i\gamma^{\text{eff}} & 0 \\ -i\gamma^{\text{eff}} & \varepsilon_{xx}^{\text{eff}} & 0 \\ 0 & 0 & \varepsilon_{xx}^{\text{eff}} \end{pmatrix}, \quad (8)$$

where diagonal components $\varepsilon_{xx}^{\text{eff}} = (\varepsilon_{xx}^{\text{eff}})' - i(\varepsilon_{xx}^{\text{eff}})''$ are the optical constituent, while the non-diagonal components $\gamma^{\text{eff}} = (\gamma^{\text{eff}})' - i(\gamma^{\text{eff}})''$ are the MO constituent of the DPT [4–8].

The most interesting case arises when the nanocomposite is near the percolation threshold, since a significant enhancement of MO effects occurs in this region. In this connection, all calculations were performed when the volume concentration X = 0.4, which corresponds to the proximity to the percolation threshold.

Let us use the Bruggeman effective medium approximation (EMA) at $0.3 < X < 0.7$, which works well for describing nanocomposites at an average concentration of magnetic (metallic) component [7–10].

In order to find ε^{eff} and γ^{eff}, we use the following equations:

$$\begin{gathered} X\frac{(\varepsilon_1-\varepsilon^{\text{EMA}})}{\varepsilon^{\text{EMA}}+(\varepsilon_1-\varepsilon^{\text{EMA}})L_{xx}}+ \\ +(1-X)\frac{(\varepsilon_0-\varepsilon^{\text{EMA}})}{\varepsilon^{\text{EMA}}+(\varepsilon_0-\varepsilon^{\text{EMA}})L_{xx}}=0, \\ X\frac{(\gamma^{\text{EMA}}-\gamma)}{\left[\varepsilon^{\text{EMA}}+(\varepsilon_1-\varepsilon^{\text{EMA}})L_{xx}\right]^2}+ \\ +(1-X)\frac{\gamma^{\text{EMA}}}{\left[\varepsilon^{\text{EMA}}+(\varepsilon_0-\varepsilon^{\text{EMA}})L_{xx}\right]^2}=0, \end{gathered} \tag{9}$$

where $\varepsilon^{\text{EMA}} = \varepsilon^{\text{eff}}$, $\gamma^{\text{EMA}} = \gamma^{\text{eff}}$, $L_{xx} = \frac{1-L}{2} = \frac{1-\frac{1}{3}}{2} = \frac{1}{3}$ is the particle form factor $\left(L = \frac{1}{3} \text{ for spherical particles}\right)$, $\varepsilon_0 = \varepsilon_0' - i\varepsilon_0''$ is the dielectric permittivity of the nonmetallic (non-ferromagnetic) component, $\varepsilon_1 = \varepsilon_1' - i\varepsilon_1''$ is the dielectric permittivity for the ferromagnetic component (the diagonal part of the corresponding DPT), $\gamma = \gamma' - i\gamma''$ is the non-diagonal component of the DPT of the ferromagnetic component [2].

CALCULATION RESULTS

We calculated the absolute values of the reflection $\frac{\Delta R}{R}$ and transmission $\frac{\Delta T}{T}$ MRE at incidence angles of $\varphi_1 = 0°$ and $\varphi_2 = 70°$, as well as the effective DPT at different wavelengths of the infrared (IR) range (from 0.8 to 10 μm) incidence on the surface of Co-Al_2O_3. If the nanocomposite is in a state below the percolation threshold, the choice of the angle $\varphi_2 = 70°$ is conditioned by its proximity to the Brewster angle, while, if the nanocomposite is in a state above the percolation threshold, the angle is determined by its proximity to the main angle of incidence for metals, which also enhances optical effects.

The results of calculations are given in Tables 1–6. Here E is the energy of the incident electromagnetic wave.

Table 1. Absolute values of reflection coefficients $\frac{\Delta R}{R}$ at normal light incidence $\frac{\Delta\rho}{\rho} = 1\%$

E, eV	λ, μm	$n_{1(Al_2O_3)}$	$n_{2(Co)}$	$k_{2(Co)}$	$\frac{\Delta R}{R}$, %		
					$\varphi_1 = 0°$		
					$\frac{\Delta\rho}{\rho} = 1\%$	$\frac{\Delta\rho}{\rho} = 5\%$	$\frac{\Delta\rho}{\rho} = 10\%$
1.550	0.8	1.76	1.90	4.95	0.117	0.583	1.167
1.240	1	1.76	2.20	5.50	0.099	0.495	0.989
0.620	2	1.74	5.15	7.00	−0.069	−0.344	−0.687
0.413	3	1.71	4.90	8.45	0.0006	0.003	0.006
0.310	4	1.68	4.70	11.00	0.043	0.214	0.429
0.248	5	1.62	4.70	14.70	0.045	0.225	0.450
0.207	6	1.56	5.00	17.50	0.039	0.195	0.389
0.177	7	1.46	5.40	20.90	0.033	0.163	0.325
0.155	8	1.32	5.80	24.00	0.028	0.140	0.280
0.138	9	1.15	6.56	27.20	0.025	0.123	0.247
0.124	10	0.85	7.10	29.50	0.023	0.114	0.228

Table 2. Absolute values of reflection coefficients $\frac{\Delta R}{R}$ at light incidence at the angle of 70°

E, eV	λ, μm	$n_{1(Al_2O_3)}$	$n_{2(Co)}$	$k_{2(Co)}$	$\frac{\Delta R}{R}$, %		
					$\varphi_2 = 70°$		
					$\frac{\Delta\rho}{\rho} = 1\%$	$\frac{\Delta\rho}{\rho} = 5\%$	$\frac{\Delta\rho}{\rho} = 10\%$
1.550	0.8	1.76	1.90	4.95	−0.277	−1.383	−2.767
1.240	1	1.76	2.20	5.50	−0.281	−1.406	−2.811
0.620	2	1.74	5.15	7.00	−0.351	−1.756	−3.512
0.413	3	1.71	4.90	8.45	−0.300	−1.500	−3.001
0.310	4	1.68	4.70	11.00	−0.226	−1.131	−2.262
0.248	5	1.62	4.70	14.70	−0.154	−0.771	−1.541
0.207	6	1.56	5.00	17.50	−0.122	−0.612	−1.224
0.177	7	1.46	5.40	20.90	−0.095	−0.473	−0.947
0.155	8	1.32	5.80	24.00	−0.076	−0.379	−0.758
0.138	9	1.15	6.56	27.20	−0.064	−0.322	−0.645
0.124	10	0.85	7.10	29.50	−0.059	−0.294	−0.588

Table 3. Absolute values of transmittance coefficients $\frac{\Delta T}{T}$ at normal light incidence

E, eV	λ, μm	$n_{1(Al_2O_3)}$	$n_{2(Co)}$	$k_{2(Co)}$	$\frac{\Delta T}{T}$, %		
					$\varphi_1 = 0°$		
					$\frac{\Delta\rho}{\rho} = 1\%$	$\frac{\Delta\rho}{\rho} = 5\%$	$\frac{\Delta\rho}{\rho} = 10\%$
1.550	0.8	1.76	1.90	4.95	1.378	6.888	13.777
1.240	1	1.76	2.20	5.50	1.513	7.567	15.134
0.620	2	1.74	5.15	7.00	1.763	8.817	17.635
0.413	3	1.71	4.90	8.45	2.023	10.114	20.228
0.310	4	1.68	4.70	11.00	2.211	11.053	22.107
0.248	5	1.62	4.70	14.70	2.243	11.213	22.427
0.207	6	1.56	5.00	17.50	2.269	11.347	22.694
0.177	7	1.46	5.40	20.90	2.298	11.491	22.982
0.155	8	1.32	5.80	24.00	2.331	11.653	23.306
0.138	9	1.15	6.56	27.20	2.442	12.208	24.416
0.124	10	0.85	7.10	29.50	2.518	12.591	25.182

Table 4. Absolute values of transmittance coefficients $\frac{\Delta T}{T}$ at light incidence at the angle of 70°

E, eV	λ, μm	$n_{1(Al_2O_3)}$	$n_{2(Co)}$	$k_{2(Co)}$	$\frac{\Delta T}{T}$, %		
					$\varphi_2 = 70°$		
					$\frac{\Delta\rho}{\rho} = 1\%$	$\frac{\Delta\rho}{\rho} = 5\%$	$\frac{\Delta\rho}{\rho} = 10\%$
1.550	0.8	1.76	1.90	4.95	−0.026	−0.128	−0.255
1.240	1	1.76	2.20	5.50	−0.023	−0.114	−0.228
0.620	2	1.74	5.15	7.00	−0.013	−0.064	−0.129
0.413	3	1.71	4.90	8.45	−0.012	−0.058	−0.117
0.310	4	1.68	4.70	11.00	−0.009	−0.047	−0.093
0.248	5	1.62	4.70	14.70	−0.007	−0.033	−0.065
0.207	6	1.56	5.00	17.50	−0.005	−0.025	−0.050
0.177	7	1.46	5.40	20.90	−0.004	−0.019	−0.038
0.155	8	1.32	5.80	24.00	−0.003	−0.015	−0.030
0.138	9	1.15	6.56	27.20	−0.002	−0.012	−0.024
0.124	10	0.85	7.10	29.50	−0.002	−0.010	−0.021

Table 5. Spectral values of ε^{EMA} at the different values of λ calculated via the coefficients n and k

E, eV	λ, μm	$n_{1(Al_2O_3)}$	$n_{2(Co)}$	$k_{2(Co)}$	ε_1	ε_0	ε^{eff}
0.539	2.30	1.73	5.15	7.27	$-26.330 - 74.881i$	2.993	$5.018 - 13.031i$
0.729	1.70	1.74	4.6	6.70	$-23.730 - 61.640i$	3.028	$4.666 - 11.622i$
1.000	1.24	1.75	3.2	6.10	$-26.970 - 39.040i$	3.063	$2.975 - 9.599i$
1.253	0.99	1.76	2.94	5.50	$-21.606 - 32.340i$	3.098	$3.033 - 8.558i$
1.494	0.83	1.76	2.53	4.95	$-18.102 - 25.047i$	3.098	$2.762 - 7.487i$
1.797	0.69	1.76	2.31	4.45	$-14.466 - 20.559i$	3.098	$2.712 - 6.634i$
2.000	0.62	1.77	2.19	4.11	$-12.096 - 18.002i$	3.133	$2.729 - 6.108i$
2.296	0.54	1.77	2.05	3.81	$-10.314 - 15.621i$	3.133	$2.661 - 5.606i$
2.480	0.50	1.77	1.88	3.55	$-9.068 - 13.348i$	3.133	$2.524 - 5.158i$
2.696	0.46	1.78	1.78	3.30	$-7.722 - 11.748i$	3.168	$2.498 - 4.782i$
3.024	0.41	1.78	1.61	3.05	$-6.710 - 9.821i$	3.168	$2.343 - 4.361i$
3.263	0.38	1.79	1.53	2.82	$-5.612 - 8.629i$	3.204	$2.325 - 4.025i$

Table 6. Spectral values of ε^{EMA} and γ^{EMA} at the different values of λ with tabulated values of ε and γ

E, eV	λ, μm	$X = 0.4$			ε^{eff}	γ^{eff}
		ε_1	ε_0	γ		
0.539	2.30	2.993	−23.835 − 57.178*i*	1.529 − 3.008*i*	4.381 − 11.119*i*	0.179 + 0.017*i*
0.729	1.70	3.028	−18.091 − 44.063*i*	0.748 − 2.051*i*	4.213 − 9.450*i*	0.134 + 0.004*i*
1.000	1.24	3.063	−13.307 − 31.657*i*	0.203 − 1.241*i*	3.857 − 7.761*i*	0.098 + 0.008*i*
1.253	0.99	3.098	−11.358 − 24.914*i*	−0.009 − 0.895*i*	3.520 − 6.829*i*	0.083 − 0.007*i*
1.494	0.83	3.098	−9.474 − 17.882*i*	−0.135 − 0.530*i*	3.018 − 5.762*i*	0.060 − 0.017*i*
1.797	0.69	3.098	−8.295 − 14.346*i*	−0.160 − 0.380*i*	2.739 − 5.160*i*	0.051 − 0.024*i*
2.000	0.62	3.133	−7.613 − 12.339*i*	−0.162 − 0.299*i*	2.580 − 4.823*i*	0.045 − 0.028*i*
2.296	0.54	3.133	−6.507 − 9.779*i*	−0.144 − 0.199*i*	2.349 − 4.301*i*	0.033 − 0.028*i*
2.480	0.50	3.133	−5.945 − 8.626*i*	−0.130 − 0.159*i*	2.240 − 4.042*i*	0.029 − 0.029*i*
2.696	0.46	3.168	−5.217 − 7.378*i*	−0.111 − 0.118*i*	2.144 − 3.745*i*	0.023 − 0.029*i*
3.024	0.41	3.168	−4.407 − 6.281*i*	−0.088 − 0.084*i*	2.059 − 3.415*i*	0.018 − 0.026*i*
3.263	0.38	3.204	−3.504 − 5.468*i*	−0.066 − 0.059*i*	2.058 − 3.103*i*	0.013 − 0.023*i*

From analyzing the values in the tables, the calculated values of the effective DPT can be seen to coincide well with the literature data, such as those given in [4].

On the basis of the performed calculations, plots of the dependence of MRE on reflection and transmission at normal light incidence and angle of incidence of 70° were constructed (Figs. 1–4).

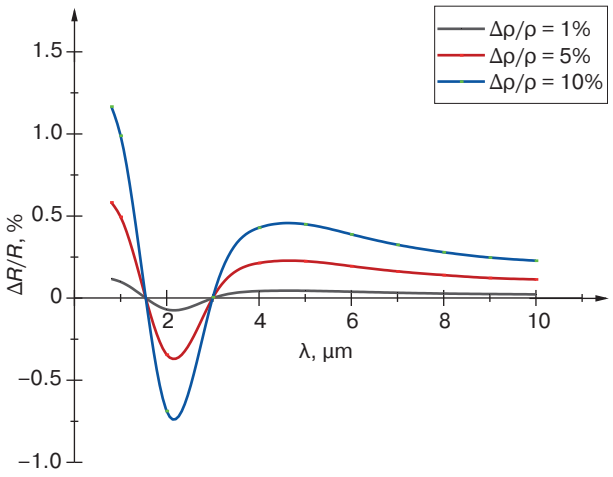

Fig. 1. Spectral dependence of MRE on reflection at normal light incidence

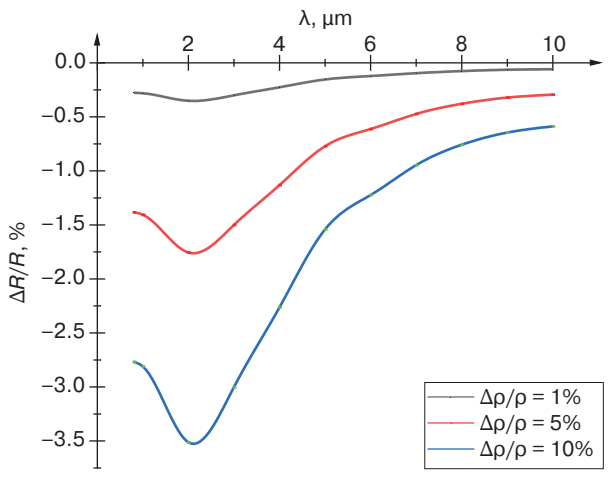

Fig. 2. Spectral dependence of MRE on reflection at $\varphi_2 = 70°$

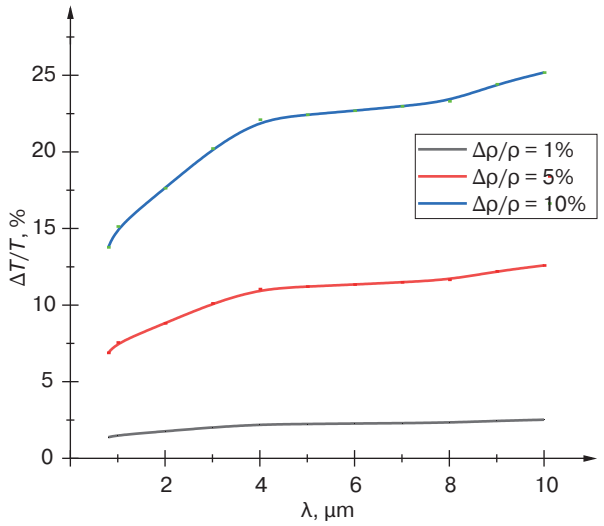

Fig. 3. Spectral dependence of MRE on transmittance at normal light incidence

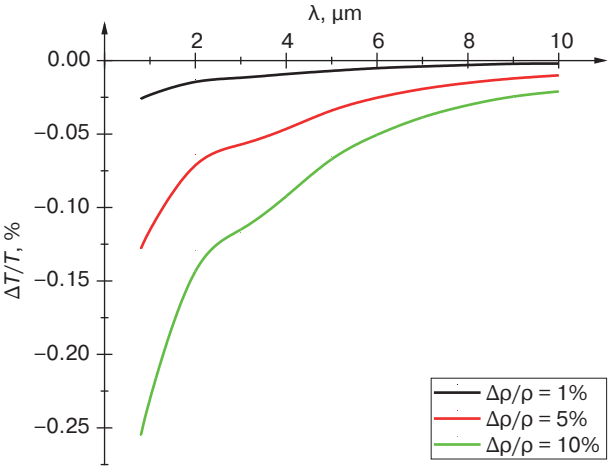

Fig. 4. Spectral dependence of MRE on transmittance at $\varphi_2 = 70^\circ$

When analyzing these graphs, we can draw the main conclusion: the spectral dependencies $\frac{\Delta R}{R}$ and $\frac{\Delta T}{T}$ in the IR range are linearly correlated with MR values $\frac{\Delta\rho}{\rho}$, and the dependence is directly proportional. The higher the MR value, the stronger the changes in the values $\frac{\Delta R}{R}$ and $\frac{\Delta T}{T}$.

It can be seen from Fig. 1 that in the near-IR region of the spectrum the MRE on reflection varies strongly, which is due to interzone transitions that significantly affect the optical characteristics of the material in the IR range. In Fig. 2, we can see a large absolute value of the parameter $\frac{\Delta R}{R}$. This can be explained by the significant role played in this region by intraband transitions, in addition to interband transitions, and the angle of incidence close to the Brewster angle (the main angle of incidence for metals) [3]. Figure 3 shows a smooth increase of the MRE on transmittance $\frac{\Delta T}{T}$, while Fig. 4 shows that as the wavelength increases (i.e., E decreases), the transmission MRE values $\frac{\Delta T}{T}$ first increase sharply and then change smoothly. By varying the wavelength λ and the real part of the refractive index n for a given film thickness d of the nanocomposite, it is possible to obtain the interference conditions under which the MRE value increases significantly [11–15].

CONCLUSIONS

The theoretical study of optical and MO spectra of Co-Al_2O_3 nanocomposites presented in this work was carried out in the framework of the MRE theory. The spectra were calculated using formulas (2)–(7). The spectra of the effective DPT were calculated in the Bruggeman approximation, which provides a good description of the nanocomposite properties at average volume concentrations of the metallic component ($X = 0.4$). As a non-contact MR measurement method for nondestructive control of any nanostructures, MRE represents a promising tool for the study of nanomaterials. The approaches described in this work are valid for the study of a wide class of nanostructures.

ACKNOWLEDGMENTS

The work was supported by the Ministry of Education and Science of the Russian Federation (State task for universities No. FGFZ-2023-0005).

Authors' contributions

M.A. Muhutdinova—literature review, computer simulation, discussion of results, and writing the text of the article.

A.N. Yurasov—computer simulation, discussion of results, writing and editing the article.

REFERENCES

1. Yurasov A.N. Magnetorefractive effect in nanostructures. *Pribory = Instruments*. 2022;4(262):22–25 (in Russ.).
2. Yurasov A.N. *Magnitoopticheskie effekty i magnitorefraktivnyi effekt v nanokompozitakh* (*Magneto-Optical Effects and Magnetorefractive Effect in Nanocomposites*). Moscow: MIREA; 2016. 55 p. (in Russ.).
3. Krinchik G.S., Artem'ev V.A. Magneto-optical properties of Ni, Co and Fe in the ultraviolet visible and infrared parts of the spectrum. *Journal of Experimental and Theoretical Physics* (*JETF*). 1968;26(6):1080–1085.
[Original Russian Text: Krinchik G.S., Artem'ev V.A. Magneto-optical properties of Ni, Co and Fe in the ultraviolet visible and infrared parts of the spectrum. *Zhurnal Eksperimental'noi i Teorieticheskoi Fiziki*. 1967;53(6):1901–1912 (in Russ.).]
4. Niklasson G.A., Granqvist C.G. Optical properties and solar selectivity of coevaporated $CoAl_2O_3$ composite films. *J. Appl. Phys*. 1984;55(9):3382–3410. https://doi.org/10.1063/1.333386
5. Bykov I.V., Gan'shina E.A., Granovskii A.B., et al. Magnetorefractive effect in granular films with tunneling magnetoresistance. *Phys. Solid State.* 2000;42(3):498–502. https://doi.org/10.1134/1.1131238
[Original Russian Text: Bykov I.V., Gan'shina E.A., Granovskii A.B., Gushchin B.C. Magnetorefractive effect in granular films with tunneling magnetoresistance. *Fizika tverdogo tela.* 2000;42(3):487–491 (in Russ.).]
6. Gushchin B.C., Gan'shina E.A., Kozlov A.A., Bykov I.V. Magnetorefractive effect in nanocomposites. *Moscow University Physics Bulletin.* 2005;60(1):57–75.
[Original Russian Text: Gushchin B.C., Gan'shina E.A., Kozlov A.A., Bykov I.V. Magnetorefractive effect in nanocomposites. *Vestnik Moskovskogo universiteta. Seriya 3. Fizika. Astronomiya*. 2005;1:45–58 (in Russ.).]
7. Yurasov A., Yashin M., Ganshina E., Granovsky A., Garshin V., Semenova D., Mirzokulov K. Simulation of magneto-optical properties of nanocomposites $(CoFeZr)_x(Al2O3)_{(1-x)}$. *J. Phys.: Conf. Ser*. 2019;1389(1):012113. http://doi.org/10.1088/1742-6596/1389/1/012113
8. Apresyan L.A., Vlasova T.V., Krasovskii V.I., et al. Effective Medium Approximations for the Description of Multicomponent Composites. *Tech. Phys.* 2020;65(7):1130–1138. https://doi.org/10.1134/S106378422007004X
[Original Russian Text: Apresyan L.A., Vlasova T.V., Krasovskii V.I., Kryshtob V.I., Rasmagin S.I. Effective Medium Approximations for the Description of Multicomponent Composites. *Zhurnal tekhnicheskoi fiziki*. 2020;90(7):1175–1183 (in Russ.). https://doi.org/10.21883/JTF.2020.07.49453.446-18]
9. Fadeev E.A., Blinov M.I., Garshin V.V. et al. Magnetic Properties of $(Co_{40}Fe_{40}B_{20})_x(SiO_2)_{(100-x)}$ Nanocomposites near the Percolation Threshold. *Bull. Russ. Acad. Sci. Phys.* 2019;83(7):835–837. https://doi.org/10.3103/S1062873819070153
[Original Russian Text: Fadeev E.A., Blinov M.I., Garshin V.V., Tarasova O.S., Gan'shina E.A., Prudnikova M.V., Prudnikov V.N., Lyakhderanta E., Ryl'kov V.V., Granovskii A.B. Properties of $(Co_{40}Fe_{40}B_{20})_x(SiO_2)_{(100-x)}$ Nanocomposites near the Percolation Threshold. *Izvestiya Rossiiskoi akademii nauk. Seriya fizicheskaya.* 2019;83(7):917–920 (in Russ.). https://doi.org/10.1134/S0367676519070159]
10. Gan'shina E.A., Pripechenkov I.M., Perova N.N., et al. Magneto-Optical Spectroscopy of Nanocomposites $(CoFeB)_x(LiNbO_3)_{(100-x)}$ with Concentrations up to the Percolation Threshold: From Superparamagnetism and Superferromagnetism to Ferromagnetism. *Phys. Metals Metallogr.* 2023;124(2):126–132. https://doi.org/10.1134/s0031918x22601949
[Original Russian Text: Gan'shina E.A., Pripechenkov I.M., Perova N.N., Kanazakova E.S., Nikolaev S.N., Sitnikov A.S., Granovskii A.B., Ryl'kov V.V. Magneto-optical spectroscopy of nanocomposites $(CoFeB)_x(LiNbO_3)_{(100-x)}$ with concentrations up to the percolation threshold: from superparamagnetism and superferromagnetism to ferromagnetism. *Fizika metallov i metallovedenie.* 2023;124(2):134–140 (in Russ.).]
11. Granovsky A., Sukhorukov Yu., Gan'shina E., Telegin A. Magnetorefractive effect in magnetoresistive materials. In: *Magnetophotonics: From Theory to Applications.* Berlin Heidelberg: Springer. 2013. P. 107–133.
12. Shkurdoda Yu.O., Dekhtyaruk L.V., Basov A.G., Chornous A.M., Shabelnyk Yu.M., Kharchenko A.P., Shabelnyk T.M. The giant magnetoresistance effect in Co/Cu/Co three-layer films. *Journal of Magnetism and Magnetic Materials*. 2019;477:88–91. https://www.doi.org/10.1016/j.jmmm.2019.01.040
13. Dekhtyaruk L.V., Kharchenko A.P., Klymenko Yu.O., Shkurdoda Yu.O., Shabelnyk Yu.M., Bezdidko O.V., Chornous A.M. Negative and Positive Effect of Giant Magnetoresistance in The Magnetically Ordered Sandwich. *2020 IEEE 10th International Conference Nanomaterials: Applications & Properties* (*NAP*). Sumy. Ukraine. 2020. P. 01NMM13-1-01NMM13-3. https://www.doi.org/10.1109/NAP51477.2020.9309694
14. Kelley C.S., Naughton J., Benson E., Bradley R.C., Lazarov V.K., Thompson S.M., Matthew J.A. Investigating the magnetic field-dependent conductivity in magnetite thin films by modelling the magnetorefractive effect. *J. Phys.: Condens. Matter*. 2014;26(3):036002. https://doi.org/10.1088/0953-8984/26/3/036002
15. Yurasov A., Yashin M., Ganshina E., et al. Simulation of magneto-optical properties of nanocomposites $(CoFeZr)_x(Al_2O_3)_{1-x}$. *J. Phys.: Conf. Ser*. 2019;1389:012113. http://doi.org/10.1088/1742-6596/1389/1/012113

СПИСОК ЛИТЕРАТУРЫ

1. Юрасов А.Н. Магниторефрактивный эффект в наноструктурах. *Приборы*. 2022. № 4(262). С. 22–25.
2. Юрасов А.Н. *Магнитооптические эффекты и магниторефрактивный эффект в нанокомпозитах.* М.: МИРЭА; 2016. 55 с.

3. Кринчик Г.С., Артемьев В.А. Магнитооптические свойства Ni, Co, и Fe в ультрафиолетовой, видимой и инфракрасной областях спектра. *Журнал экспериментальной и теоретической физики*. 1967;53(6):1901–1912.
4. Niklasson G.A., Granqvist C.G. Optical properties and solar selectivity of coevaporated $CoAl_2O_3$ composite films. *J. Appl. Phys*. 1984;55(9):3382–3410. https://doi.org/10.1063/1.333386
5. Быков И.В., Ганьшина Е.А., Грановский А.Б., Гущин В.С. Магниторефрактивный эффект в гранулированных пленках с туннельным магнитосопротивлением. *Физика твердого тела*. 2000;42(3):487–491.
6. Гущин В.С., Ганьшина Е.А., Козлов А.А., Быков И.В. Магниторефрактивный эффект в нанокомпозитах. *Вестник Московского университета. Серия 3. Физика. Астрономия*. 2005;1:45–58.
7. Yurasov A., Yashin M., Ganshina E., Granovsky A., Garshin V., Semenova D., Mirzokulov K. Simulation of magneto-optical properties of nanocomposites $(CoFeZr)_x(Al2O3)_{(1–x)}$. *J. Phys.: Conf. Ser*. 2019;1389(1):012113. http://doi.org/10.1088/1742-6596/1389/1/012113
8. Апресян Л.А., Власова Т.В., Красовский В.И., Крыштоб В.И., Расмагин С.И. Приближения эффективной среды для описания многокомпонентных композитов. *Журнал технической физики* (*ЖТФ*). 2020;90(7):1175–1183. https://doi.org/10.21883/JTF.2020.07.49453.446-18
9. Фадеев Е.А., Блинов М.И., Гаршин В.В., Тарасова О.С., Ганьшина Е.А., Прудникова М.В., Прудников В.Н., Ляхдеранта Э., Рыльков В.В., Грановский А.Б. Магнитные свойства нанокомпозитов $(Co_{40}Fe_{40}B_{20})_x(SiO_2)_{(100–x)}$ вблизи порога перколяции. *Известия РАН. Серия физическая*. 2019;83(7):917–920. https://doi.org/10.1134/S0367676519070159
10. Ганьшина Е.А., Припеченков И.М., Перова Н.Н., Каназакова Е.С., Николаев С.Н., Ситников А.С., Грановский А.Б., Рыльков В.В. Магнитооптическая спектроскопия нанокомпозитов $(CoFeB)_x(LiNbO_3)_{(100–x)}$ до порога перколяции: от суперпарамагнетизма и суперферромагнетизма до ферромагнетизма. *Физика металлов и металловедение*. 2023;124(2):134–140.
11. Granovsky A., Sukhorukov Yu., Gan'shina E., Telegin A. Magnetorefractive effect in magnetoresistive materials. In: *Magnetophotonics: From Theory to Applications.* Berlin Heidelberg: Springer. 2013. P. 107–133.
12. Shkurdoda Yu.O., Dekhtyaruk L.V., Basov A.G., Chornous A.M., Shabelnyk Yu.M., Kharchenko A.P., Shabelnyk T.M. The giant magnetoresistance effect in Co/Cu/Co three-layer films. *Journal of Magnetism and Magnetic Materials*. 2019;477:88–91. https://www.doi.org/10.1016/j.jmmm.2019.01.040
13. Dekhtyaruk L.V., Kharchenko A.P., Klymenko Yu.O., Shkurdoda Yu.O., Shabelnyk Yu.M., Bezdidko O.V., Chornous A.M. Negative and Positive Effect of Giant Magnetoresistance in The Magnetically Ordered Sandwich. *2020 IEEE 10th International Conference Nanomaterials: Applications & Properties* (*NAP*). Sumy. Ukraine. 2020. P. 01NMM13-1-01NMM13-3. https://www.doi.org/10.1109/NAP51477.2020.9309694
14. Kelley C.S., Naughton J., Benson E., Bradley R.C., Lazarov V.K., Thompson S.M., Matthew J.A. Investigating the magnetic field-dependent conductivity in magnetite thin films by modelling the magnetorefractive effect. *J. Phys.: Condens. Matter*. 2014;26(3):036002. https://doi.org/10.1088/0953-8984/26/3/036002
15. Yurasov A., Yashin M., Ganshina E., et al. Simulation of magneto-optical properties of nanocomposites $(CoFeZr)_x(Al_2O_3)_{1–x}$. *J. Phys.: Conf. Ser*. 2019;1389:012113. http://doi.org/10.1088/1742-6596/1389/1/012113

About the authors

Muza A. Mukhutdinova, Student, Institute for Advanced Technologies and Industrial Programming, MIREA – Russian Technological University (78, Vernadskogo pr., Moscow, 119454 Russia). E-mail: mukhutdinova-03@mail.ru. https://orcid.org/0009-0001-5013-5208

Alexey N. Yurasov, Dr. Sci. (Phys.-Math.), Professor, Department of Nanoelectronics, Institute for Advanced Technologies and Industrial Programming, MIREA – Russian Technological University (78, Vernadskogo pr., Moscow, 119454 Russia). E-mail: alexey_yurasov@mail.ru. ResearcherID M-3113-2016, Scopus Authors ID 6602974416, RSCI SPIN-code 4259-8885, https://orcid.org/0000-0002-9104-3529

Об авторах

Мухутдинова Муза Александровна, студент, Институт перспективных технологий и индустриального программирования, ФГБОУ ВО «МИРЭА – Российский технологический университет» (119454, Россия, Москва, пр-т Вернадского, д. 78). E-mail: mukhutdinova-03@mail.ru. https://orcid.org/0009-0001-5013-5208

Юрасов Алексей Николаевич, д.ф.-м.н., профессор, профессор кафедры наноэлектроники, Институт перспективных технологий и индустриального программирования, ФГБОУ ВО «МИРЭА – Российский технологический университет» (119454, Россия, Москва, пр-т Вернадского, д. 78). E-mail: alexey_yurasov@mail.ru. ResearcherID M-3113-2016, Scopus Authors ID 6602974416, SPIN-код РИНЦ 4259-8885, https://orcid.org/0000-0002-9104-3529

Translated from Russian into English by Lyudmila O. Bychkova
Edited for English language and spelling by Thomas A. Beavitt

Mathematical modeling

Математическое моделирование

UDC 621.396.969.1
https://doi.org/10.32362/2500-316X-2024-12-3-65-77
EDN TUXBXL

RESEARCH ARTICLE

High-resolution 2D-DoA sequential algorithm of azimuth and elevation estimation in automotive distributed system of coherent MIMO radars

Igor V. Artyukhin @

Lobachevsky State University of Nizhny Novgorod, Nizhny Novgorod, 603950 Russia
@ *Corresponding author, e-mail: artjukhin@rf.unn.ru*

Abstract

Objectives. One of the main tasks of radiolocation involves the problem of increasing spatial resolution of the targets in the case of limited aperture of the radar antenna array and short length of time samples (snapshots). Algorithms must be developed to provide high angular resolution and low computational complexity. In order to conform with the existing Advanced Driver Assistance Systems requirements, modern cars are equipped with more than one radar having a common signal processing scheme to improve performance during target detection, positioning, and recognition as compared to a single radar. The present study aims to develop a two-dimensional Direction-of-Arrival algorithm with low computation complexity as part of distributed coherent automotive radar system for cases involving short time samples (snapshots).

Methods. A virtual antenna array formation algorithm is formulated according to the two-dimensional Capon method. A proposed modification of two-dimensional Capon algorithm is based on sequentially estimating the directions of arrival for the distributed radar system. The Monte Carlo method is used to compare the effectiveness of the considered algorithms.

Results. The 2D-DoA sequential algorithm of azimuth and elevation estimation is proposed. The comparative analysis results for the developed algorithm and classical 2D Capon method based on numerical simulation using Monte Carlo method are presented. The proposed scheme of DoA estimation for coherent signal processing of distributed radars is shown to lead to an improvement of the main considered metrics representing the probability of correctly estimating the number of targets, mean square error, and square error compared to a single radar system. The proposed low-computational algorithm shows the gain in complexity compared to full 2D Capon algorithm.

Conclusions. The proposed two-stage algorithm for estimating the directions of arrival of signals in azimuth and elevation planes can be applied to the distributed system of coherent radars with several receiving and transmitting antennas representing multiple input multiple output (MIMO) radars. The algorithm is based on sequentially estimating the directions of arrival, implying estimation in the azimuthal plane at the first stage and estimation in the vertical plane at the second stage. The performance of a coherent radar system with limited antenna array configuration of separate radar is close in characteristics to a high-performance 4D-radar with a large antenna array system.

Keywords: automotive distributed radars, coherent signal processing, high-resolution algorithms, 2D Capon algorithm

• **Submitted:** 18.07.2023 • **Revised:** 18.03.2024 • **Accepted:** 05.04.2024

For citation: Artyukhin I.V. High-resolution 2D-DOA sequential algorithm of azimuth and elevation estimation in automotive distributed system of coherent MIMO radars. *Russ. Technol. J.* 2024;12(3):65–77. https://doi.org/10.32362/2500-316X-2024-12-3-65-77

Financial disclosure: The author has no a financial or property interest in any material or method mentioned.

The author declares no conflicts of interest.

НАУЧНАЯ СТАТЬЯ

Двумерный алгоритм с последовательной оценкой углов прихода сигналов в системе когерентных распределенных автомобильных радаров с несколькими приемными и передающими антеннами

И.В. Артюхин @

Нижегородский государственный университет им. Н.И. Лобачевского, Нижний Новгород, 603950 Россия
@ *Автор для переписки, e-mail: artjukhin@rf.unn.ru*

Резюме

Цели. Одной из актуальных задач в радиолокации является проблема повышения пространственного разрешения целей при ограниченной апертуре антенной решетки радара и короткой выборке входных отсчетов. Разрабатываемые алгоритмы должны обеспечивать высокое угловое разрешение и иметь малую вычислительную сложность. В настоящее время автомобили для выполнения требований систем безопасности и помощи водителю оснащаются не одним, а несколькими радарами с общей схемой обработки сигналов для улучшения характеристик при обнаружении, позиционировании и распознавании целей по сравнению с одиночным радаром. Цель работы – разработка двумерного алгоритма оценки угловых координат с низкой вычислительной сложностью в системе распределенных когерентных автомобильных радаров для случая короткой выборки входных отсчетов.

Методы. Использованы алгоритм формирования виртуальной антенной решетки, двумерный метод Кейпона. Предложена модификация метода Кейпона на основе последовательной оценки углов прихода сигналов применительно к системе распределенных радаров. Для сравнения эффективности рассматриваемых алгоритмов используется метод Монте-Карло.

Результаты. Представлен алгоритм с последовательной оценкой азимута и угла места для системы распределенных когерентных автомобильных радаров. Приведены результаты сравнительного анализа предложенного алгоритма и классического двумерного метода Кейпона на основе численного моделирования при помощи метода Монте-Карло. Показано, что предложенная схема приводит к улучшению целевых метрик (вероятности правильного определения числа целей, среднеквадратической и систематической ошибок измерения азимута и угла места) по сравнению с одиночным радаром. Последовательный алгоритм обеспечивает выигрыш в использовании вычислительных ресурсов по сравнению с полным двумерным методом Кейпона.

Выводы. Предложенный двумерный метод оценки углов прихода сигналов в азимутальной и угломестной плоскостях может быть применен для распределенной системы бистатических когерентных радаров с несколькими приемными и передающими антеннами (MIMO-радаров). Метод основан на последовательной оценке углов прихода (на первом шаге – в азимутальной плоскости, на втором – в вертикальной). Характеристики системы когерентных радаров с ограниченной конфигурацией антенной решетки, сравнимы с характеристиками высокопроизводительного 4D-радара со значительно большим числом элементов антенной решетки.

Ключевые слова: распределенные автомобильные радары, когерентная обработка, алгоритмы сверхразрешения, двумерный алгоритм Кейпона

• **Поступила:** 18.07.2023 • **Доработана:** 18.03.2024 • **Принята к опубликованию:** 05.04.2024

Для цитирования: Артюхин И.В. Двумерный алгоритм с последовательной оценкой углов прихода сигналов в системе когерентных распределенных автомобильных радаров с несколькими приемными и передающими антеннами. *Russ. Technol. J*. 2024;12(3):65–77. https://doi.org/10.32362/2500-316X-2024-12-3-65-77

Прозрачность финансовой деятельности: Автор не имеет финансовой заинтересованности в представленных материалах или методах.

Автор заявляет об отсутствии конфликта интересов.

INTRODUCTION

Recent developments in the field of automotive electronics have given rise to a new generation of radars called 4D radars[1]. Such devices allow simultaneous measurement of three spatial coordinates (distance, azimuth, and elevation) and velocity (Doppler shift). At the same time, the high spatial resolution enables recognition of overlapping images, such as a pedestrian standing by a fence or a motorcycle driving next to a truck.

One way to improve angular resolution is to increase the number of transmitters (Tx) and receivers (Rx). However, this approach is limited by the complexity of hardware implementation and high cost of the final product. Currently, the number of antennas ranges from a few units to several dozen per radar. For example, the Continental ARS540 radar (Xilinx, Germany) is equipped with 12 transmitters and 16 receivers[2]. The S80 automotive radar released by Uhnder, USA, has a similar configuration [1]. In the more advanced Phoenix radar by Arbe (Israel)[3], up to 48 Tx and 48 Rx are implemented.

Given the limitation on the number of physical antennas, the angular resolution can be improved through applying additional high-resolution (HR) methods for neighboring signal sources (targets). Among classical HR algorithms, mention multiple signal classification (MUSIC), estimation of signal parameters via rotational invariant techniques (ESPRIT), Capon method, minimum polynomial method, and their variations [2–6] should be distinguished. However, these methods, while highly efficient, require large computational resources, especially when using antenna array systems (AAS) with a sufficiently large number of antennas.

In practice, when processing signals in automotive radars, the estimation of direction of arrival (DoA) is typically performed using only one sequence of short pulses (the so-called "frame"), which gives one snapshot (a time sample) in each radar [3, 7]. Thus, for the considered problem, the number of time samples is less than the number of AAS elements (the so-called "short sample"), resulting in the complexity of using the above-mentioned HR methods associated with the inversion of the ill-conditioned correlation matrix of such short input process.

The second technique for increasing angular resolution is based on implementing a coherent radar with multiple receiving and transmitting channels known as the multiple-input multiple-output (MIMO) radar. MIMO radars equipped with N_{Tx} Tx and N_{Rx} Rx antennas form a virtual AAS equivalent to that of a traditional system equipped with a single Tx antenna and $N_{\text{Tx}} \times N_{\text{Rx}}$ Rx antennas (called multiple-input single-output (MISO) radars). Thus, MIMO radars provide an efficient path to achieve high angular resolution with fewer real antennas [7–9]. However, they require all received signals to be coherent and that the waveform be orthogonal. When constructing MIMO radars, different orthogonalization methods are used, such as time or code division of signals [8, 9].

Using the MIMO technology, Arbe's Phoenix radar can create up to 2304 virtual antennas providing an angular resolution (3 dB beamwidth of antenna pattern) of 1.25° and 1.5° in azimuth and elevation, respectively. At the same time, the field of view (FoV) is ±60° in the azimuth plane and ±15° in elevation. Following the same approach, the Continental ARS540 radar can create 192 virtual antennas with 1.2° azimuth resolution and 2.3° elevation resolution.

In order to satisfy existing requirements of advanced driver assistance systems (ADAS), modern cars are equipped with several sensors capable of operating as a single unit and having a common (centralized) signal processing. The advantages of such systems include a significant improvement in their performance when solving detection-, positioning-, and target-recognition tasks as compared to a single radar (traditional or MIMO).

[1] https://autotech.news/the-future-of-automotive-radar-4d-imaging-radar/. Accessed February 07, 2024.

[2] https://www.xilinx.com/publications/presentations/continental-ARS540-powered-by-xilinx.pdf. Accessed August 21, 2023.

[3] https://arberobotics.com/wp-content/uploads/2021/04/4D_Imaging_Radar_Product_Overview.pdf. Accessed August 21, 2023.

Two approaches to integrating measurements from different radars are typically distinguished, based on coherent and incoherent signal processing. The incoherent scheme involves combining signals of single radars operating in monostatic mode [10, 11]. The coherent scheme is based on creating a joint virtual AAS of distributed radars operating in the bistatic measurement mode, which requires full or partial time/frequency synchronization of signals between radars [12].

The present paper considers the 2D DoA estimation method for coherent signal processing in the distributed automotive radar system (DRS) for short length of time samples. This method should provide high angular resolution by coherent signal processing in distributed radars with a small number of real antennas instead of using a single high-performance 4D radar with large AAS. At the same time, 1° azimuth resolution and 2° elevation are considered as necessary characteristics.

1. CREATING VIRTUAL AAS FOR DISTRIBUTED COHERENT RADAR SYSTEM

We consider a distributed system consisting of two coherent MIMO radars. Assume that this system has real N_{Tx} transmitters and N_{Rx} receivers. The total number of antennas of virtual AAS equals to $N_{\text{virt}} = N_{\text{Tx}} \cdot N_{\text{Rx}}$.

The location of virtual antennas is defined as the convolution of coordinates of real receivers and transmitters [13, 14]. The coordinates of the mth virtual antenna may be calculated from the following formula:

$$\boldsymbol{\rho}^{(m)} = \mathbf{r}_{\text{Tx}}^{(p)} + \mathbf{r}_{\text{Rx}}^{(q)} - \mathbf{r}_0, \qquad (1)$$

where $\mathbf{r}_{\text{Tx}}^{(p)}$ is the position vector of coordinates of the pth element of the transmitter; $\mathbf{r}_{\text{Rx}}^{(q)}$ is the position vector of coordinates of the qth element of the receiver; $\mathbf{r}_0$ is the position vector determining the choice of the coordinate system; $m = q \cdot p$. Here it should be noted that, under certain conditions of the radar AAS architecture, several virtual antennas can have similar space coordinates.

Thus, equation (1) can be rewritten in the following form:

$$\boldsymbol{\rho}^{(m)} = \mathbf{r}_{\text{Tx}}^{(p)} + \mathbf{r}_{\text{Rx}}^{(q)} - \mathbf{r}_{\text{Tx}}^{(1)} - \mathbf{r}_{\text{Rx}}^{(1)}, \qquad (2)$$

where $\mathbf{r}_{\text{Tx}}^{(1)}$ and $\mathbf{r}_{\text{Rx}}^{(1)}$ are the position vector of coordinates of the first transmitting and first receiving AAS elements, respectively.

The properties of the virtual AR can be controlled by changing coordinates of real Rx and Tx antennas. The selection of antenna position is generally aimed at obtaining a virtual array having a larger aperture, resulting in the improved angular resolution of close objects. At the same time, the concept of virtual AAS allows the application of traditional AAS processing (including HR algorithms) to estimate angular coordinates. The basic idea of virtual AAS is to match its output signal with that generated by some real AAS. Although such a match is unambiguous in free space, multipath propagation determines the optimal configuration of real AAS by considering matching criteria. It is shown in [14] that, in the presence of a reflected signal from the Earth, either all transmitters or all receivers should have the same height above the Earth's surface. The simplest form of such configuration for real transmitting and receiving antennas is the L-shaped AAS.

An example of virtual AAS configuration for the distributed system consisting of two coherent radars with the L-shaped AAS is shown in Fig. 1. Transmitters are marked with a cross, while receivers are marked with a circle. The AASs of single radars are arranged symmetrically with respect to the vertical axis (radar center).

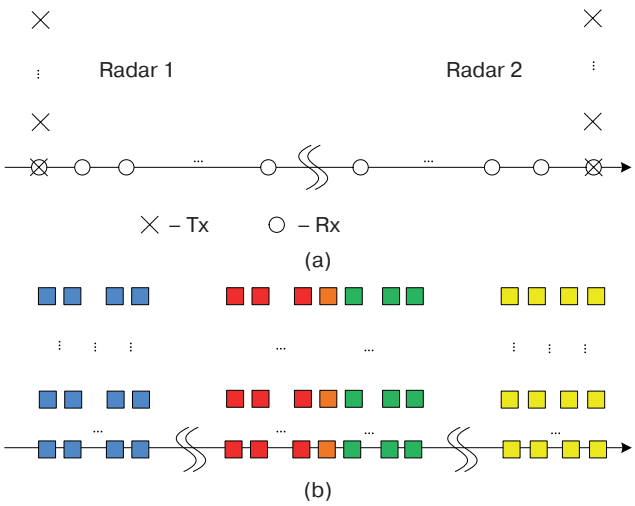

Fig. 1. General geometry of the distributed radar system: (a) AAS consisting of two L-type radars; (b) virtual AAS

The resulting virtual AAS consists of two virtual monostatic arrays (highlighted in blue and yellow colors in Fig. 1b) and one virtual bistatic array located in the middle. The bistatic AAS consists of twice the number of elements of the virtual single radar array [13, 14].

The virtual antennas formed using the bistatic response of the left radar are shown in red, while those of the right radar are shown in green. The middle elements highlighted in orange in the virtual AAS contain overlapping bistatic measurements from the right and left radars. This position of antennas in the middle column is necessary for considering and compensating for the phase difference occurring between bistatic signals in the virtual AAS under non-ideal time/frequency synchronization.

2. DESCRIPTION OF THE EXPLOITED ALGORITHMS

2.1. Phase compensation algorithm

We propose a signal phase compensation algorithm consisting of two stages. The first stage is used for non-zero installment angle α of single radars (Fig. 2). If the single radar installment angle is zero, then the first stage is skipped, and only the second stage is applied.

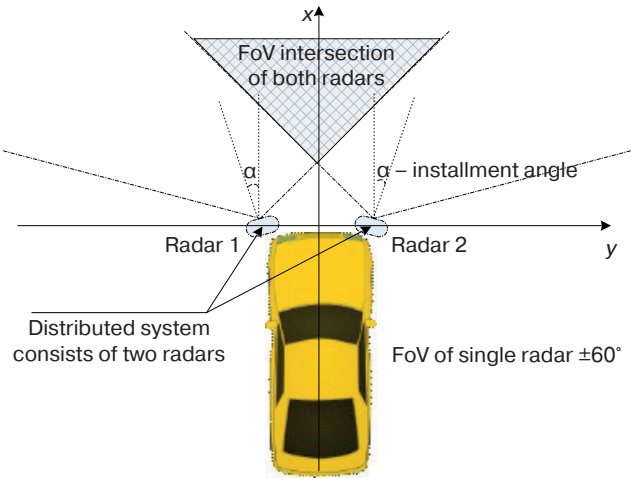

Fig. 2. General geometry of the distributed radar system. Top view

First stage: compensating for the additional phase incursion related to the non-zero installment angle of a single radar.

We denote the signals of virtual bistatic arrays (responses) from the left and right radars by matrices $\mathbf{Y}_i$ (i = 1, 2). We introduce the pth component of the AAS scanning vector $\mathbf{s}(\alpha)$ in azimuth for the radar installment angle α as follows:

$$s_p(\alpha) = \exp(2\pi j d_\lambda (p-1)\sin(\alpha)), \quad p = \overline{1,N}, \qquad (3)$$

where N is the number of antenna elements in the horizontal plane of a single radar, j is an imaginary unit.

In order to compensate for the additional phase incursion related to the non-zero installment angle of a single radar, the following transformation is performed:

$$\mathbf{Z}_1 = \mathbf{G}_1 \cdot \mathbf{Y}_1, \quad \mathbf{Z}_2 = \mathbf{G}_2 \cdot \mathbf{Y}_2, \qquad (4)$$

where

$$\mathbf{G}_1 = \mathbf{diag}\{\mathbf{s}\}, \mathbf{G}_2 = \mathbf{diag}\{\mathbf{s}^*\} \qquad (5)$$

and $\mathbf{diag}\{\mathbf{s}\}$ is a diagonal matrix, the elements of vector $\mathbf{s}$ lie on the main diagonal, and * is the sign of complex conjugation.

We introduce matrix $\mathbf{Z}$ of dimension $N_{Tx}/2 \times 2N$ containing signals $\mathbf{Z}_1$ and $\mathbf{Z}_2$:

$$\mathbf{Z} = [\mathbf{Z}_1, \mathbf{Z}_2]. \qquad (6)$$

Second stage: the jump in phases between bistatic radar measurements is compensated by taking into account the radar phase difference in the average element of the constructed virtual AAS.

We extract a separate row consisting of $2N$ elements: $\{z(1), z(2), \ldots z(2N)\}$ from the complete set $\mathbf{Z}$. The virtual antenna array (selected row) consists of $2N - 1$ elements with overlapping measurements in the middle element (Fig. 3).

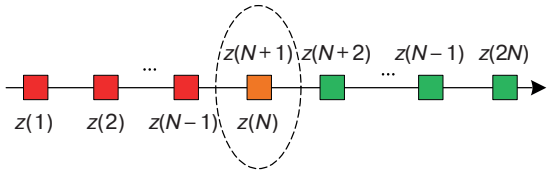

Fig. 3. Illustration of the sample construction for a separate row of the virtual array

We shall find the phase difference in the average element $\Delta\Phi = \text{phase}(z(N)) - \text{phase}(z(N+1))$ and compensate the obtained difference for antenna elements with indices $N + 2, \ldots, 2N$, as follows:

$$\{z(N+2), z(N+3), \ldots z(2N)\} \cdot \exp(-j \cdot \Delta\Phi). \qquad (7)$$

The transformed signals used to estimate DoA consist of the following $2N - 1$ elements:

$$\begin{aligned} &\{z(1), z(2), \ldots z(N),\ z(N+2) \cdot \exp(-j\Delta\Phi), \ldots \\ &z(N+3) \cdot \exp(-j\Delta\Phi), \ldots z(2N) \cdot \exp(-j\Delta\Phi)\}. \end{aligned} \qquad (8)$$

The element with index $N + 1$ from the complete set is not used in the final set (Fig. 4).

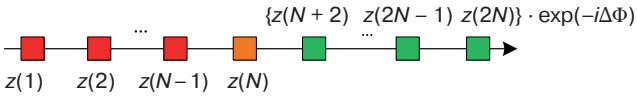

Fig. 4. Construction of samples for a separate row of the virtual array

2.2. Two-dimensional algorithm for estimating DoA

We consider two methods for estimating the azimuth and target elevation: the classical two-dimensional (2D) Capon algorithm and the proposed (new) two-step method for sequential estimation of azimuth and elevation.

The nonparametric 2D Capon method is selected as the basic approach. Although this method does not

require priori knowledge of the target quantity (or its prior estimation), which simplifies the DoA estimation, it has high computational complexity related to finding the inverse matrix and the two-dimensional search for extrema [2, 13]. This algorithm is based on the search for maxima of the two-dimensional resolution function $\eta_C(\varphi, \theta)$:

$$\eta_C(\varphi,\theta) = \frac{1}{\mathbf{S}(\varphi,\theta)^H \mathbf{M}_{2D}^{-1} \mathbf{S}(\varphi,\theta)}, \quad (9)$$

where $\mathbf{M}_{2D}$ is the estimation of the correlation matrix of the input process of the two-dimensional AAS, while $\mathbf{S}(\varphi, \theta)$ is the corresponding scanning vector.

The DoA estimation method proposed in the paper consists in the sequential estimation of azimuth (first step) and elevation (second step). We consider the proposed DoA estimation scheme in detail.

The first step involves implementing the one-dimensional Capon algorithm. Let there be an $m \times n$ virtual AAS (marked with blue squares in Fig. 5 on the left). A single time sample is used for estimating DoA, which can be represented mathematically using matrix $\mathbf{A}$ (see Fig. 5 on the right).

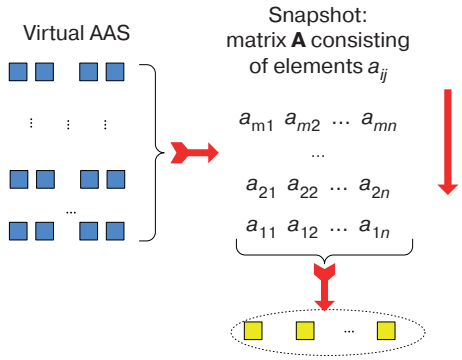

Fig. 5. Example of constructing samples for estimation in the azimuth plane

We select a horizontal row of length n (one-dimensional AAS is yellow squares marked with an ellipse in Fig. 5) from full virtual AAS. In this case, the entire matrix $\mathbf{A}$ is used to estimate the correlation matrix of one-dimensional AAS. Single rows of matrix $\mathbf{A}$ can be interpreted as "time samples" for one-dimensional AAS. We compile matrix $\mathbf{A}$ in the following form:

$$\mathbf{A} = \begin{bmatrix} a_{11} & a_{21} & \dots & a_{m1} \\ a_{12} & a_{22} & \dots & a_{m2} \\ \dots & \dots & \dots & \dots \\ a_{1n} & a_{2n} & \dots & a_{mn} \end{bmatrix}, \quad (10)$$

allowing the one-dimensional resolution function for the Capon method to be represented as the following expression:

$$\eta(\varphi) = \frac{1}{\mathbf{S}(\varphi)^H \mathbf{M}_{1D}^{-1} \mathbf{S}(\varphi)}, \quad (11)$$

where matrix $\mathbf{M}_{1D} = \frac{1}{L} \cdot \mathbf{A} \cdot \mathbf{A}^H$, $L = m$ is the number of rows in virtual AAS, $(\bullet)^H$ is Hermite conjugation.

Solving the maximization problem (11), we obtain k azimuth estimates: $\varphi_1, \dots, \varphi_k$.

In the second step, the 2D Capon algorithm for elevation estimation is implemented. However, unlike the full 2D Capon method, the search for maxima of resolution function $\eta_C(\varphi, \theta)$ is performed only at fixed values of the target azimuths $\varphi_1, \dots, \varphi_k$ found in the first step:

$$\eta_C(\varphi,\theta)\big|_{\varphi=\varphi_l} = \frac{1}{\mathbf{S}(\varphi,\theta)^H \mathbf{M}_{2D}^{-1} \mathbf{S}(\varphi,\theta)}\Bigg|_{\varphi=\varphi_l},$$

$$\varphi_l \text{ are fixed, } l = \overline{1,k}. \quad (12)$$

Thus, the problem of finding maxima for two-dimensional function $\eta_C(\varphi, \theta)$ (9) has been reduced to k one-dimensional hill-climbing problems (12). The solution to (12) is elevation estimates $\theta_1, \dots, \theta_k$.

The flowchart of the proposed algorithm is presented in Fig. 6.

2.3. Spatial smoothing procedure

In real-world problems, only a single snapshot is used to estimate DoAs. In this case, correlation matrices $\mathbf{M}_{1D}$ and $\mathbf{M}_{2D}$ are degenerate. For such situation, a spatial smoothing procedure for the input data is applied [3]. For this purpose, subarrays are selected in main AAS whose optimal size is $Q \approx 0.7N_{dim}$ [3, 5] for each N_{dim} dimension.

In order to explain the spatial smoothing procedure, the subarray formation on the example of the L-type radar system with 6T8R configuration is considered. Then the bistatic virtual array is 6×15 in size, and the size of subarray for spatial smoothing would be 4×10 when using the 2D Capon algorithm (marked in red in Fig. 7a). In case of the 1D Capon algorithm, the subarray size is 1×10 (marked in green in Fig. 7b).

After selecting the subarray, several samples are generated. Each sample is a part of the received signal corresponding to the shifted copies of the selected subarray (so-called forward spatial smoothing). The number of samples can be doubled by applying the inverse smoothing procedure [3, 5]. The spatial smoothing results in $L_{2D} = 36$ and $L_{1D} = 12 \times 6 = 72$ spatial samples for the 2D and 1D Capon algorithms, respectively.

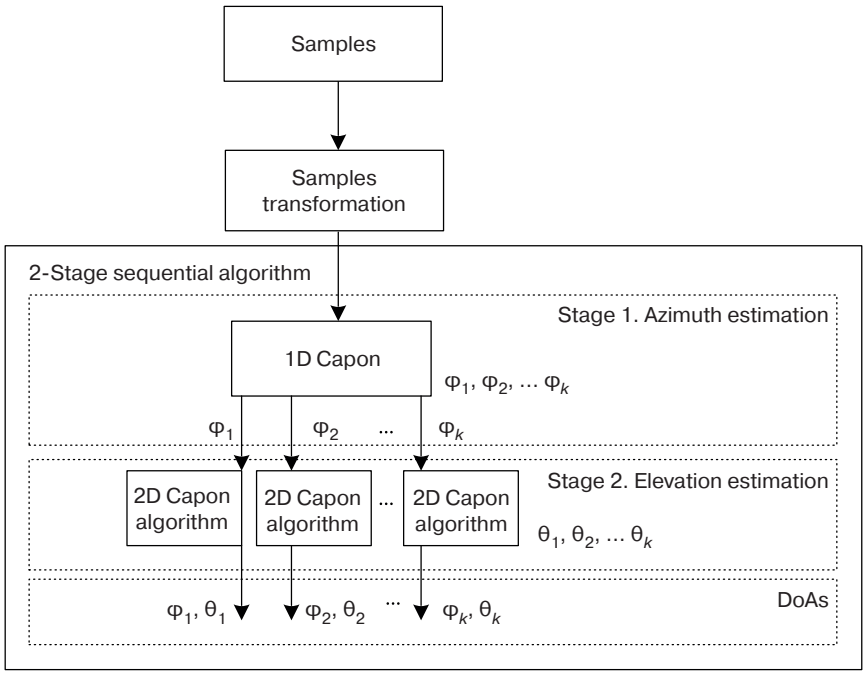

Fig. 6. Sequential algorithm for DoA estimation

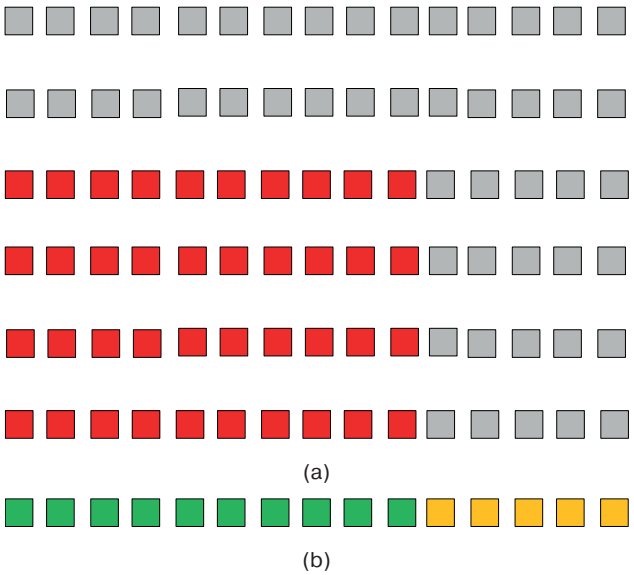

Fig. 7. Subarray configuration:
(a) subarray for the 2D Capon algorithm;
(b) subarray for the 1D Capon algorithm

2.4. Estimating computational resources

For estimating the required computational resources in the hardware implementation of algorithms, only the complex multiplication operation is considered as the costliest procedure [15, 16]. The computational complexity of the full 2D Capon method is presented in Tables 1, 2. The computational resource estimation for the proposed sequential DoA estimation algorithm is collected in Tables 3, 4.

The numerical estimates of computational resources are presented in Tables 2, 4 for the following case:

- AAS of a single *L*-type 6T8R radar;
- virtual array size (bistatic measurements): 6 × 15;
- a single snapshot;
- spatial smoothing procedure is applied.

The parameters "number of antenna elements" and "number of time samples" in Tables 2 and 4 are parameters after the spatial smoothing procedure.

Table 1. Computational costs of the 2D Capon method

Procedure	Number of operations
Estimation of the correlation matrix	$L_{2D}(N_{2D})^2 + (N_{2D})^2$
Matrix inversion	$4(N_{2D})^2$
Angles scan (Capon resolving function)	$(N_{2D})^2 + N_{2D}$
Search for maxima	$4J_1N_{steps}$
Total complexity	$(N_{2D})^2(L_{2D}+6) + N_{2D} + 4J_1N_{steps}$

Table 2. Computational cost of the 2D Capon method

Parameter	Value
Number of antenna elements	$N_{2D} = 40$
Number of time samples	$L_{2D} = 36$
Number of targets	$J_1 = 2$
Number of steps (points) to find maxima	$N_{steps} = N_hN_v$, $N_h = N_v = 100$
Total complexity	147240

Table 3. Computational cost of the sequential DoA estimation algorithm

Procedure	Number of operations
Stage 1 (1D Capon)	
Estimation of the correlation matrix	$L_{1D}(N_{1D})^2 + (N_{1D})^2$
Matrix inversion	$4(N_{1D})^2$
Scanning by resolution function angles	$(N_{1D})^2 + N_{1D}$
Search for maxima	$4J_1N_h$
Stage 2 (2D Capon)	
Estimation of the correlation matrix	$4(L_{2D}(N_{2D})^2 + (N_{2D})^2)$
Matrix inversion	$4(N_{2D})^2$
Angles scan (Capon resolving function)	$(N_{2D})^2 + N_{2D}$
Search for maxima	$2 \cdot 4J_2N_v$
Total complexity	$(N_{2D})^2(L_{2D}+6) + N_{2D} + 2 \cdot 4J_2N_v + + (N_{1D})^2(L_{2D}+6) + N_{1D} + 4J_1N_h$

Table 4. Computational cost of the sequential DoA estimation algorithm

Parameter	Value
Number of antenna elements	$N_{1D} = 10$
Number of time samples	$L_{1D} = 72$
Number of targets	$J_2 = 1$
Total complexity	76650

The computational complexity of the full 2D Capon method is 147240 operations (complex multiplications) and 76650 operations per the sequential DoA estimation algorithm for given parameters. Thus, the computational resource gain of the proposed algorithm is 1.9 times higher as compared to the classical 2D Capon algorithm.

3. NUMERICAL SIMULATION RESULTS

We assume that the distributed system consists of two coherent millimeter-wave (77 GHz) radars, the sensor spacing is 1.48 m, and the installment angle is 0° (forward-facing radars). The antenna array system of the single radar has the *L*-shaped 6T8R configuration shown in Fig. 8.

The AAS period is 0.575λ (horizontal plane) and 1.93λ (vertical plane). The single radar parameters provide FoV of ±60° in the azimuth plane and ±15° in the vertical plane. The main beam width at half power level (−3 dB) is 11.25° in the horizontal plane and 4.46° in the vertical plane.

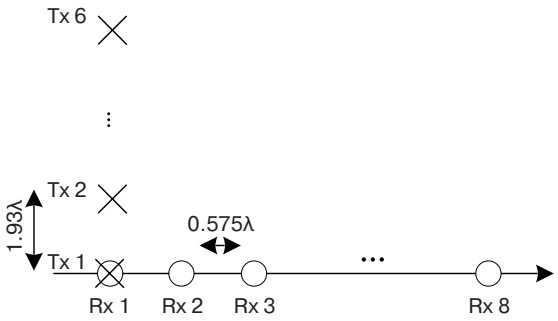

Fig. 8. AAS of the single *L*-type 6T8R radar

For the DRS, given the resulting virtual bistatic AAS, the main beam width in the vertical plane does not change; however, it decreases to ≈6° in the horizontal plane compared to a single radar.

In order to illustrate the efficiency of the distributed coherent radar system, two scenarios for spatial arrangement of two close targets are considered. In the first scenario shown in Fig. 9a, two targets are located symmetrically with respect to the *x*-axis with angular distance of 1° in the azimuth plane sharing the same elevation of 0°. The angular distance between the targets is 11 times smaller than the AAS beam width of the single radar. In the second scenario (Fig. 9b), the two targets have the same azimuth of 0° and are located symmetrically with respect to the *x*-axis in the vertical plane with an angular distance of 2°. The general arrangement of targets and radars is shown in Fig. 9c. The angular distance between targets is approximately 2.2 times smaller than the AAS beam width of a single radar in the vertical plane.

The full 2D Capon method for a single radar and the distributed system is used as the baseline algorithm for comparison with the proposed algorithm for sequential azimuth and elevation estimation for the distributed radar system (DRS). For DoA estimation, a single snapshot is taken.

The efficiency of the algorithms is compared using the Monte Carlo method. For each SNR value, a statistical ensemble of 2000 experiments is generated. Here, three main metrics are considered as functions of the SNR parameter:

1. The probability of correctly estimating the number of close targets *p*:

$$p = \frac{m}{n}, \tag{13}$$

where *m* is the number of experiments with correctly detected number of targets, while *n* is the total number of experiments.

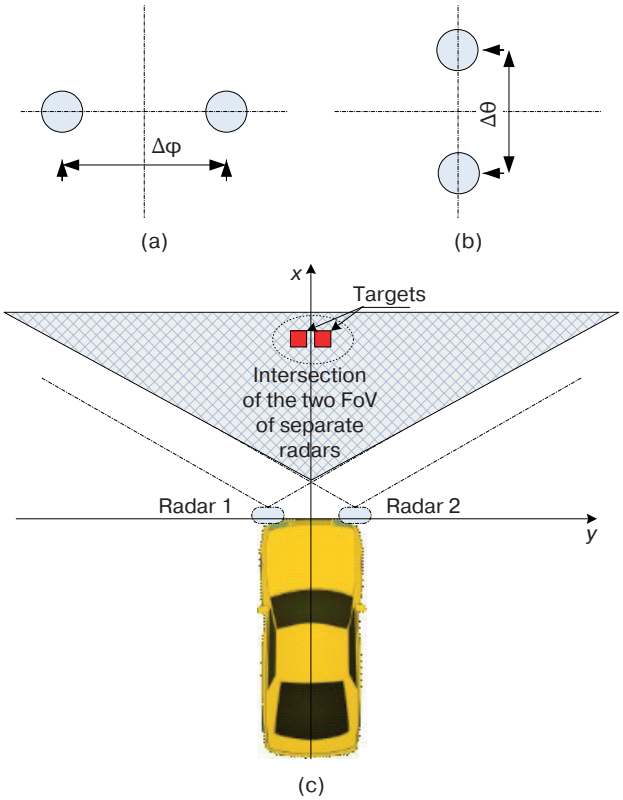

Fig. 9. Spatial arrangement scenarios for two close targets:
(a) scenario 1; (b) scenario 2; (c) general geometry of the distributed system consisting of two radars

2. The mean square error (MSE) is the following:

$$MSE = \sqrt{\frac{1}{J}\sum_{k=1}^{J}\sigma_k^2},$$
$$\sigma_k^2 = \frac{1}{m-1}\sum_{i=1}^{m}\left(\hat{\varphi}_{ki} - \bar{\varphi}_k\right)^2,\ \bar{\varphi}_k = \frac{1}{m}\sum_{i=1}^{m}\hat{\varphi}_{ki}, \quad (14)$$

where $\hat{\varphi}_{km}$ is DoA estimate for the kth target in the mth experiment.

3. The systematic error (SE) is the following:

$$SE = \sqrt{\frac{1}{J}\sum_{k=1}^{J}\left(\bar{\varphi}_k - \varphi_k\right)^2}. \quad (15)$$

The generalized numerical simulation results for the proposed algorithm of sequential azimuth and elevation estimation are presented in Table 5. It can be seen that azimuth and elevation resolutions (1° and 2°, respectively) are achieved at SNR of 36 dB (scenario 1) and 20 dB (scenario 2) for the probability of estimating the number of targets equal to 0.5 correctly.

The comparison of metrics as functions of the SNR parameter for the considered algorithms under different scenarios is shown in Figs. 10 and 11. The full set of metrics under study consists of five graphs. The left part presents MSE and SE metrics as a function of SNR for azimuth estimation, while the right part presents that for elevation estimation. The MSE and SE metrics are presented making allowance for an additional constraint on the probability of detecting correctly the number of close targets ($p > 0.5$).

Table 5. Generalized numerical simulation results for the proposed algorithm of sequential azimuth and elevation estimation

Scenario	Resolution		Accuracy		SNR
	Azimuth, Δφ	Elevation, Δθ	Azimuth	Elevation	
1	1°	–	0.12° (MSE) 0.11° (SE)	0.6° (MSE) 0.04° (SE)	36 dB
2	–	2°	0.08° (MSE) 0.02° (SE)	0.45° (MSE) 0.04° (SE)	20 dB

Scenario 1 (Fig. 9a): two targets have azimuths ±0.5° and the same elevation of 0°.

The black dashed curve with asterisks corresponds to the proposed sequential algorithm for DRS; the black dashed curve with circles corresponds to DRS for the full 2D Capon algorithm; the blue curve with triangles/red curve with crosses is the DoA estimation for the single radar (left/right); the full 2D Capon algorithm is used. It can be seen from the graphs that the single radars have failed to reach the target metric level of correctly estimating the number of targets at $p = 0.5$. Thus, the results for SNR/SE metrics are not available in graphs.

The simulation results for the current scenario show that the proposed algorithm for sequential DoA estimation outperforms the full 2D Capon algorithm in terms of metrics for correctly estimating the number of targets (for large SNR values) and MSE due to the larger number of spatial samples during azimuth estimation at the first stage (72 *vs* 36, see Section 2.4). At the same time, SE metrics for two algorithms have close values.

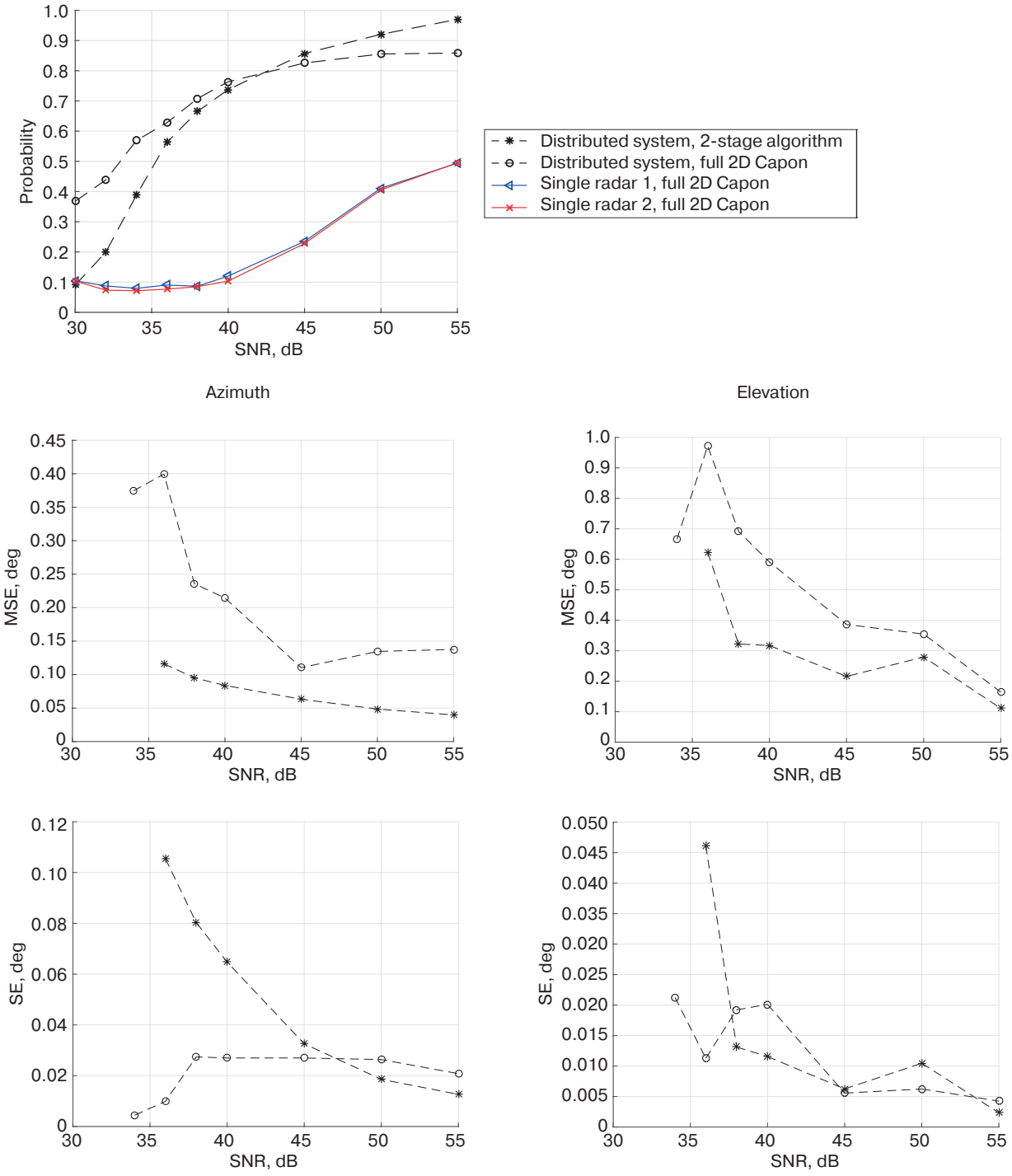

Fig. 10. Metrics as a function of SNR. Scenario 1

Scenario 2 (Fig. 9b): two targets have the same azimuth of 0° and elevation of ±1° (angular distance of 2° in the vertical plane).

The results of the study show that the sequential algorithm for estimating directions of arrival leads to an improvement in SNR and SE metrics. While a single radar can also distinguish between two close targets in Scenario 2 due to the same apertures of AASs of the single radar and the distributed system in the vertical plane, the single radar with the full 2D Capon algorithm loses in SNR and SE metrics to DRS with the two-step algorithm.

The advantage of the proposed algorithm for DoA sequential estimation compared to the full 2D Capon algorithm can be explained by a more accurate azimuth estimation at the first stage of the method due to a larger number of spatial samples (72 *vs* 36), while the classical 2D Capon algorithm is compelled to estimate azimuth and elevation simultaneously with a shorter spatial sample length.

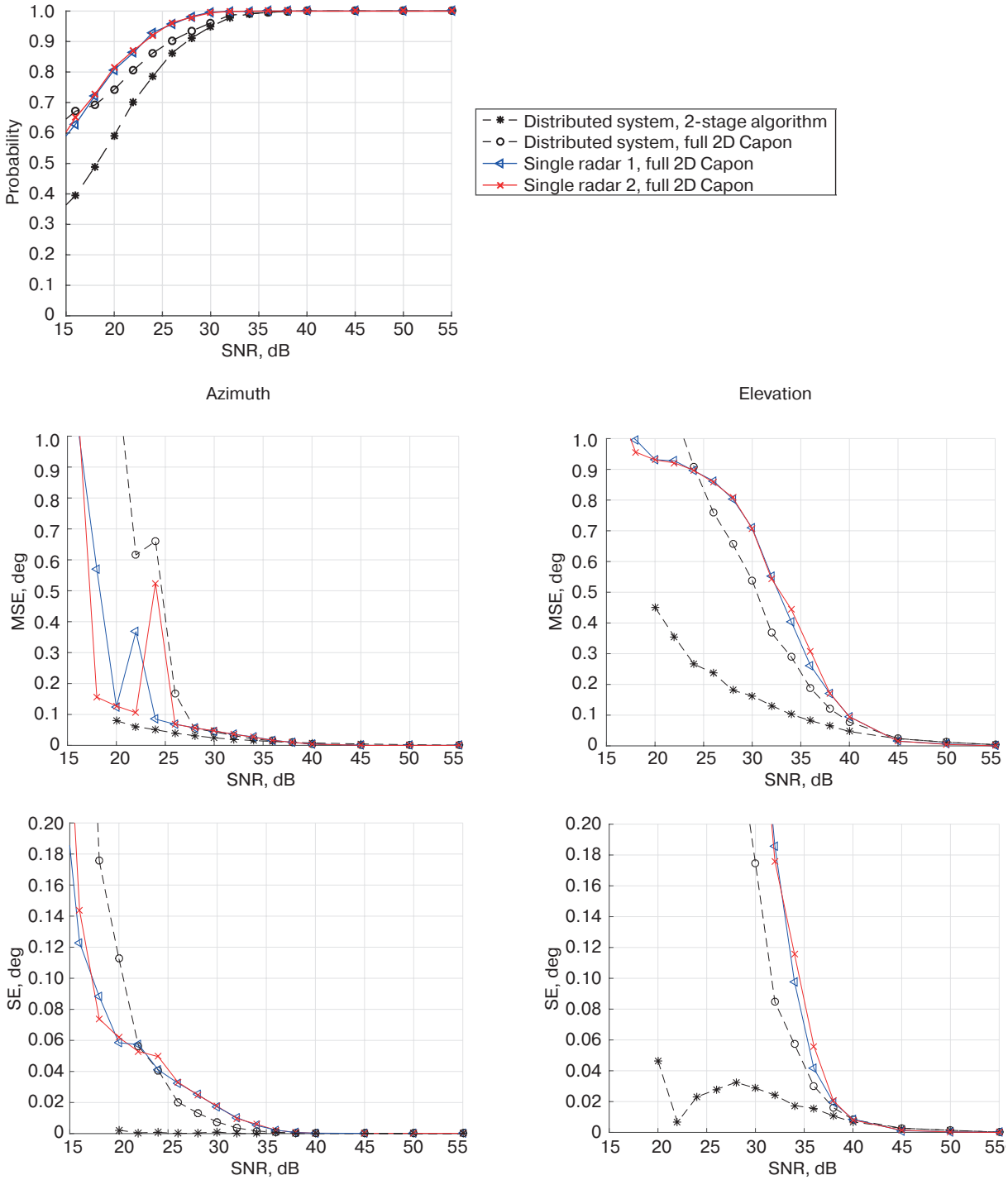

Fig. 11. Metrics as a function of SNR. Scenario 2

CONCLUSIONS

A two-dimensional method for estimating directions of arrival in azimuth and elevation planes for the distributed system of bistatic coherent MIMO-radars has been proposed. The method, which is based on the sequential estimation of DoAs (in the azimuth plane at the first stage and in the elevation plane at the second stage), ensures 1.9 times gain (at selected system parameters) in terms of use of computational resources as compared to the full classical 2D Capon method.

The comparative numerical simulation based on the Monte-Carlo method shows that the proposed scheme for coherent processing of distributed radar signals for DoA estimation leads to an improvement in target metrics (probability of correctly estimating the number of targets, MSE and SE) compared to a single radar. The performance of the system comprising coherent radars having a limited AAS configuration is comparable to that of a high-performance 4D radar with a much larger number of AAS elements.

REFERENCES

1. Giannini V., Goldenberg M., Eshrahi A., et al. 9.2 A 192-Virtual-Receiver 77/79GHz GMSK Code-Domain MIMO Radar System-on-Chip. In: *2019 IEEE International Solid-State Circuits Conference* (*ISSCC*), San Francisco, CA, USA. 2019. P. 164–166. https://doi.org/10.1109/ISSCC.2019.8662386
2. Godara L.C. *Smart Antennas*. CRC Press; 2004. 472 p.
3. Tuncer T.E., Friedlander B. (Eds.). *Classical and Modern Direction-of-Arrival Estimation*. Academic Press, Inc.; 2009. 456 p. https://doi.org/10.1016/C2009-0-19135-3
4. Ermolaev V.T., Flaksman A.G., Elokhin A.V., et al. Minimal Polynomial Method for Estimating Parameters of Signals Received by an Antenna Array. *Acoust. Phys.* 2018;64(1):83–90. https://doi.org/10.1134/S1063771018010050
   [Original Russian Text: Ermolaev V.T., Flaksman A.G., Elokhin A.V., Kuptsov V.V. Minimal Polynomial Method for Estimating Parameters of Signals Received by an Antenna Array. *Akusticheskii Zhurnal*. 2018;64(1):78–85 (in Russ.). https://doi.org/10.7868/S0320791918010057]
5. Ermolaev V.T., Flaksman A.G., Elokhin A.V., et al. Angular Superresolution of the Antenna-Array Signals Using the Root Method of Minimum Polynomial of the Correlation Matrix. *Radiophys. Quantum Electron*. 2018;61(3):232–241. https://doi.org/10.1007/s11141-018-9884-5
   [Original Russian Text: Ermolaev V.T., Flaksman A.G., Elokhin A.V., Shmonin O.A. Angular Superresolution of the Antenna-Array Signals Using the Root Method of Minimum Polynomial of the Correlation Matrix. *Izvestiya Vysshikh Uchebnykh Zavedenii. Radiofizika*. 2018;61(3):261–272 (in Russ.).]
6. Rodionov A.A., Turchin V.I. Processing of Antenna-Array Signals on the Basis of the Interference Model Including a Rank-Deficient Correlation Matrix. *Radiophys. Quantum Electron*. 2017;60(1):54–64. https://doi.org/10.1007/s11141-017-9776-0
   [Original Russian Text: Rodionov A.A., Turchin V.I. Processing of Antenna-Array Signals on the Basis of the Interference Model Including a Rank-Deficient Correlation Matrix. *Izvestiya Vysshikh Uchebnykh Zavedenii. Radiofizika*. 2017;60(1):60–71 (in Russ.).]
7. Patole S.M., Torlak M., Wang D., Ali M. Automotive radars: A review of signal processing techniques. *IEEE Signal Processing Magazine.* 2017;34(2):22–35. https://doi.org/10.1109/MSP.2016.2628914
8. Ermolaev V.T., Semenov V.Yu., Flaksman A.G., Artyukhin I.V., Shmonin O.A. The method of forming virtual receiving channels in the automobile MIMO-radar. *Radiotekhnika = J. Radioengineering*. 2021;85(7):115–126 (in Russ.).
9. Li J., Stoica P. *MIMO Radar Signal Processing*. Wiley-IEEE Press; 2009. 448 p. ISBN 978-0-4701-7898-0
10. Folster F., Rohling H., Lubbert U. An automotive radar network based on 77 GHz FMCW sensors. In: *IEEE International Radar Conference*. 2005. P. 871–876. https://doi.org/10.1109/RADAR.2005.1435950
11. Artyukhin I.V., Averin I.M., Flaksman A.G., Rubtsov A.E. Direction-of-Arrival Estimation Algorithm in Automotive Distributed Non-Coherent Multi-Radar Systems. *Zhurnal radioelektroniki = J. Radio Electronics*. 2023;4:1–20 (in Russ.). https://doi.org/10.30898/1684-1719.2023.4.2
12. Gottinger M., Hoffmann M., Christmann M., Schutz M., Kirsch F., Gulden P., Vossiek M. Coherent Automotive Radar Networks: The Next Generation of Radar-Based Imaging and Mapping. *IEEE Journal of Microwaves*. 2021;1(1):149–163. https://doi.org/10.1109/JMW.2020.3034475
13. Richards M.A. *Fundamentals of Radar Signal Processing*. 2nd edition. New York: McGraw-Hill; 2014. 656 p.
14. Ermolaev V.T., Flaksman A.G., Shmonin O.A. Using the Concept of a Virtual Antenna Array in a MIMO Radar in the Presence of Reflections from the Ground Surface. *Radiophys. Quantum Electron*. 2020;63(3):218–226. https://doi.org/10.1007/s11141-021-10047-1
    [Original Russian Text: Ermolaev V.T., Flaksman A.G., Shmonin O.A. Using the Concept of a Virtual Antenna Array in a MIMO Radar in the Presence of Reflections from the Ground Surface. *Izvestiya Vysshikh Uchebnykh Zavedenii. Radiofizika*. 2020;63(3):240–249(in Russ.).]
15. Björnson E., Hoydis J., Sanguinetti L. Massive MIMO Networks: Spectral, Energy, and Hardware Efficiency. *Foundations and Trends® in Signal Processing.* 2017;11(3–4):154–655. http://doi.org/10.1561/2000000093
16. Gentilho E., Scalassara P.R., Abrão T. Direction-of-Arrival Estimation Methods: A Performance-Complexity Tradeoff Perspective. *J. Sign. Process. Syst.* 2020;92(2):239–256. https://doi.org/10.1007/s11265-019-01467-4

СПИСОК ЛИТЕРАТУРЫ

1. Giannini V., Goldenberg M., Eshrahi A., et al. 9.2 A 192-Virtual-Receiver 77/79GHz GMSK Code-Domain MIMO Radar System-on-Chip. In: *2019 IEEE International Solid-State Circuits Conference* (*ISSCC*), San Francisco, CA, USA. 2019. P. 164–166. https://doi.org/10.1109/ISSCC.2019.8662386
2. Godara L.C. *Smart Antennas*. CRC Press; 2004. 472 p.
3. Tuncer T.E., Friedlander B. (Eds.). *Classical and Modern Direction-of-Arrival Estimation*. Academic Press, Inc.; 2009. 456 p. https://doi.org/10.1016/C2009-0-19135-3
4. Ермолаев В.Т., Флаксман А.Г., Елохин А.В., Купцов В.В. Метод минимального многочлена для оценки параметров сигналов, принимаемых антенной решеткой. *Акустический журнал*. 2018;64(1):78–85. https://doi.org/10.7868/S0320791918010057
5. Ермолаев В.Т., Флаксман А.Г., Елохин А.В., Шмонин О.А. Угловое сверхразрешение сигналов в антенной решетке с помощью корневого метода минимального многочлена корреляционной матрицы. *Известия вузов. Радиофизика*. 2018;61(3):261–272.
6. Родионов А.А., Турчин В.И. Обработка сигналов в антенных решётках на основе модели помехи, включающей корреляционную матрицу неполного ранга. *Известия вузов. Радиофизика*. 2017;60(1):60–71.
7. Patole S.M., Torlak M., Wang D., Ali M. Automotive radars: A review of signal processing techniques. *IEEE Signal Processing Magazine.* 2017;34(2):22–35. https://doi.org/10.1109/MSP.2016.2628914
8. Ермолаев В.Т., Семенов В.Ю., Флаксман А.Г., Артюхин И.В., Шмонин О.А. Метод формирования виртуальных приемных каналов в автомобильном MIMO-радаре. *Радиотехника*. 2021;85(7):115–126.
9. Li J., Stoica P. *MIMO Radar Signal Processing*. Wiley-IEEE Press; 2009. 448 p. ISBN 978-0-4701-7898-0
10. Folster F., Rohling H., Lubbert U. An automotive radar network based on 77 GHz FMCW sensors. In: *IEEE International Radar Conference*. 2005. P. 871–876. https://doi.org/10.1109/RADAR.2005.1435950
11. Артюхин И.В., Аверин И.М., Флаксман А.Г., Рубцов А.Е. Алгоритм оценки углов прихода сигналов в системе распределенных некогерентных автомобильных радаров. *Журнал радиоэлектроники*. 2023;4:1–20. http://jre.cplire.ru/jre/apr23/2/text.pdf
12. Gottinger M., Hoffmann M., Christmann M., Schutz M., Kirsch F., Gulden P., Vossiek M. Coherent Automotive Radar Networks: The Next Generation of Radar-Based Imaging and Mapping. *IEEE Journal of Microwaves*. 2021;1(1):149–163. https://doi.org/10.1109/JMW.2020.3034475
13. Richards M.A. *Fundamentals of Radar Signal Processing*. 2nd edition. New York: McGraw-Hill; 2014. 656 p.
14. Ермолаев В.Т., Флаксман А.Г., Шмонин О.А. Применение концепции виртуальной антенной решетки в MIMO-радаре при наличии отражений от земной поверхности. *Известия вузов. Радиофизика*. 2020;63(3):240–249.
15. Björnson E., Hoydis J., Sanguinetti L. Massive MIMO Networks: Spectral, Energy, and Hardware Efficiency. *Found. Trends® Sign. Process.* 2017;11(3–4):154–655. http://doi.org/10.1561/2000000093
16. Gentilho E., Scalassara P.R., Abrão T. Direction-of-Arrival Estimation Methods: A Performance-Complexity Tradeoff Perspective. *J. Sign. Process. Syst.* 2020;92(2):239–256. https://doi.org/10.1007/s11265-019-01467-4

About the author

Igor V. Artyukhin, Engineer, Department of Statistical Radiophysics and Mobile Communication Systems, Faculty of Radiophysics, National Research Lobachevsky State University of Nizhny Novgorod (23, Gagarina pr., Nizhny Novgorod, 603022 Russia). E-mail: artjukhin@rf.unn.ru. Scopus Author ID 57216223873, https://orcid.org/0009-0008-5139-6443

Об авторе

Артюхин Игорь Владимирович, электроник 1 категории, кафедра статистической радиофизики и мобильных систем связи, Радиофизический факультет, ФГАОУ ВО «Национальный исследовательский Нижегородский государственный университет им. Н.И. Лобачевского» (603022, Россия, Нижний Новгород, пр-т Гагарина, д. 23). E-mail: artjukhin@rf.unn.ru. Scopus Author ID 57216223873, https://orcid.org/0009-0008-5139-6443

Translated from Russian into English by K. Nazarov
Edited for English language and spelling by Thomas A. Beavitt

Mathematical modeling

Математическое моделирование

UDC 519.63
https://doi.org/10.32362/2500-316X-2024-12-3-78-92
EDN WBOETG

RESEARCH ARTICLE

Analyzing and forecasting the dynamics of Internet resource user sentiments based on the Fokker–Planck equation

Julia P. Perova [@], **Sergey A. Lesko, Andrey A. Ivanov**

MIREA – Russian Technological University, Moscow, 119454 Russia
[@] *Corresponding author, e-mail: jul-np@yandex.ru*

Abstract

Objectives. The study aims to theoretically derive the power law observed in practice for the distribution of characteristics of sociodynamic processes from the stationary Fokker–Planck equation and apply the non-stationary Fokker–Planck equation to describe the dynamics of processes in social systems.

Methods. During the research, stochastic modeling methods were used along with methods and models derived from graph theory, as well as tools and technologies of object-oriented programming for the development of systems for collecting data from mass media sources, and simulation modeling approaches.

Results. The current state of the comment network graph can be described using a vector whose elements are the average value of the mediation coefficient, the average value of the clustering coefficient, and the proportion of users in a corresponding state. The critical state of the network can be specified by the base vector. The time dependence of the distance between the base vector and the current state vector forms a time series whose values can be considered as the "wandering point" whose movement dynamics is described by the non-stationary Fokker–Planck equation. The current state of the comment graph can be determined using text analysis methods.

Conclusions. The power law observed in practice for the dependence of the stationary probability density of news distribution by the number of comments can be obtained from solving the stationary Fokker–Planck equation, while the non-stationary equation can be used to describe processes in complex network structures. The vector representation can be used to describe the comment network states of news media users. Achieving or implementing desired or not desired states of the whole social network can be specified on the basis of base vectors. By solving the non-stationary Fokker–Planck equation, an equation is obtained for the probability density of transitions between system states per unit time, which agree well with the observed data. Analysis of the resulting model using the characteristics of the real time series to change the graph of comments of users of the RIA Novosti portal and the structural parameters of the graph demonstrates its adequacy.

Keywords: social networks, modeling of social processes, network graph, network graph characteristics, Fokker–Planck equation, monitoring, management, nonlinear dynamics, power law of distribution

• **Submitted:** 12.01.2023 • **Revised:** 17.11.2023 • **Accepted:** 08.04.2024

For citation: Perova J.P., Lesko S.A., Ivanov A.A. Analyzing and forecasting the dynamics of Internet resource user sentiments based on the Fokker–Planck equation. *Russ. Technol. J*. 2024;12(3):78–92. https://doi.org/10.32362/2500-316X-2024-12-3-78-92

Financial disclosure: The authors have no a financial or property interest in any material or method mentioned.

The authors declare no conflicts of interest.

НАУЧНАЯ СТАТЬЯ

Анализ и прогнозирование динамики настроений пользователей интернет-ресурсов на основе уравнения Фоккера – Планка

Ю.П. Перова [@], **С.А. Лесько**, **А.А. Иванов**

МИРЭА – Российский технологический университет, Москва, 119454 Россия
[@] *Автор для переписки, e-mail: jul-np@yandex.ru*

Резюме

Цели. Цель работы – вывод наблюдаемого на практике степенного закона распределения характеристик социодинамических процессов из стационарного уравнения Фоккера – Планка и проверка возможности применения нестационарного уравнения Фоккера – Планка для описания динамики процессов в социальных системах.

Методы. При проведении исследований были использованы методы моделирования стохастических процессов, методы и модели теории графов, инструменты и технологии объектно-ориентированного программирования для разработки систем сбора данных из массмедиа-источников, методы имитационного моделирования.

Результаты. Наблюдаемое текущее состояние графа сети комментариев может быть описано с помощью вектора, элементами которого являются среднее значение коэффициента посредничества, среднее значение коэффициента кластеризации, доля пользователей в конкретном состоянии. Критическое состояние сети может быть задано базовым вектором. Зависимость от времени расстояния между базовым вектором и текущим вектором состояния образует временной ряд, значения которого можно рассматривать как «блуждающую точку», динамика перемещений которой описывается нестационарным уравнением Фоккера – Планка. Текущее состояние графа комментариев можно определить с помощью методов текстовой аналитики.

Выводы. Наблюдаемый на практике степенной закон зависимости стационарной плотности вероятности распределения новостей по числу комментариев может быть получен из решения стационарного уравнения Фоккера – Планка, а нестационарное уравнение может быть использовано для описания процессов в сложных сетевых структурах. Для описания состояний сети комментариев пользователей новостных массмедиа можно использовать векторное представление. Достижение или реализация желаемых, или нежелательных состояний всей социальной сети могут быть заданы на основе базовых векторов. Решение нестационарного уравнения Фоккера – Планка позволяет получить уравнение для плотности вероятности переходов между состояниями системы в единицу времени, которые хорошо согласуются с наблюдаемыми данными. Анализ полученной модели с использованием характеристик реального временного ряда для изменения графа комментариев читателей официальной страницы в социальной сети «ВКонтакте» информационного агентства «РИА Новости» и структурных параметров графа показывает ее адекватность.

Ключевые слова: социальные сети, моделирование социальных процессов, сетевой граф, характеристики сетевого графа, уравнение Фоккера – Планка, мониторинг, управление, нелинейная динамика, степенной закон распределения

• **Поступила:** 12.01.2023 • **Доработана:** 17.11.2023 • **Принята к опубликованию:** 08.04.2024

Для цитирования: Перова Ю.П., Лесько С.А., Иванов А.А. Анализ и прогнозирование динамики настроений пользователей интернет-ресурсов на основе уравнения Фоккера – Планка. *Russ. Technol. J*. 2024;12(3):78–92. https://doi.org/10.32362/2500-316X-2024-12-3-78-92

Прозрачность финансовой деятельности: Авторы не имеют финансовой заинтересованности в представленных материалах или методах.

Авторы заявляют об отсутствии конфликта интересов.

INTRODUCTION

One of the most important trends in mathematical sociology consists in methods for describing the behavior of users of social networks and information resources. In practical terms, the creation of models describing the manifestation dynamics of user opinions and preferences can be used to develop systems for the automated monitoring of social sentiment along with trends of its change. The advantage of these systems over traditional methods for studying public opinion is their technological feasibility.

Significantly, the dynamics of changes in the opinions and attitudes of Internet users can be attributed to stochastic processes. While on the one hand, the presence of the human factor (many people having different opinions, preferences, etc.) creates randomness of changes due to the great variety of user behavioral patterns, this also introduces elements of purposefulness into the dynamics of changes on the other hand.

In [1], a model describing the spatial and temporal diffusion of information in social networks based on a stochastic partial differential equation is considered. The creation and study of a non-autonomous diffusion logistic model with Dirichlet boundary conditions demonstrates that information diffusion in social networks is strongly influenced by the diffusion coefficient and the internal growth rate (information dissemination or rumors can be considered as resembling viruses that do not possess a physical form).

Among the most promising for modelling dynamics of changes in social sentiment are models created on the basis of stochastic differential equations, for example, the Fokker–Planck equation, which accounts for both ordered ("drift") and random changes ("diffusion"). The Fokker–Planck equation is widely used to analyze and model the behavior of time series when describing processes in complex systems [2–5].

In addition to the Fokker–Planck equation, approaches for modeling on the basis of differential equations include the Liouville equations [5, 6], diffusion equations [4, 7], and some others.

In addition to describing dynamic processes from the Fokker–Planck equation, stationary solutions can be obtained, which can describe the condition of any system in a stationary state, for example, when its evolution has already ended resulting in no changes having occurred.

For modeling social processes, not only models based on partial differential equations are used but also such as those based on game-theory approaches, as well as management decisions carried out on their basis [8].

Since the dynamics of processes in network structures is inextricably linked to their topology, their structural characteristics should be taken into account. In [9], for example, a methodology for analyzing topics in a social network is presented, which includes collecting, processing, and classifying information, as well as measuring the time between publications. This data is then used to create a timeline.

On this basis, a graph is constructed for tracking changes in the popularity of specific topics discussed on social media. This graph can also be used to visualize related events based on social sentiment, as well as to identify periods of active discussions on specific topics. In [10], the Kronecker graph model is used to study community detection on graphs, overlapping community detection, as well as community detection in incomplete networks with missing links and in complete networks.

The use of nature-like algorithms is also gaining popularity for investigating the link structure of social networks. In particular, in [11], swarm-like algorithms are used in social network analysis to optimize the process of solving link prediction and community detection problems. With increasing network sizes, finding similarities between their nodes becomes a rather resource-intensive process.

Although the study of processes occurring in complex systems involving the human factor shows that the power law of distribution $\rho(x) \sim x^{-\gamma}$ (where γ is the characteristic degree) is fulfilled very often for the observed parameter characteristics of these processes [12–17], its theoretical foundation requires further study. In order to carry out a deeper study of the

behavior and analysis of complex social systems, it will be necessary to identify the nature of processes that give rise to the degree law.

In this regard, studying the possibility of applying the Fokker–Planck equation to model the dynamics of social processes looks very promising.

1. DATA COLLECTION AND PROCESSING

Several news portals and one of the online communities of the VKontakte social network dedicated to discussing the news of the RIA Novosti information resource[1] were selected for study. This resource was chosen based on its recognizability and popularity in Russian society; it ranks first among media resources (for March 2022) according to Brand Analytics[2], is among the top 3 most quoted news agencies in mass media and social media (for March 2022), and ranks first[3] by these indicators in the Russian Internet segment.

First, a special software application (parser) was used to download the desired range of news from January 1, 2019 to April 2022 from the official RIA Novosti community in the VKontakte social network using the developed parser and the network application programming interface[4]. Within the social network, each post has its own unique address, where {owner_id} is the community unique identifier (for RIA_Novosti, it is "-15755094"), while {post_id} is the unique identifier of the post (news). Each post (news) has a number of basic parameters such as: unique identifier of the post in the social network; post text; date and time of publication; and number of views and user comments. Comments have the following parameters: unique identifier in the social network community; unique user identifier; comment text; date and time of appearance; comment hierarchy level; and connection by comment level with parent comment (which user comments on which other user when discussing the news).

Since comments could be left by chatbots, spammers, and unscrupulous users who write comments on a professional basis, it is necessary to introduce data-scrubbing rules. Users writing more than 7,365 comments during a year (more than 20 comments per day on average) or who write with a frequency of more than one comment per 5 min are considered as unscrupulous.

When analyzing the obtained data, it is necessary to determine to what distribution law the observed distribution density obeys. For this, the following three most frequently observed distribution laws are examined: Gaussian $\rho(x) = e^{-\frac{x^2}{2\sigma^2}} \Big/ \sigma\sqrt{2\pi}$; exponential $\rho(x) = ae^{-\alpha x}$, and power series $\rho(x) \sim \beta x^{-\gamma}$. When processing the collected data using linearization in appropriate coordinates, the closest linearization is observed for the power law (Fig. 1). For other laws, worse linearization is observed.

The straight line drawn in Fig. 1 shows that the trend line is well described by the linear approximation $y = -0.76 - 1.48z$, where $y = \ln\{\rho(x)\}$, $z = \ln\{x\}$, $\ln\{\beta\} = -0.76$, and the correlation coefficient is 0.95.

In order to confirm the conclusion about linear approximation, the behavior of the residuals can be studied in order to test the hypothesis that they are normally distributed with mean equal to zero and have homogeneous variance. The equation is derived from residuals calculated based on the actually observed values for the natural logarithm of the fraction of commenters who have written a certain number of comments. The calculated value of the mathematical expectation for the distribution of residuals is equal to 0.25, while the variance is 0.13. The test of the slope hypothesis (two-sample F-test for variances) shows that the variance of residuals (calculated relative to the trend line) equal to 2.11 ($0.13 << 2.11$) is significantly smaller than that of the deviation of linear regression points from the mean value of the observed data ($\Sigma y_i/n = \Sigma\ln\{\rho(x_i)\}/n$). Thus, it can be concluded from the obtained data that the distribution of residuals is very close to normal, while the obtained regression is significant. This supports the conclusion that the natural logarithm of the fraction of commenters who have written these comments depends linearly on the natural logarithm of the number of comments, which confirms the fulfillment of the power law.

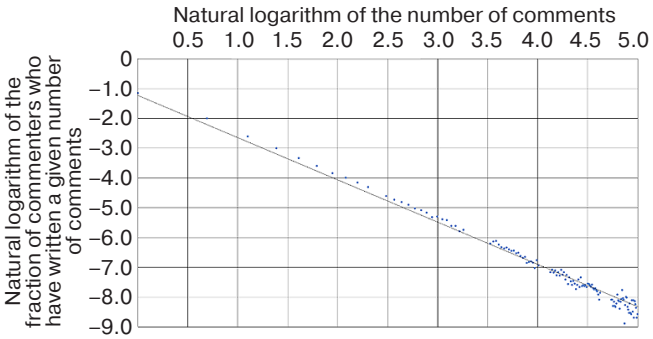

Fig. 1. Linearization of the observed data for the power series distribution of the fraction of commenters to the number of comments made

[1] https://vk.com/ria (in Russ.). Accessed September 02, 2023.
[2] https://br-analytics.ru/mediatrends/media/?period=202203 (in Russ.). Accessed September 02, 2023.
[3] https://www.mlg.ru/ratings/media/federal/11110/#internet (in Russ.). Accessed September 02, 2023.
[4] https://dev.vk.com/guide (in Russ.). Accessed September 02, 2023.

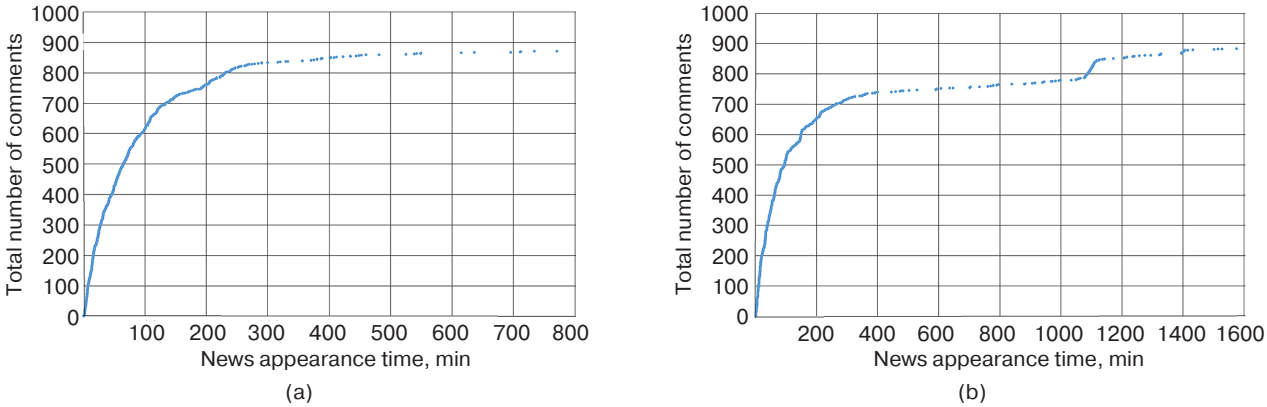

Fig. 2. Observed dynamics of change in the number of comments to news items

It is also of interest in research to analyze the dynamics of change in the number of comments on news of great public interest over time (such news gathers hundreds of comments during the viewing period).

Observing this dynamic of change shows that it can have both S-shaped and two-stage character. For demonstrating such dynamics of commenting on RIA Novosti news by VKontakte users, the following several news items are selected:

1. "Zelensky had left Ukraine and moved to Poland, Volodin said" (see Fig. 2a, where the dynamics of comments has an S-shaped character)[5, 6], origin date and time: 2022-03-04 16:13:27 UTC +03:00). The total number of comments is 894. The number of first-level comments (comments on the news itself) is 433, while the number of second-level comments (first-level comments on the comments) is 461. The total number of views is 118764. The average appearance time of the first-level comments is 73 min while that of the second-level comments is 74 min.
2. "Soon the city will be liberated, he stated" (see Fig. 2b, where the dynamics of comments has a two-stage character)[7, 8], origin date and time: 2022-04-10 17:14:40 UTC +03:00). The total number of comments is 901. The number of first-level comments is 173 and the number of second-level comments is 728. The total number of views is 173607. The average appearance time of the first-level comments is 75 min and that of the second-level comments is 82 min.

In our view, this can be related to the difference in the average appearance time of the second-level comments (the time interval between the appearance of the first-level comments and the commentary on these comments), as well as to the ratio between the number of comments of the first and second levels. For the first news item, the average appearance time intervals of the first and second-level comments practically coincide; for the second news item, there is a slight increase in the average appearance time interval of the second-level comments (time lag occurs). In addition, their number significantly exceeds the number of comments of the first-level for the second news item.

The following task of further theoretical research can be formulated: what is the nature of commenting news and blogs, and what features of these complex social systems result in describing the probability density of comment distribution on the number of comments using the power law, whose dynamics have a complex two-step character over many cases.

2. SOLVING THE STATIONARY FOKKER–PLANCK EQUATION

In general, the Fokker–Planck equation has the following form:

$$\frac{\partial \rho(x,t)}{\partial t} = -\frac{\partial}{\partial x}[\mu(x)\rho(x,t)] + \frac{1}{2}\cdot\frac{\partial^2}{\partial x^2}[D(x)\rho(x,t)], \quad (1)$$

where $\rho(x, t)$ is the time t dependent probability density of distribution over states x (in our case, state x is the number of comments observed at time t); $D(x)$ is the state-dependent coefficient determining the random change of state x (diffusion); $\mu(x)$ is the state x dependent coefficient determining the purposeful change of state x (drift).

As applied to our model, $D(x)$ can be interpreted as the user activities caused by a spontaneous impulse arising from reading news item or comments of other users in case the event described in the news item or blog is not significantly important. The user is ready to

[5] https://vk.com/ria?w=wall-15755094_34243579 (in Russ.). Accessed September 02, 2023.
[6] https://ria.ru/20220304/zelenskiy-1776545154.html (in Russ.). Accessed September 02, 2023.
[7] https://vk.com/ria?w=wall-15755094_35202266 (in Russ.). Accessed September 02, 2023.
[8] https://ria.ru/20220410/ukraina-1782778315.html (in Russ.). Accessed September 02, 2023.

spend time on commenting or responding to another commenter (the user has a spontaneous desire to respond to this news item). The coefficient $\mu(x)$ can be interpreted as purposeful behavior caused by the desire to respond to a news item or blog event that is essential for the user as well as to comment on another user's comment in case it addresses an important topic from this user perspective (the user is constantly interested in this topic).

For building the model, assumptions about the dependence of $D(x)$ and $\mu(x)$ on state x should be made and two conditions should be considered. First, the dimensionality of the terms included in Eq. (1) should be taken into account; second, it can be assumed that as the state x grows (the number of possible comments, the importance of the news or blog), values $D(x)$ and $\mu(x)$ should also increase. Physical considerations suggest that all terms of Eq. (1) should have the same dimensionality, which $\rho(x, t)$ has. Both the first and the second condition would be satisfied if dependencies of $D(x)$ and $\mu(x)$ on state x have the following form: $\mu(x) = \mu_0 x$ and $D(x) = D_0 x^2$. The coefficients μ_0 and D_0 have dimensionality $1/t$.

The solution of the stationary Fokker–Planck equation is written as follows:

$$-\frac{d}{\partial x}[\mu(x)\rho(x)]+\frac{1}{2}\cdot\frac{d^2}{dx^2}[D(x)\rho(x)]=0$$

under the following assumptions: $\mu(x) = \mu_0 x$ and $D(x) = D_0 x^2$ has the form $\rho(x) = [\gamma - 1]x^{-\gamma}$, which corresponds to the power law observed in practice.

According to the results obtained from analyzing the observed data, $\gamma = 1.48$, and $\gamma - 1 = 0.48$, the natural logarithm $(\gamma - 1)$ is -0.73, which is equal to $\ln\{\beta\} = -0.76$ with sufficiently high precision (see the resulting linearization equation: $y = -0.76 - 1.48z$, where $y = \ln\{\rho(x)\}$, $z = \ln\{x\}$, $\ln\{\beta\} = \ln\{\gamma - 1\} - 0.76$, and the correlation coefficient is 0.95). This generally indicates the adequacy of the developed model. Note that the terms of the stationary equation for $\rho(x)$ should also have the same dimensionality. The solution of the stationary equation includes expression $2\left[1-\frac{\mu_0}{D_0}\right]=\gamma$ which does not depend on t.

Deriving the power law can be described as follows. We substitute expressions for $\mu(x)$ and $D(x)$ into the stationary Fokker–Planck equation.

Substituting $D(x)$ and $\mu(x)$ into Eq. (1), the following is obtained:

$$-\mu_0 x\frac{d\rho(x)}{dx}-\mu_0\rho(x)+\frac{1}{2}D_0x^2\frac{d^2\rho(x)}{dx^2}+$$
$$+2D_0x\frac{d\rho(x)}{dx}+D_0x\rho(x)=0.$$

We denote $2\left[1-\frac{\mu_0}{D_0}\right]=\gamma$, then

$$x^2\frac{d^2\rho(x)}{dx^2}+[2+\gamma]x\frac{d\rho(x)}{dx}+\gamma\rho(x)=0.$$

The solution of the resulting equation can be sought in the form $\rho(x)=\sum_k C_k x^q$, where C_k are constant coefficients at corresponding roots of the characteristic equation having the form $q(q-1)+[2+\gamma]q+\gamma=0$. This equation has two roots: $q_1 = -1$ and $q_2 = -\gamma$. Thus, for $\rho(x)$, we obtain: $\rho(x) = C_1x^{-1} + C_2x^{-\gamma}$. The constant coefficients C_1 and C_2 are found using the normalization condition for function $\rho(x)$, as follows:

$$\int_1^\infty \rho(x)dx = C_1\ln x\Big|_1^\infty + C_2\frac{x^{1-\gamma}}{1-\gamma}\Big|_1^\infty \equiv 1.$$

The integral is calculated from 1 to ∞, since there may be users who have written a very large number of comments on news items, but there cannot be commenters who have written less than one comment. Given that at $x\to\infty$, $\ln x\big|_\infty = \infty, C_1 = 0$ and $C_2 = \gamma - 1$, respectively, we finally obtain: $\rho(x) = [\gamma - 1]x^{-\gamma}$.

3. SOLVING THE NON-STATIONARY FOKKER–PLANCK EQUATION AND ANALYZING THE MODEL

We briefly derive the solution for the non-stationary Fokker–Planck equation. Using the Laplace transform method for the Fokker–Planck equation, the following can be written:

$$s\overline{G(s,x)}-\rho(x,0)=$$
$$=-\frac{d}{dx}\left[\mu(x)\overline{G(s,x)}\right]+\frac{1}{2}\cdot\frac{d^2}{dx^2}\left[D(x)\overline{G(s,x)}\right]. \quad (2)$$

Substituting the corresponding derivatives and dependencies of $\mu(x)$ and $D(x)$ into Eq. (2), we obtain the following:

$$x^2\frac{d^2\overline{G(s,x)}}{dx^2}+2\left[2-\frac{\mu_0}{D_0}\right]x\frac{d\overline{G(s,x)}}{dx}+$$
$$+2\left[1-\frac{\mu_0+s}{D_0}\right]\overline{G(s,x)}=-\frac{\delta(x-x_0)}{D_0}. \quad (3)$$

The solution of Eq. (3) will be found in the form: $\overline{G(s,x)}=\sum_k C_k x^q$, where C_k are the coefficients for the roots of the characteristic equation which has the following form:

$$q(q-1)+2\left[2-\frac{\mu_0}{D_0}\right]q+2\left[1-\frac{\mu_0+s}{D_0}\right]=0.$$

The solution to the non-stationary Fokker–Planck Eq. (3) under the $\mu(x)$ and $D(x)$ assumptions takes the following form:

$$\rho(x,t)=\int\frac{\left[\frac{[\ln x]^2}{D_0 t}+\left[\frac{1}{2}-\frac{\mu_0}{D_0}\right]\ln x-1\right]}{\sqrt{2\pi D_0 t^3}}\times \\ \times e^{-\left[\frac{[\ln x]^2}{2D_0 t}+\left[\frac{3}{2}-\frac{\mu_0}{D_0}\right]\ln x+\left[\frac{1}{2}-\frac{\mu_0}{D_0}\right]^2\frac{D_0 t}{2}\right]}dt. \quad (4)$$

The probability that the number of comments by time t reaches a certain number L can be found by the formula: $P(L,t)=1-\int_0^L\rho(x,t)dx$. The dependence of the number of comments on time t is described by equation: $N(t) = P(L, t)L$.

To analyze the obtained solution, simulation modeling is carried out. As an example, we select L = 100 and three sets of μ_0 and D_0 values: μ_0 = 0.45 and D_0 = 0.50 conventional units ($\mu_0 < D_0$ is curve 1 in Fig. 3a), μ_0 = 0.50 and D_0 = 0.50 conventional units ($\mu_0 = D_0$ is curve 2 in Fig. 3), and μ_0 = 0.55 and D_0 = 0.50 conventional units ($\mu_0 > D_0$ is curve 3 in Fig. 3a). The calculations show that, as μ_0 increases relative to D_0, the growth rate of curves for the number of comments $N(t)$ at the selected model parameters μ_0, D_0, and L increases (Fig. 3a).

A two-step curve can be obtained by using the distribution density function accounting for delay time τ, as follows:

$$\rho(x,t-\tau)=\int\frac{\left[\frac{[\ln x]^2}{D_0(t-\tau)}+\left[\frac{1}{2}-\frac{\mu_0}{D_0}\right]\ln x-1\right]}{\sqrt{2\pi D_0[t-\tau]^3}}\times \\ \times e^{-\left[\frac{[\ln x]^2}{2D_0[t-\tau]}+\left[\frac{3}{2}-\frac{\mu_0}{D_0}\right]\ln x+\left[\frac{1}{2}-\frac{\mu_0}{D_0}\right]^2\frac{D_0(t-\tau)}{2}\right]}dt. \quad (5)$$

Confirmation of the compliance between the theoretical model and the observed data (Figs. 2 and 3b) can be obtained on the assumption that two processes with different coefficients μ_0 and D_0 can occur simultaneously. Moreover, the sum of partial fractions of processes should be equal to 1, i.e., $P_{com}(L, t) = \alpha_1 P_1(L, t) + \alpha_2 P_2(L, t)$. As a purely illustrative modeling example, the following model parameters are selected for the process of commenting on the news item or blog itself: $\mu_{0,1}$ = 0.55, $D_{0,1}$ = 0.50. For commenting on comments: $\mu_{0,2}$ = 0.50, $D_{0,2}$ = 0.50, τ = 50 conventional units, α_1 = 0.75, α_2 = 0.25, and L = 100 ($\mu_{0,1} > \mu_{0,2}$ is selected based on the assumption that commenting on a news item is a more primary process for users than commenting on comments), where $\alpha_1 + \alpha_2 = 1$.

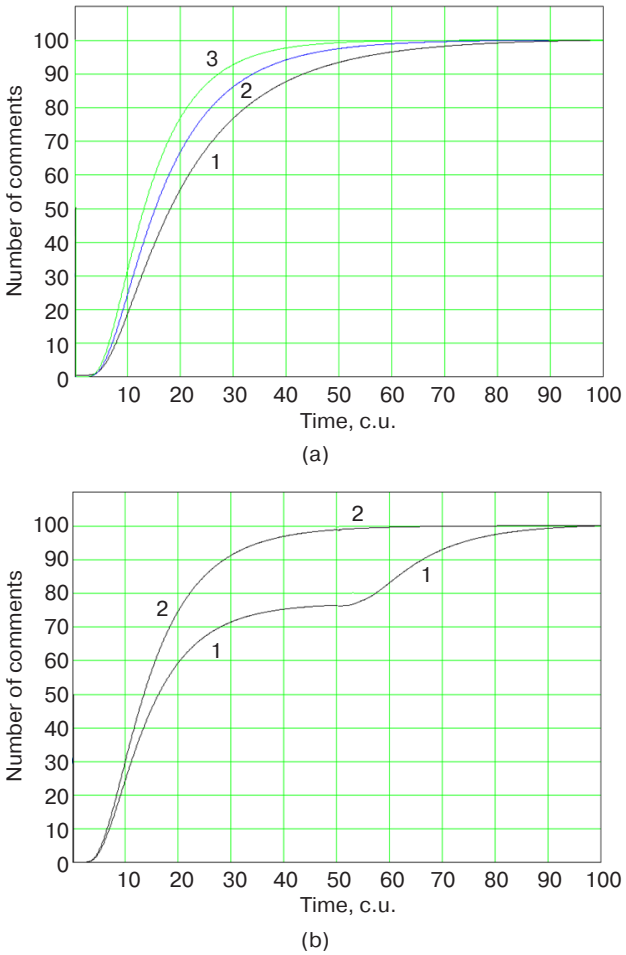

Fig. 3. Dynamics of change over time in the number of comments to the news item in the simulation model based on the Fokker–Planck equation:
(a) 1 process,
(b) 2 parallel processes

As indicated earlier, the plateau in curve 1 in Fig. 3b may be due to a significant difference in the average appearance time of the second-level comments (the time interval between the appearance of the first-level comment and the comment on a given comment), which may result in implementation of two-stage dynamics in the appearance of comments.

The results of modeling the dynamics of the change in the number of comments $N(t)$ over time with allowance for two processes running in parallel are shown in Fig. 3b. The results show a good compliance between the real data and theoretical calculations.

4. MODELING THE DYNAMICS OF THE INTERNET MASS MEDIA USER SENTIMENT BASED ON THE FOKKER–PLANK EQUATION AND CHANGES IN THE PARAMETERS OF THEIR COMMENT NETWORK GRAPHS

It is proposed to use vector representation to describe the states of the comment network. The elements of the vectors serve as allowed values of the network parameters (density, mediation coefficient average, value clustering coefficient average, elasticity, and others), as well as characteristics like fraction of users who can be attributed, based on the analysis of comment texts, to one of the following groups: 1) loyalist (unconditionally supports the actions of the government and authorities); 2) oppositionist; 3) "troll" (a user who uses the resource to blow the whistle); and 4) undecided or neutral. Achieving or implementing the desirable or undesirable states of the entire social network as a whole can be based on base vectors.

The time change in the value of the distance between the base vector and the vector of the current state can be considered as a "wandering point" on segment $[L_{min}, L_{max}]$ or as a random (or almost random) time series. Some given value of this distance (the state upon reaching which management decisions should be made) can be regarded as a trap or a point of the acceptable implementation threshold, where a "wandering point" can fall over time. This allows building probabilistic sociodynamic models for forecasting the dynamics of social sentiment.

The diffusion model is commonly used in the conventional description of the "wandering point" behavior. However, it cannot be considered reliable in this case. As a rule, time series describing processes in complex systems (for example, financial indicators of stock and commodity exchanges) are not stationary due to various reasons including the presence of human factor. Their sample distribution functions have the time dependent mathematical expectation, which contradicts the simple diffusion model and shows the non-stationarity of time series.

In this regard, it is intended to consider more complex models of the "wandering point" behavior, for example, based on the Fokker–Planck equations.

The graph structure obtained from processing news comments is shown in Fig. 4. When visualizing the obtained data in color, the graph nodes, depending on their state (attribution to one of 4 types), can be marked in different colors (oppositionists in green-sand color, "trolls" in red, loyalists in blue, and undecided in green). The links in the figure show mutual commenting of users by each other. Thus, one can estimate their state by the color of the nodes and the interaction by the graph edges.

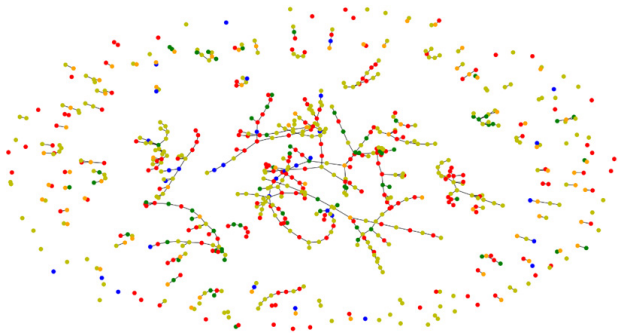

Fig. 4. Graph structure for comments to the news item under consideration

It is evident from Fig. 4 that this structure has many unconnected single vertices. In a connected component of the graph presented separately in Fig. 5, the closed oval lines (representing the core of the graph in Fig. 4) show the users commenting on themselves.

We consider the elements of the network state vector to be used in our model:

1. The fraction of nodes having a certain state (e.g., users who are negative about some social life event).
2. The clustering coefficient is a measure for the link density of a given node with its neighbors. The ratio of the real number of links connecting the nearest neighbors of a given node *i* to the maximum possible one (such that all the nearest neighbors of a given node would be connected to each other directly) is called the node clustering coefficient; its value lies on interval [0, 1]. The higher its value is, the more significant this node is in the process of information exchange.
3. The mediation degree shows the ratio of the number of shortest paths between all pairs of network nodes passing through a given node to the total number of all shortest paths in the network. Its value lies on the interval [0, 1]. The larger its value, the more significant is the role of a given node in information exchange.

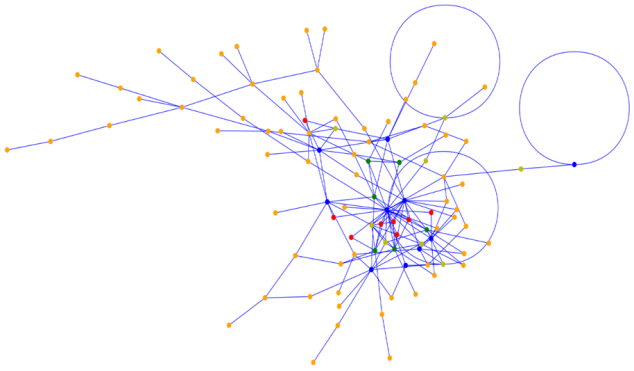

Fig. 5. Graph of user interconnections by comments

We define the values for the elements of the network state base vector (denoted by θ). They specify the threshold values, whose passing through is undesirable in terms of state management. Given that any community usually contains from 0.10 to 0.15 fraction of participants always disagreeing on any issue, we take the fraction of those who are negative about the considered event to be 0.12. The desired average value (over all nodes) of the clustering coefficient for such network is also assumed to be small, for example, equal to 0.05; the average degree of node mediation in such network is also equal to 0.05. Thus, the basis vector would have the following form: θ = (0.12; 0.05; 0.05).

Note that the number of parameters used to describe the network state may be larger. Only those considered the most important are selected. In addition, the selected parameters are normalized (lie in interval [0, 1]) so that they have the same effect on calculating the distance metric.

In the proposed approach, different graphs of news commenting on certain topics on a selected info resource during a day can be combined into a single structure through links between nodes that refer to users. In this way, a large graph describing the activity of users of a given network info resource during a day can be identified. Next, it is possible to define the elements of the current state vector that describes its characteristics.

Changes in this vector components for each day during a certain time would form some time series.

For describing the change in the value of the distance between the value of the current state vector and a given basis vector over time, the solution of the non-stationary Fokker–Planck equation is considered, which may allow the construction of probabilistic sociodynamic models for predicting the dynamics of social sentiment.

We formulate the boundary value problem, whose solution describes the process of changing the value of the distance between the value of the current state vector in the comment network graph and a given basis vector over time.

First boundary condition. When selecting the first boundary condition, we assume the following: state $x = L_{\min}$ (the left boundary of the segment of possible states) determines the state whose passing through should be avoided (the area to the left of this state on the segment is undesirable). The probability of detecting such a system state may be non-zero, while the probability density determining the flow in state $x = L_{\min}$ should be taken as equal to 0, since the states should not exceed this boundary (here the reflection condition is implemented). Thus:

$$\rho(x,t)\big|_{x=L_{\min}} = 0. \tag{6a}$$

Second boundary condition. We limit the area of possible states to the right by some value $x = L_{\max}$ (the metric used in calculations cannot be larger than the value of the vector whose elements have maximum values in the space of selected coordinates). The probability of detecting such state over time is different from zero. However, the probability density determining the flow in state $x = L_{\max}$ should be set equal to zero (the distance between the current and the base state vector is limited by the maximum values of possible coordinates in the applied vector space (the condition of reflection from the boundary is implemented)):

$$\rho(x,t)\big|_{x=L_{\max}} = 0. \tag{6b}$$

When formulating the boundary value problem, the initial condition should be specified. Since the state of the system (the distance between the basis vector and the current state vector) can be equal to some value x_0 at time $t = 0$, the initial condition can be specified in the following form:

$$\rho(x,t=0) = \begin{cases} \int \delta(x-x_0)dx = 1, & x = x_0, \\ 0, & x \neq x_0. \end{cases} \tag{6c}$$

Briefly, the solution to this boundary value problem has the following form. Using the Laplace transform method for the Fokker–Planck equation, the following can be written:

$$\begin{gathered} s\overline{G(s,x)} - \rho(x,0) = \\ = -\frac{d}{dx}\left[\mu(x)s\overline{G(s,x)}\right] + \frac{1}{2}\cdot\frac{d^2}{dx^2}\left[D(x)s\overline{G(s,x)}\right]. \end{gathered} \tag{7}$$

Substituting the corresponding derivatives and dependencies of $\mu(x)$ and $D(x)$ into Eq. (7), we obtain the following:

$$\begin{gathered} x^2\frac{d^2\overline{G(s,x)}}{dx^2} + 2\left[2 - \frac{\mu_0}{D_0}\right]x\frac{d\overline{G(s,x)}}{dx} + \\ + 2\left[1 - \frac{\mu_0 + s}{D_0}\right]\overline{G(s,x)} = -\frac{\delta(x-x_0)}{D_0}. \end{gathered} \tag{8}$$

The solution to this equation is found in the form: $\overline{G(s,x)} = \sum_k C_k x^q$, where C_k are the coefficients for the roots of the following characteristic equation: $q(q-1) + 2\left[2 - \frac{\mu_0}{D_0}\right]q + 2\left[1 - \frac{\mu_0 + s}{D_0}\right] = 0.$

We shall seek the solution in the form of two functions: $\overline{G_1(s,x)}$ on interval $[L, x_0]$ and $\overline{G_2(s,x)}$ on

interval $[x_0, 1]$ using the cross-linking condition of functions $\overline{G_1(s,x)}$ and $\overline{G_2(s,x)}$ at point $x = x_0$. The presence of the δ-function in the equation results in the solution remaining continuous at point $x = x_0$ but having a discontinuity of the derivative there.

At $L_{\min} \le x \le x_0$

$$\overline{G_1(s,x)} = C_1 x^{-[1+\alpha]+\beta\sqrt{k+s}} + C_2 x^{-[1+\alpha]-\beta\sqrt{k+s}}.$$

At $x_0 \le x \le L_{\max}$

$$\overline{G_2(s,x)} = C_3 x^{-[1+\alpha]+\beta\sqrt{k+s}} + C_4 x^{-[1+\alpha]-\beta\sqrt{k+s}}.$$

After appropriate transformations, we obtain the following:

- at $L_{\min} \le x \le x_0$,

$$\overline{G_1(s,x)} = \frac{x_0^{\alpha} x^{-[1+\alpha]} \operatorname{sh}\left\{\left[\beta \ln\left(\frac{L_{\max}}{x_0}\right)\right]\sqrt{k+s}\right\}}{\beta D_0 \sqrt{k+s}} \times \times \frac{\operatorname{sh}\left\{\left[\beta \ln\left(\frac{x}{L_{\min}}\right)\right]\sqrt{k+s}\right\}}{\operatorname{sh}\left\{\left[\beta \ln\left(\frac{L_{\max}}{L_{\min}}\right)\right]\sqrt{k+s}\right\}};$$

- at $x_0 \le x \le L_{\max}$,

$$\overline{G_2(s,x)} = \frac{x_0^{\alpha} x^{-[1+\alpha]} \operatorname{sh}\left\{\left[\beta \ln\left(\frac{x_0}{L_{\min}}\right)\right]\sqrt{k+s}\right\}}{\beta D_0 \sqrt{k+s}} \times \times \frac{\operatorname{sh}\left\{\left[\beta \ln\left(\frac{x}{L_{\max}}\right)\right]\sqrt{k+s}\right\}}{\operatorname{sh}\left\{\left[\beta \ln\left(\frac{L_{\max}}{L_{\min}}\right)\right]\sqrt{k+s}\right\}}.$$

We perform the following inverse Laplace transformations:

$$\overline{G_1(s,x)} = \frac{A(s)}{B(s)} = \sum_{n=1}^{M} \frac{A(s_n)}{B(s_n)} \cdot e^{s_n t},$$

where s_n are simple non-zero roots of $B(s)$,

$$B(s) = \sqrt{k+s} \cdot \operatorname{sh}\left\{[\beta \ln L]\sqrt{k+s}\right\},$$

$$A(s) = sh\left\{[\beta \ln x_0]\sqrt{k+s}\right\} \cdot \operatorname{sh}\left\{\left[\beta \ln \frac{x}{L}\right]\sqrt{k+s}\right\}.$$

After appropriate transformations, we obtain the following at $L_{\min} \le x \le x_0$:

$$\rho_1(x,t) = 2 \cdot \frac{x_0^{\alpha} x^{-[1+\alpha]} e^{-kt}}{D_0 \beta^2 \ln\left(\frac{L_{\max}}{L_{\min}}\right)} \cdot \sum_{n=1}^{M} \frac{\sin\left\{\pi n \frac{\ln\left(\frac{L_{\max}}{x_0}\right)}{\ln\left(\frac{L_{\max}}{L_{\min}}\right)}\right\} \cdot \sin\left\{\pi n \frac{\ln\left(\frac{x}{L_{\min}}\right)}{\ln\left(\frac{L_{\max}}{L_{\min}}\right)}\right\}}{\cos \pi n} \cdot e^{-\frac{\pi^2 n^2 t}{\left[\beta \ln\left(\frac{L_{\max}}{L_{\min}}\right)\right]^2}}.$$

Similarly, at $x_0 \le x \le L_{\max}$,

$$\rho_2(x,t) = -4 \cdot \frac{x_0^{\alpha} x^{-[1+\alpha]} e^{-kt}}{D_0 \beta^2 \ln L} \cdot \sum_{n=1}^{M} \frac{\sin\left\{\pi n \frac{\ln\left(\frac{x_0}{L}\right)}{\ln L}\right\} \cdot \sin\left\{\pi n \frac{\ln x}{\ln L}\right\}}{\cos \pi n} \cdot e^{-\frac{\pi^2 n^2 t}{[\beta \ln L]^2}}.$$

Accounting for $\alpha = \frac{1 - 2 \cdot \frac{\mu_0}{D_0}}{2} = \frac{1}{2} - \frac{\mu_0}{D_0}$, $\beta^2 = \frac{2}{D_0}$ and $k = \frac{\alpha^2}{\beta^2}$, we obtain the following:

- at $L_{min} \le x \le x_0$,

$$\rho_1(x,t) = -2 \cdot \frac{x_0^{\alpha} x^{-[1+\alpha]} \cdot e^{-\frac{D_0 \alpha^2}{2} t}}{\ln\left(\frac{L_{max}}{L_{min}}\right)} \cdot \sum_{n=1}^{M} \frac{\sin\left\{\pi n \frac{\ln\left(\frac{L_{max}}{x_0}\right)}{\ln\left(\frac{L_{max}}{L_{min}}\right)}\right\} \cdot \sin\left\{\pi n \frac{\ln\left(\frac{x}{L_{min}}\right)}{\ln\left(\frac{L_{max}}{L_{min}}\right)}\right\}}{\cos \pi n} \cdot e^{-\frac{\pi^2 n^2 D_0 t}{2\left[\ln\left(\frac{L_{max}}{L_{min}}\right)\right]^2}}; \quad (9a)$$

- at $x_0 \le x \le L_{max}$,

$$\rho_2(x,t) = 2 \cdot \frac{x_0^{\alpha} x^{-[1+\alpha]} \cdot e^{-\frac{D_0 \alpha^2}{2} t}}{\ln\left(\frac{L_{max}}{L_{min}}\right)} \cdot \sum_{n=1}^{M} \frac{\sin\left\{\pi n \frac{\ln\left(\frac{x_0}{L_{min}}\right)}{\ln\left(\frac{L_{max}}{L_{min}}\right)}\right\} \cdot \sin\left\{\pi n \frac{\ln\left(\frac{x}{L_{max}}\right)}{\ln\left(\frac{L_{max}}{L_{min}}\right)}\right\}}{\cos \pi n} \cdot e^{-\frac{\pi^2 n^2 D_0 t}{2\left[\ln\left(\frac{L_{max}}{L_{min}}\right)\right]^2}}, \alpha = \frac{1}{2} - \frac{\mu_0}{D_0}. \quad (9b)$$

The probability that the system state will be in the interval from L_{min} to L_{max} by time t (i.e., the threshold state (θ) will not be reached) can be calculated as follows:

$$P(\theta,t) = \int_{L_{min}}^{x_0} \rho_2(x,t)dx + \int_{x_0}^{L_{max}} \rho_1(x,t)dx. \quad (10)$$

The probability $Q(\theta, t)$ that the threshold state θ will be reached or surpassed by time t is calculated using the following formula:

$$Q(\theta, t) = 1 - P(\theta, t). \quad (11)$$

Defining the boundaries of the interval of possible states from L_{min} to L_{max} will be discussed later on.

Using sentiment analysis tools, all user comments during a day can be categorized into positive and negative to obtain a time series. The time series of daily activity of users (with negative attitudes) of the RIA Novosti official community on the VKontakte social network on commenting on news from January 2013 to December 2020 is presented in Fig. 6. The activity is defined as the ratio of the total number of unique comments left by users on all news items during the day to the total number of unique views of all published news items by users during the day.

It should be noted that visitors in general are very reluctant to leave comments. The total number of those who make them is unlikely to exceed 1–2% of all portal viewers.

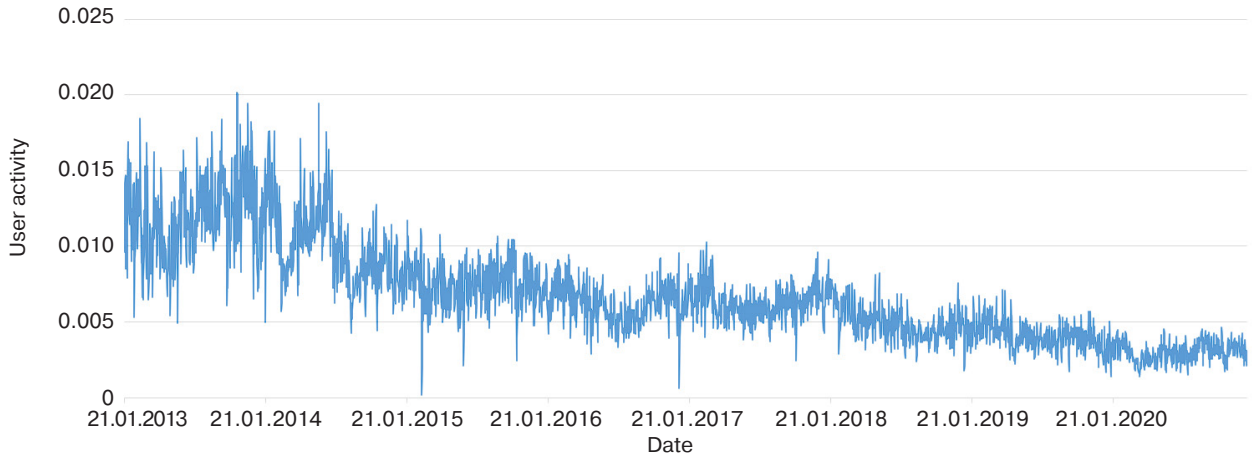

Fig. 6. Time series of RIA Novosti portal user activity in commenting on news from January 2013 to December 2020

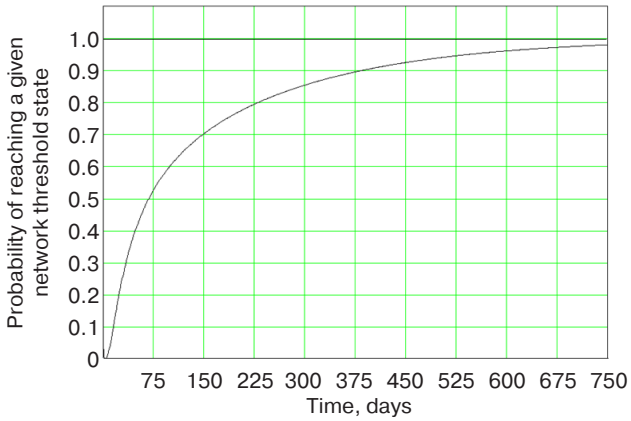

Fig. 7. Time dependence of the probability of reaching a given network threshold state for the considered example at time point May 15, 2019

It is possible to construct an aggregated comment graph for a day, as well as to define its characteristics and state vector (changing from day to day).

We shall discuss selecting the boundaries for the interval of possible states from L_{min} to L_{max}. For the comment graph of the RIA Novosti portal users, the elements of the current state vector at the time moment of May 15, 2019 (which is taken as $t = 0$) are equal to $X(t) = (0.0035; 0.07; 0.12)$: the fraction of negative comments is 0.0035, while the clustering coefficient average is 0.07, and the average degree of node mediation is 0.12. The baseline vector of the desired state is defined as $\theta = (0.0025; 0.05; 0.05)$: the fraction of negative comments is 0.0025, the clustering coefficient average is 0.05, and the average degree of node mediation is 0.05. The value for the fraction of negative comments equal to 0.0025 is selected for model validation, since the time of observing this value actually in the time series graph is known. The model's adequacy can be evaluated by comparing the forecast modeling results with the real value. The distance between the given base vector of the desired state $\theta = (0.0025; 0.05; 0.05)$ and the current state vector $X(t)$ at time $t = 0$ is $x_0 = 0.073$. Analyzing the dynamics of the time series of changes in the state of the network for several previous days and using the model equations, the inverse problem can be solved to determine values for model parameters μ_0 and D_0. In this case, $\mu_0 = 0.0002$ and $D_0 = 0.0009$.

The right boundary of the interval of possible states L_{max} can be given as the distance between the basis vector (θ) and the vector of maximum possible values of network parameters $X(t) = (1; 1; 1)$. In the considered case, $L_{max} = 1.70$. For reliability of consideration, the left boundary can be defined, for example, as half the length of a given basis vector (in this case, $|\theta| = 0.071$), so that L_{min} is equal to 0.035.

The results show that under the prevailing conditions with no impact on the user network, the desired state can be achieved with a probability of 0.8 on the 225th day, and with a probability of 0.9 on the 375th day (Fig. 7), which is roughly what actually happened, according to the observed data.

5. ALGORITHM FOR PREDICTING THE ACHIEVEMENT OF A GIVEN STATE OF THE COMMENT NETWORK GRAPH OF NEWS MEDIA USERS

On the basis of the studies and the developed model for the dynamics of change in the sentiment of Internet media users based on the Fokker–Planck equation, as well as changes in the parameters of the graphs of their comment networks, an algorithm is created for their prediction consisting of the following steps:

a) Date and time stamped collection of text comments and metadata of users on a certain topic from online news media resources.
b) Data processing using text analytics tools and sentiment analysis, obtaining the user comment graph on a certain topic, and calculating its characteristics (network density, mediation coefficient average, clustering coefficient average, elasticity, and fraction of users with a particular sentiment).
c) Specifying the value for elements of the base vector determining the achievement of the desired or undesired state (θ), as well as forming a time series of changes in the graph of user comments on a certain topic over time based on the processed data and the given vector.
d) Specifying step duration τ (hour, day, week, etc.). Based on the values of the time series at several steps for a given τ, determining model parameters μ_0 and D_0 by numerical calculations using the observed data and Eqs. (5) and (6).
e) Accepting the last average value of the distance metric between the base vector and the current network state vector as initial state x_0 and using the obtained values for μ_0 and D_0 along with Eqs. (5) and (6). Performing calculations and obtaining the time dependence of the probability of achieving the desired or undesired state. Then the probability value can be specified (e.g., 0.95), as well as the time to reach the specified probability level can be estimated (time prediction).

CONCLUSIONS

In the work, the following results have been obtained:

1. The stationary distribution of news in terms of the number of comments to them observed in practice corresponds to the power law: $\rho(x) = [\gamma - 1]x^{-\gamma}$, where $\rho(x)$ is the fraction of news in their total

number having x comments while γ is the index of power.

2. The dynamics of change over time in the number of comments to a news item or blog can have both S-shaped form and two-stage form due to a significant difference in the average appearance time of second-level comments (the time interval between the appearance of the first-level comment and the comment to this comment), i.e., the value of the average delay.
3. On the basis of certain assumptions, the power law for dependence of the stationary probability density of news distribution on the number of comments (states x) observed in practice can be obtained from the solution to the stationary Fokker–Planck equation. In particular, assuming that coefficient $\mu(x)$ responsible in the Fokker–Planck equation for the purposeful change of the system state x (x is the current number of comments on the news item) depends linearly on state x, while coefficient $D(x)$ responsible for the random change depends on x quadratically. All this suggests that the Fokker–Planck equation can be used for describing processes occurring in complex network structures.
4. Solving the non-stationary Fokker–Planck equation under the assumptions of a linear dependence of $\mu(x)$ on state x and a quadratic dependence of $D(x)$ on state x yields an equation for the probability density of transitions between states of the system per unit time, which corresponds well with the observed data with regard for the effect of the delay time between the appearance of a first-level comment and the comment on that comment.
5. The good correspondence of the models developed on the basis of the Fokker–Planck equation with the observed data provides a basis for the creation of algorithms for monitoring and predicting the public opinion evolution for users of news info resources.
6. The parameters of comment network graphs can be obtained using both off-the-shelf tools and libraries of the Python language used to analyze complex networks, as well as the additionally developed software.
7. The analysis of the resulting model using the characteristics of the real time series to change the comment graph for users of the RIA Novosti portal and structural parameters of the graph shows its adequacy and consistency. The results show that given no impact on the user network, the desired state in terms of the number of negative commenters can be reached with probability 0.8 on the 225th day and with probability 0.9 on the 375th day, which is approximately what actually happened, according to the observed data.
8. The model based on the Fokker–Planck equation justifies the development of a practically significant algorithm for predicting the achievement of a given state of the comment network graph for news media users.
9. The complex dynamics of processes in complex social systems can be described by models other than those based on the Fokker–Planck equation. For example, the models developed by the present authors for describing the stochastic dynamics of state changes in complex social systems with provision for processes of self-organization and the presence of memory are discussed in [18–21]. For the development of the present model, the authors considered graphical schemes of transition probabilities between possible states of the described systems taking previous states into account, which accounts for memory and describes not only Markovian but also non-Markovian processes.

ACKNOWLEDGMENTS

The study is financially supported by the Russian Science Foundation, grant No. 22-21-00109 “Development of models for forecasting the dynamics of social sentiments based on analyzing time series of text content of social networks using the Fokker–Planck equations and nonlinear diffusion.”

Authors’ contribution. All authors equally contributed to the research work.

REFERENCES

1. Du B., Lian X., Cheng X. Partial differential equation modeling with Dirichlet boundary conditions on social networks. *Bound. Value Probl*. 2018;2018(1):50. https://doi.org/10.1186/s13661-018-0964-4
2. Lux T. Inference for systems of stochastic differential equations from discretely sampled data: a numerical maximum likelihood approach. *Ann. Finance*. 2013;9(2):217–248. http://doi.org/10.1007/s10436-012-0219-9
3. Hurn A., Jeisman J., Lindsay K. Teaching an Old Dog New Tricks: Improved Estimation of the Parameters of Stochastic Differential Equations by Numerical Solution of the Fokker–Planck Equation. In: Dungey M., Bardsley P. (Eds.). *Proceedings of the Australasian Meeting of the Econometric Society*. 2006. The Australian National University, Australia. P. 1–36.
4. Elliott R.J., Siu T.K., Chan L. A PDE approach for risk measures for derivatives with regime switching. *Ann. Finance*. 2007;4(1):55–74. http://dx.doi.org/10.1007/s10436-006-0068-5

5. Orlov Y.N., Fedorov S.L. Nonstationary time series trajectories generation on the basis of the Fokker–Planck equation. *TRUDY MFTI = Proceedings of MIPT*. 2016;8(2):126–133 (in Russ.).
6. Chen Y., Cosimano T.F., Himonas A.A., Kelly P. An Analytic Approach for Stochastic Differential Utility for Endowment and Production Economies. *Comput. Econ*. 2013;44(4):397–443. http://doi.org/10.1007/s10614-013-9397-4
7. Savku E., Weber G.-W. Stochastic differential games for optimal investment problems in a Markov regime-switching jump-diffusion market. *Ann. Oper. Res*. 2020;132(6):1171–1196. https://doi.org/10.1007/s10479-020-03768-5
8. Krasnikov K.E. Mathematical modeling of some social processes using game-theoretic approaches and making managerial decisions based on them. *Russ. Technol. J*. 2021;9(5):67–83 (in Russ.). https://doi.org/10.32362/2500-316X-2021-9-5-67-83
9. Kirn S.L., Hinders M.K. Dynamic wavelet fingerprint for differentiation of tweet storm types. *Soc. Netw. Anal. Min*. 2020;10(1):4. https://doi.org/10.1007/s13278-019-0617-3
10. Hoffmann T., Peel L., Lambiotte R., Jones N.S. Community detection in networks without observing edges. *Sci. Adv*. 2020;6(4):1478. https://doi.org/10.1126/sciadv.aav1478
11. Pulipati S., Somula R., Parvathala B.R. Nature inspired link prediction and community detection algorithms for social networks: a survey. *Int. J. Syst. Assur. Eng. Manag.* 2021. https://doi.org/10.1007/s13198-021-01125-8
12. Dorogovtsev S.N., Mendes J.F.F. Evolution of networks. *Adv. Phys*. 2002;51(4):1079–1187. http://doi.org/10.1080/00018730110112519
13. Newman M.E.J. The structure and function of complex networks. *SIAM Rev*. 2003;45(2):167–256. https://doi.org/10.1137/S003614450342480
14. Dorogovtsev S.N., Mendes J.F.F., Samukhin A.N. Generic scale of the scale-free growing networks. *Phys. Rev. E*. 2001;63(6):062101. https://doi.org/10.1103/PhysRevE.63.062101
15. Golder S., Wilkinson D., Huberman B. Rhythms of Social Interaction: Messaging Within a Massive Online Network. In: Steinfield C., Pentland B.T., Ackerman M., Contractor N. (Eds.). *Communities and Technologies.* 2007. https://doi.org/10.1007/978-1-84628-905-7_3
16. Kumar R., Novak J., Tomkins A. Structure and evolution of online social networks. In: *Proceedings of the 12th ACM SIGKDD International Conference on Knowledge Discovery and data Mining*, KDD ’06. 2006. P. 611–617. https://doi.org/10.1145/1150402.1150476
17. Mislove A., Marcon M., Gummadi K.P., Druschel P., Bhattacharjee B. Measurement and analysis of online social networks. In: *Proceedings of the 7th ACM SIGCOMM Conference on Internet Measurement*, IMC’07. 2007. P. 29–42. https://doi.org/10.1145/1298306.1298311
18. Zhukov D., Khvatova T., Zaltsman A. Stochastic Dynamics of Influence Expansion in Social Networks and Managing Users’ Transitions from One State to Another. In: *Proceedings of the 11th European Conference on Information Systems Management* (ECISM 2017). 2017. P. 322–329.
19. Zhukov D., Khvatova T., Millar C., Zaltcman A. Modelling the stochastic dynamics of transitions between states in social systems incorporating self-organization and memory. *Technol. Forecast. Soc. Change*. 2020;158:120134. https://doi.org/10.1016/j.techfore.2020.120134
20. Zhukov D., Khvatova T., Istratov L. A stochastic dynamics model for shaping stock indexes using self-organization processes, memory and oscillations. In: *Proceedings of the European Conference on the Impact of Artificial Intelligence and Robotics* (ECIAIR 2019). 2019. P. 390–401.
21. Zhukov D.O., Zaltcman A.D., Khvatova T.Yu. Forecasting Changes in States in Social Networks and Sentiment Security Using the Principles of Percolation Theory and Stochastic Dynamics. In: *Proceedings of the 2019 IEEE International Conference “Quality Management, Transport and Information Security, Information Technologies”* (IT&QM&IS). 2019. Article number 8928295. P. 149–153. https://doi.org/10.1109/ITQMIS.2019.8928295

About the authors

Julia P. Perova, Senior Lecturer, Department of Telecommunications, Institute of Radio Electronics and Informatics, MIREA – Russian Technological University (78, Vernadskogo pr., Moscow, 119454 Russia). E-mail: jul-np@yandex.ru. Scopus Author ID 57431908700, https://orcid.org/0000-0003-4028-2842

Sergey A. Lesko, Dr. Sci. (Eng.), Docent, Professor of the Cybersecurity Information and Analytical Systems Department, Institute of Cybersecurity and Digital Technologies, MIREA – Russian Technological University (78, Vernadskogo pr., Moscow, 119454 Russia). E-mail: sergey@testor.ru. Scopus Author ID 57189664364, https://orcid.org/0000-0002-6641-1609

Andrey A. Ivanov, Student, MIREA – Russian Technological University (78, Vernadskogo pr., Moscow, 119454 Russia). E-mail: heliosgoodgame@gmail.com. https://orcid.org/0009-0002-7199-2871

Об авторах

Перова Юлия Петровна, старший преподаватель, кафедра телекоммуникаций, Институт радиоэлектроники и информатики, ФГБОУ ВО «МИРЭА – Российский технологический университет» (119454, Россия, Москва, пр-т Вернадского, д. 78). E-mail: jul-np@yandex.ru. Scopus Author ID 57431908700, https://orcid.org/0000-0003-4028-2842

Лесько Сергей Александрович, д.т.н., доцент, профессор кафедры «Информационно-аналитические системы кибербезопасности», Институт кибербезопасности и цифровых технологий, ФГБОУ ВО «МИРЭА – Российский технологический университет» (119454, Россия, Москва, пр-т Вернадского, д. 78). E-mail: sergey@testor.ru. Scopus Author ID 57189664364, https://orcid.org/0000-0002-6641-1609

Иванов Андрей Андреевич, магистрант, ФГБОУ ВО «МИРЭА – Российский технологический университет» (119454, Россия, Москва, пр-т Вернадского, д. 78). E-mail: heliosgoodgame@gmail.com. https://orcid.org/0009-0002-7199-2871

Translated from Russian into English by K. Nazarov
Edited for English language and spelling by Thomas A. Beavitt

Mathematical modeling

Математическое моделирование

UDC 330.4
https://doi.org/10.32362/2500-316X-2024-12-3-93-103
EDN YSWUJG

RESEARCH ARTICLE

Analysis of approaches to identification of trend in the structure of the time series

Ulyana S. Mokhnatkina,
Denis V. Parfenov,
Denis A. Petrusevich @

MIREA – Russian Technological University, Moscow, 119454 Russia
@ *Corresponding author, e-mail: petrusevich@mirea.ru, petrdenis@mail.ru*

Abstract

Objectives. The study set out to compare the forecasting quality of time series models that describe the trend in different ways and to form a conclusion about the applicability of each approach in describing the trend depending on the properties of the time series.

Methods. A trend can be thought of as the tendency of a given quantity to increase or decrease over the long term. There is also an approach in which a trend is viewed as some function, reflecting patterns in the behavior of the time series. In this case, we discuss the patterns that characterize the behavior of the series for the entire period under consideration, rather than short-term features. The experimental part involves STL decomposition, construction of ARIMA models (one of the stages of preparation for which includes differentiation, i.e., removal of the trend and transition to a weakly stationary series), construction of ACD models (average conditional displacement) and other approaches. Time-series models based on various trend models are compared with respect to the value of the maximum likelihood function. Many of the combinations have not been constructed before (Fourier series as a trend model, combination of ACD model for trend with seasonal models). Example forecasts of macroeconomic statistics of the Russian Federation and stock prices of Sberbank on the Moscow Exchange in the time range of 2000–2021 are presented.

Results. In the experiments, The LOESS method obtained the best results. A combination of polynomial model for trend description and ARIMA for seasonally description and combination of ACD algorithm for trend and ETS for seasonal model obtained good forecasts in case of seasonal time series, while Fourier time series as a trend model also achieved close quality of prediction.

Conclusions. Since the LOESS method for groups of seasonal and non-seasonal series gives the best results for all indicators, this method can be recommended for obtaining the most accurate results for series of different nature. Trend modeling using Fourier series decomposition leads to quite accurate results for time series of different natures. For seasonal series, one of the best results is given by the combination of modeling a trend on the basis of a polynomial and seasonality in the form of the ARIMA model.

Keywords: dynamic series, macroeconomic statistics, ARIMA, ACD, time series, trend, maximum likelihood function, trend modeling

• **Submitted:** 21.06.2023 • **Revised:** 08.02.2024 • **Accepted:** 09.04.2024

For citation: Mokhnatkina U.S., Parfenov D.V., Petrusevich D.A. Analysis of approaches to identification of trend in the structure of the time series. *Russ. Technol. J.* 2024;12(3):93–103. https://doi.org/10.32362/2500-316X-2024-12-3-93-103

Financial disclosure: The authors have no a financial or property interest in any material or method mentioned.

The authors declare no conflicts of interest.

НАУЧНАЯ СТАТЬЯ

Анализ подходов к определению тренда в структуре временного ряда

У.С. Мохнаткина,
Д.В. Парфенов,
Д.А. Петрусевич @

МИРЭА – Российский технологический университет, Москва, 119454 Россия
@ *Автор для переписки, e-mail: petrusevich@mirea.ru, petrdenis@mail.ru*

Резюме

Цели. Основная цель – сравнить качество прогнозирования моделей временных рядов, по-разному описывающих тренд, и сформировать заключение о применимости каждого подхода при описании тренда в зависимости от свойств временного ряда.

Методы. Тренд может рассматриваться как склонность рассматриваемой величины к возрастанию или убыванию в долгосрочной перспективе. Также встречается подход, при котором тренд является функцией некоторого вида, отражающей закономерности в поведении рассматриваемого временного ряда (речь идет о закономерностях, характеризующих поведение ряда для всего рассматриваемого периода, а не краткосрочные особенности). В работе рассматривается разложение STL, построение моделей ARIMA, использование моделей ACD (усредненного условного смещения) и другие подходы. Хотя разложение на тренд, сезонность, остаток и является общеупотребительной практикой, многие комбинации, представленные в вычислительном эксперименте, построены впервые (например, использование ряда Фурье для моделирования тренда, совмещение модели сезонности и модели тренда на основе алгоритма ACD). Во второй части работы представлен вычислительный эксперимент, в котором модели, использующие различные подходы к понятию тренда, его выделению и обработке, сравниваются по значению функции максимального правдоподобия и по прогнозу на тестовый период для динамических рядов макроэкономической статистики РФ; цены акций Сбербанка РФ на Московской бирже временного периода 2000–2021 гг.

Результаты. Во всех экспериментах один из наиболее точных прогнозов сделан при помощи метода LOESS. Для сезонных рядов достаточно точные результаты показывает моделирование тренда на основе многочлена и сезонности на основе функций ARIMA, совмещение модели тренда на основе алгоритма ACD и сезонности на основе ETS и моделирование на основе ряда Фурье.

Выводы. Метод LOESS для групп сезонных и несезонных рядов дает наилучший результат по всем показателям, поэтому можно рекомендовать именно этот метод для получения наиболее точных результатов для рядов различной природы. Моделирование тренда с помощью разложения в ряд Фурье приводит к достаточно точным результатам на временных рядах различной природы. Для сезонных рядов один из лучших результатов дает комбинация моделирования тренда на основе многочлена и сезонности в виде модели ARIMA.

Ключевые слова: динамические ряды, макроэкономическая статистика, ARIMA, ACD, временные ряды, тренд, функция максимального правдоподобия, моделирование тренда

• **Поступила:** 21.06.2023 • **Доработана:** 08.02.2024 • **Принята к опубликованию:** 09.04.2024

Для цитирования: Мохнаткина У.С., Парфенов Д.В., Петрусевич Д.А. Анализ подходов к определению тренда в структуре временного ряда. *Russ. Technol. J*. 2024;12(3):93–103. https://doi.org/10.32362/2500-316X-2024-12-3-93-103

Прозрачность финансовой деятельности: Авторы не имеют финансовой заинтересованности в представленных материалах или методах.

Авторы заявляют об отсутствии конфликта интересов.

INTRODUCTION

Within the scope of the presented work, various approaches to the definition of the trend of a time series existing in modern science are analyzed. Since there is no single approach to the definition of a trend, the concept can be given a number of definitions depending both on the characteristics of the series and the approach chosen by the researcher. However, a trend is usually understood as an increasing or decreasing propensity of a time series in the predicted area. In medicine, trend is typically considered as the general direction of change in the average level of characteristics in a data set [1]. This definition can be generalized to the presence of a constant unidirectional change in the quantity under study [2–4]. It is important to note the presence of the noise component of the time series, which can affect the values of the series in both downward and upward directions. For this reason, researchers are interested in the component of long-term trend, i.e., the characteristics of changes in the studied value over a long period of time [5–8]. There is also a way to identify the trend in functional form, which is the analysis of the process at a deeper level, where the same terminology is used.

The article considers several methods of trend extraction, providing forecasts for the test period of time series models (for cases where the model enables making a forecast), and comparing different approaches in terms of the quality of forecasts for the test period. In terms of processed data, we used the time series of macroeconomic statistics of the Russian Federation[1], as well as data of the stack quote of Sberbank of the Russian Federation (RF Sberbank) on the Moscow Exchange[2]. All the models under consideration were tuned on the 2000–2020 study period (following removal of the crisis years 2008 and 2014, the data were joined). However, since the models studied in this paper do not depend on a specific time period, the conclusions can be extended to other time processes.

The researcher generally has at hand many models of different natures (based on neural networks, standard autoregressive integrated moving average model (ARIMA)[3], exponential time smoothing (ETS), generalized autoregressive conditional heteroscedastic (GARCH), etc.), each of which makes its own prediction for the target period. The models built in computational experiments can be used (as the accuracy of their predictions for the test period shows) in a common set of predictors. The presented approach is relevant due to the possibility to build combinations of models for describing trends and seasonal components (if any) of time series that have not been used before. This will make it possible to add new models and methods to the existing set of applied models and methods, as well as to explain when the dynamics of the time process can be better described in comparison with other models. The struggle to improve the quality of time series forecasting remains important regardless of the breadth of the researcher's toolkit.

The aim of the work is to build various trend models, to compare the accuracy of their forecasts for the test period with standard models, and to draw conclusions about the possibility of further use of various models for trend in time series forecasting.

Within the concept of STL (seasonal trend decomposition based on locally estimated scatterplot smoothing) [9], trend T_t is a deterministic part of the time series y_t, which may also contain seasonal component S_t and noise component R_t. The series can be represented in additive (1) or multiplicative (2) form:

$$y_t = S_t + T_t + R_t, \quad (1)$$

$$y_t = S_t \times T_t \times R_t, \quad (2)$$

where t is time.

If variable substitution and unit conversion based on logarithmization are possible, approaches (1) and (2) are equivalent [9]:

$$\ln y_t = \ln(S_t \times T_t \times R_t) = \ln S_t + \ln T_t + \ln R_t.$$

[1] Unified archive of economic and sociological data. Dynamic series of macroeconomic statistics of the Russian Federation. Index of money incomes of the population; real volume of agricultural production. http://sophist.hse.ru/hse/nindex.shtml (in Russ.). Accessed November 03, 2023.

[2] Sberbank (SBER) stock price. https://www.moex.com/ru/issue.aspx?board=TQBR&code=SBER (in Russ.). Accessed November 03, 2023.

[3] Autoregressive and moving average model or Box–Jenkins model.

In order to find out the presence of a trend, a statistical hypothesis approach can be used—in particular, the Mann–Kendall criterion [10, 11].

Methods for estimating the trend of a time series are divided into parametric and non-parametric methods. In terms of parametric methods, a trend is understood as a function of one or more variables. Examples of parametric methods are the methods of trend estimation in the form of a function, where the parameters characterizing the trend can be calculated using the least squares method, polynomial fitting, logarithmic, step, exponential, harmonic, logistic functions, piecewise linear function, autoregressive (AR) model, etc. Non-parametric methods include the moving average (MA) model, median smoothing method, ETS model, application of frequency filters, etc. The experimental part of the work considers the selection of logarithmic, linear and exponential functions to describe the trend, as well as the application of the Bayesian approach [12]. Since describing monotonic areas of growth and decline of the studied value, these methods can be applied only for a monotonic time series. In the case when the initial series is not monotonic, it is necessary to perform preliminary processing, dividing the series into monotonic parts, and describing each part separately [13–17].

The experimental section of the work also studies the method of describing a trend using polynomials of the second order and higher. Since the polynomial function not in generally monotonic, computational problems may arise along with the question of choosing a specific type of function (degree of the polynomial). This problem is also characteristic of spline interpolation. Among other things, in polynomial interpolation the function can deviate strongly from the fixed values at the nodes. For example, the function $1/(1+x^2)$ problem is known [18].

Let us consider the average conditional displacement ACD (average conditional displacement) algorithm [15] for trend estimation and solving problems on this basis [12, 13]. Compared to spline interpolation [19, 20] for describing the behavior of some function on a given segment, the ACD algorithm and related algorithms have the useful property of preserving monotonicity. Similar ideas also find application in works based on other approaches [14].

In addition to the above trend description methods, mathematical models of time series based on neural networks (long-short term memory (LSTM), gated recurrent unit (GRU), etc.) are widely used [21–25]. Often such models better describe long-term patterns in the data compared to ARIMA models based on statistics [24, 26]. There are known works where models of different types are integrated into a single framework [22, 23]. Researchers are currently making attempts to analyze the characteristics and features of time series using neural networks [26].

The experimental section of the work presents the construction of trend models based on different methods, combining the models with information on the seasonality of the process, checking the quality of forecasts and corresponding conclusions concerning the ability of the obtained model to adjust to the values of the time series and the quality of the forecast for the test period.

TREND EXTRACTION METHODS UNDER CONSIDERATION

One of the most commonly used models for describing a time series is ARIMA(*p, d, q*) [9], which consists of the autoregressive part of AR (for a model of order *p* the values of the series *X* are made dependent on *p* of their previous values):

$$X_t = c + \varphi_1 X_{t-1} + ... + \varphi_p X_{t-p},$$

where φ_i, $i = \overline{1, p}$ are the function coefficients; and from the moving average MA part of order *q* [9]:

$$X_t = \varepsilon_t + \theta_1 \varepsilon_{t-1} + ... + \theta_q \varepsilon_{t-q},$$

where θ_i, $i = \overline{1, q}$ are the function coefficients. The order *d* denotes the number of differentiations of the series.

When building the model, the trend is eliminated by switching to the stationary time difference (multiple differentiation of the series until the test for stationarity is fulfilled) [9, 27]. Thus, the model description and the forecasting process are performed with the transformed stationary time series. The ARIMA model remains one of the most widely used models in the field of time series forecasting. In the computational part of the study, its results are compared with the forecasts of other models.

In the averaged conditional bias algorithm [15] for estimating a trend and solving related problems [16, 17], time series segments are approximated by monotonic functions of the following form:

$$f(x) = y_l + k(x - x_l), \quad (3)$$

where y_l is the value of the function $f(x)$ at the leftmost position of the segment at $x = x_l$, k is the slope coefficient of the line $f(x)$ (see Figure).

Since the trend estimation is constructed by successive calculation of monotone segments, the mentioned problems do not arise, as in the case of polynomial interpolation or spline interpolation.

As a part of the computational experiment, the quality of ARIMA and ACD model predictions was compared with the results of models based on neural networks (LSTM, GRU) and models with bagging [28] applied to time series data. Bagging involves generating

a set of pseudo-samples from the series data. The final forecast is obtained by averaging or weighted averaging of forecasts for the test period constructed for each pseudo-sample [28].

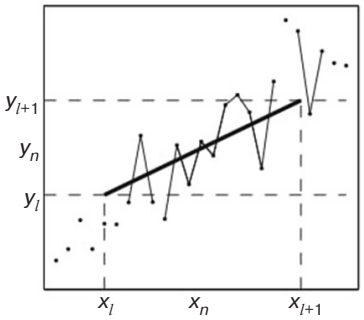

Fig. Diagram of the monotonic segment construction by time series segment according to the ACD algorithm [15]

In order to evaluate model forecasts, measures of forecast vector closeness and the vector of real values of the time series are considered [9]:

$$\mathrm{RMSE} = \sqrt{\frac{\sum_t (\tau(t) - ts(t))^2}{N}}, \qquad \mathrm{MAE} = \frac{\sum_t |\tau(t) - ts(t)|}{N}. \tag{4}$$

Here RMSE is the root mean square error; MAE is the mean absolute error; $\tau(t)$ are the real values of the time series; $ts(t)$ is the forecast of the mathematical model; N is the length of the forecasting interval (often coincides with the length of the seasonality interval; since we are talking here about time series with annual seasonality, $N = 12$ months).

COMPUTATIONAL EXPERIMENT

In the experiment, time series models are built and compared. The following series are used for modeling: monetary incomes of the population, real volume of agricultural production according to macroeconomic statistics of the Russian Federation (monthly indicators, dimensionless) and stocks of RF Sberbank on the Moscow Exchange (monthly indicators, rubles). The last year in the data is used as a test period for which forecasts are made by all models. The rest of the data is used for training and tuning the models. Since the time series models that participate in the experiment use only time series data for tuning without considering external factors, we excluded data around the 2008 and 2014 crises prior to tuning the models. Data from the previous and the next period relative to the crisis year are joined together. Graphs of the money income series, as well as its autocorrelation function (ACF) and partial autocorrelation function (PACF) [9], are presented and described in detail in [29, Figs. 3 and 4]. Graphs for a series of real agricultural output are presented and described in detail in [29, Figs. 5 and 6].

The maximum likelihood function and MAE/RMSE estimates used in model comparison show the closeness of the forecast to the real data of the test period. The results of processing the index of money income of the population are presented in Table 1 (the best models according to various criteria are marked in bold).

First five trend models are polynomials whose coefficients are estimated using the least squares method. A seasonality model is superimposed on the forecast. The next five models are characterized by the fact that the forecast on the constructed polynomial trend model is made via ARIMA.

When forecasting using hyperbolic/indicative/logarithmic function, the trend is modeled using the corresponding function. Based on the obtained regression model, the trend is forecast for the test period with subsequent imposition of seasonality information. The model coefficients are also calculated using the least squares method.

Fourier series expansion is used to describe the trend model for the training period. Forecasting is performed using ARIMA similarly to the methods presented above but with imposition of the seasonality model.

Interpolation of a tabulated function (which, in general, corresponds to the measurements on which the time series is constructed) can be performed using splines. Interestingly, while such an interpolation method is highly accurate, it cannot be used to make predictions. However, it is possible to compare how splines and other models are fitted to the series data.

When using the STL model (locally estimated scatterplot smoothing (LOESS) method) [30, 31] the series is divided into components: trend, seasonality, noise.

A similar approach is taken when applying the ACD algorithm. After building the trend model on the basis of ACD, the forecast for the test period is carried out.

Hybrid models, in which seasonality is superimposed on a trend model and predicted using ETS or ARIMA, are also studied.

Computational experiment follows the methodology used in [29]. The first part uses a time series of monthly indicators of money income of the population. The series has annual seasonality. The test period is 2018. The results are summarized in Table 1 (accuracy is 0.01). Prior to the experiment, the data of the series were transformed into the range [0, 1]. The best models in terms of forecast accuracy for the test period or the value of the logarithm of the maximum log-likelihood function (LLF) are highlighted in bold type.

Table 1. Household money income models according to macroeconomic statistics of the Russian Federation and their forecasts for the test period

Trend estimation	LLF	MAE	RMSE
1st degree polynomial $y = a_0 + a_1 x$	−364.650	0.192	0.193
2nd degree polynomial $y = a_0 + a_1 x + a_2 x^2$	−363.084	0.042	0.046
3rd degree polynomial $y = a_0 + \sum_{i=1}^{3} a_i x^i$	−362.139	0.055	0.062
4th degree polynomial $y = a_0 + \sum_{i=1}^{4} a_i x^i$	**−362.746**	**0.016**	**0.020**
5th degree polynomial $y = a_0 + \sum_{i=1}^{5} a_i x^i$	−363.487	0.081	0.086
1st degree polynomial + ARIMA	−364.151	0.145	0.147
2nd degree polynomial + ARIMA	−362.863	0.024	0.027
3rd degree polynomial + ARIMA	−362.453	0.026	0.033
4th degree polynomial + ARIMA	**−362.668**	**0.014**	**0.019**
5th degree polynomial + ARIMA	**−362.746**	**0.016**	**0.020**
Hyperbolic function $y = a_0 + a_{-1} / x$	−361.679	0.105	0.107
Logarithmic function $y = a_0 + a_1 \ln x$	−363.174	0.050	0.054
Exponential function $y = \exp(a_0 + a_1 x)$	−364.967	0.221	0.222
Interpolation by splines	−362.688	–	–
Fourier series expansion	−362.783	0.020	0.027
Exponential smoothing	−363.073	0.040	0.044
LOESS method	**−362.719**	**0.015**	**0.019**
ACD algorithm	−362.959	0.030	0.034
ACD + ARIMA trend	−362.198	0.060	0.074
ACD + ETS trend	**−361.777**	**0.010**	**0.012**

The most accurate results (MAE and RMSE columns) are obtained when considering a hybrid model with trend estimation by ACD algorithm with information on seasonality of the time series and its forecast for the test period via ETS. The method of trend estimation using a polynomial of the fourth degree with the addition of seasonality information and a random component based on the ARIMA(0, 4, 1) model has good performance in terms of forecast accuracy for the test period. The values of the likelihood function are smaller as compared to the previous method. The same values of error and model quality for trend estimation using LOESS method. These models have almost the same values of accuracy of fitting to the data of the series (LLF) as the modeling of the series based on splines.

The next method of trend estimation in terms of accuracy of results and quality of adjustment to the initial series uses a polynomial of the fourth degree modeled and predicted by linear regression method. The same indicators have the method of trend estimation using a polynomial of the fifth degree with a forecast for the test period by the ARIMA(3, 5, 1) method.

Fairly good estimates of forecast accuracy and likelihood function when modeling the trend using Fourier series expansion, polynomials of the second and third degree with forecasting using the ARIMA method. Slightly lower forecast accuracy is obtained when modeling the trend using the ACD algorithm.

While classical ARIMA and ETS methods have less accurate prediction performance for the test period, they are far from useless.

The lowest values for the logarithm of the maximum likelihood function pertain to the methods of trend estimation using the exponential function, as well as those using the polynomial of the first degree. However, these models also have the worst prediction accuracy results for the test period. The worst method of trend modeling by all indicators is the one using the hyperbolic function.

A similar computational experiment was conducted for the time series of monthly indicators of the index of real agricultural production (a detailed analysis of the characteristics of the series is given in [29]). Data from 2000–2020 are used for training. The series has annual seasonality. The test period is 2021. The results are summarized in Table 2. The best models in terms of forecast accuracy for the test period or the value of the logarithm of the maximum likelihood function are highlighted in bold font.

The lowest values for the logarithm of the maximum likelihood function have the hybrid model with trend estimation by the ACD algorithm with information on the seasonality of the time series and its prediction for the test period using ETS. However, this method does not have the most accurate results of forecasts for the test period (MAE and RMSE columns).

The best MAE results for forecasting for the test period are obtained using the method of trend estimation

Table 2. Models of the index of real volume of agricultural production according to macroeconomic statistics of the Russian Federation and their forecasts for the test period

Trend estimation	LLF	MAE	RMSE
1st degree polynomial $y = a_0 + a_1 x$	−395.597	0.084	0.097
2nd degree polynomial $y = a_0 + a_1 x + a_2 x^2$	−395.871	0.096	0.105
3rd degree polynomial $y = a_0 + \sum_{i=1}^{3} a_i x^i$	−396.132	0.112	0.117
4th degree polynomial $y = a_0 + \sum_{i=1}^{4} a_i x^i$	−396.173	0.114	0.119
5th degree polynomial $y = a_0 + \sum_{i=1}^{5} a_i x^i$	−397.175	0.171	0.185
1st degree polynomial + ARIMA	−395.567	0.083	0.096
2nd degree polynomial + ARIMA	−395.734	0.090	0.100
3rd degree polynomial + ARIMA	−395.830	0.093	0.103
4th degree polynomial + ARIMA	−395.836	0.094	0.103
5th degree polynomial + ARIMA	−396.031	0.102	0.107
Hyperbolic function $y = a_0 + a_{-1} / x$	−394.600	0.079	0.124
Logarithmic function $y = a_0 + a_1 \ln x$	**−395.058**	**0.069**	**0.101**
Exponential function $y = \exp(a_0 + a_1 x)$	**−395.310**	**0.075**	**0.095**
Interpolation by splines	−396.028	–	–
Fourier series transformations	**−395.648**	**0.076**	**0.089**
Exponential smoothing	−395.343	0.078	0.096
LOESS method	−395.379	0.079	0.097
ACD algorithm	−396.643	0.145	0.153
ACD + ARIMA trend	−397.140	0.170	0.195
ACD + ETS trend	−400.076	0.121	0.121

Table 3. Time series models of RF Sberbank stocks and their forecasts for the test period

Trend estimation	LLF	MAE	RMSE
1st degree polynomial $y = a_0 + a_1 x$	−4979.271	0.105	0.128
2nd degree polynomial $y = a_0 + a_1 x + a_2 x^2$	−4950.327	0.199	0.215
3rd degree polynomial $y = a_0 + \sum_{i=1}^{3} a_i x^i$	−4881.779	0.440	0.465
4th degree polynomial $y = a_0 + \sum_{i=1}^{4} a_i x^i$	−4986.211	0.108	0.114
5th degree polynomial $y = a_0 + \sum_{i=1}^{5} a_i x^i$	−5019.458	0.079	0.119
1st degree polynomial + ARIMA	−4993.657	0.070	0.093
2nd degree polynomial + ARIMA	-4995.075	0.067	0.089
3rd degree polynomial + ARIMA	−4997.347	0.063	0.083
4th degree polynomial + ARIMA	−5006.537	0.067	0.085
5th degree polynomial + ARIMA	−5006.588	0.062	0.079
Hyperbolic function $y = a_0 + a_{-1} / x$	−4880.421	0.443	0.451
Logarithmic function $y = a_0 + a_1 \ln x$	−4923.877	0.288	0.300
Exponential function $y = \exp(a_0 + a_1 x)$	−4992.214	0.072	0.094
Interpolation by splines	−5013.558	–	–
Fourier series transformations	−5014.470	0.038	0.054
Exponential smoothing	−4976.059	0.117	0.145
LOESS method	**−5013.578**	**0.004**	**0.006**
ACD algorithm	−4996.171	0.077	0.086
ACD + ARIMA trend	−4987.216	0.145	0.162
ACD + ETS trend	−4979.289	0.170	0.191

using logarithmic and exponential functions (the best models are highlighted in bold). Models with Fourier series expansion, exponential smoothing, hyperbolic function, as well as those based on the LOESS method, have close values to them.

The best results in terms of RMSE for forecasting for the test period are those obtained using the method of trend estimation based on Fourier series expansion. The error values of trend modeling with exponential function, exponential smoothing, LOESS method and with polynomial of the first degree with forecasting both on the basis of ARIMA and linear regression are acceptable.

The lowest value of the likelihood function after the hybrid model with ACD trend and ETS forecast is obtained using the method of modeling the trend based on a polynomial of the fifth degree with linear regression forecasting. This value is slightly higher for the hybrid model with ACD trend and time series seasonality information predicted by ARIMA. We can also note the models with trend estimation using third- and fourth-degree polynomials. However, this group of models has some of the worst indicators for forecast accuracy.

When estimating the trend using polynomials, it is important to note that the accuracy decreases as the degree of the polynomial increases. This property also holds when combining trend estimation using polynomials with the ARIMA model.

In the examples presented above, seasonal time series are processed. Let us consider the performance of various methods of trend estimation on a non-seasonal time series of RF Sberbank stocks[4] (rubles). Data from 2000–2021 are used for training. The test period is 2022. Graphs of ACF and PACF functions are presented and described in detail in [29, Fig. 7]. The modeling and forecasting results are presented in Table 3. The best

[4] Sberbank (SBER) stock price. https://www.moex.com/ru/issue.aspx?board=TQBR&code=SBER (in Russ.). Accessed November 03, 2023.

models in terms of prediction accuracy for the test period or the value of the logarithm of the maximum likelihood function are highlighted in bold font.

Since there is no seasonality for stock market data, the forecast result depends entirely on the trend model and the random component.

The behavior of the series is described best by the spline function and LOESS models. At good values of the likelihood function, the trend model with the LOESS method has the most accurate forecasts. The error is 0.004 for MAE and 0.006 for RMSE. Low LLF values also correspond to trend modeling using a fifth-degree polynomial with linear regression prediction and using Fourier series expansion. These models also have some of the best accuracy values after the LOESS method model.

In contrast to the modeling of seasonal series, the other models are less well adjusted to the behavior of the series. These models are characterized by deterioration of accuracy as LLF values increase.

In trend modeling with polynomial, as the degree of the polynomial increases, starting from the fourth degree, accuracy increases, which may be partly due to overtraining. This is also true for the combination of series modeling with polynomial and ARIMA; however, the accuracy performance improves as the degree of the polynomial increases from the first degree onwards.

CONCLUSIONS

When modeling the trend for seasonal series, overlaying information on seasonal and random components affects the quality of forecasts. The best results are shown by the methods of trend modeling using Fourier series expansion and LOESS method. The combination of trend modeling with polynomial and ARIMA method for seasonality also has quite accurate results. While the indicators are worse when using polynomials for trend estimation with linear regression forecast than when using the combination of polynomial with ARIMA model, the behavior dynamics of accuracy indicators is the same for them.

It is interesting to note that the ACD algorithm performed best on the data of monetary incomes of the population. This time series has heterogeneous dispersion. Data forecasting using the ACD algorithm can be very useful for heteroscedastic series.

Trend modeling using exponential and logarithmic functions did not demonstrate outstanding results. Such methods are also computationally more complex than their polynomial equivalents. The logarithmic function model has limitations on the data values due to the lack of a real logarithm of a negative argument. The hyperbolic function model is one of the worst performing, both in terms of likelihood function and accuracy estimates.

Unlike trend estimation using the exponential function, trend extraction using exponential smoothing led to one of the best results. However, the main disadvantage of this method is the uncertain smoothing coefficient.

When working with non-seasonal time series, the forecast quality depends only on the trend and noise components. Models with Fourier series expansion, LOESS method and spline function fit the data best. However, it is difficult to make forecasts based on splines due to their orientation to data interpolation.

Since the LOESS method for a group of non-seasonal series also gives the best or close to the best results for all indicators, this method can be recommended for obtaining the most accurate results for series of different nature. The modeling of the trend using Fourier series decomposition can also be highlighted based on the sufficiently accurate results for time series of different natures obtained using this approach.

Authors' contribution. All authors equally contributed to the research work.

REFERENCES

1. Allen R. Time series methods in the monitoring of intracranial pressure. Part 1: Problems, suggestion for a monitoring scheme and review of appropriate techniques. *J. Biomed. Eng*. 1983;5(1):5–18. https://doi.org/10.1016/0141-5425(83)90073-0
2. Blom J.A., Ruyter J.F., Saranummi F., Beneken J.W. Detection of trends in monitored variables. In: Carson E.R., Cramp D.G. (Eds.). *Computer and Controls in Clinical Medicine*. New York: Plenum; 1985. P. 153–174. https://doi.org/10.1007/978-1-4613-2437-9_6
3. Challis R.E., Kitney R.I. Biomedical signal processing (in four parts). Part I: Time domain methods. *Med. Biol. Eng. Comput*. 1990;28(6):509–524. https://doi.org/10.1007/bf02442601
4. Haimowitz I.J., Kohane I.S. Automated trend detection with alternative temporal hypotheses. In: *Proceedings of the 13th International Joint Conference of Artificial Intelligence IJCAI-93*. 1993. P. 146–151.
5. Helsel D.R., Hirsch R.M., Ryberg K.R., Archfield S.A. *Statistical Methods in Water Resources*. USGS Science Publishing Network, Reston Publishing Service Center; 2018. 458 p. ISBN 978-1-4113-4348-1. https://doi.org/10.3133/tm4a3
6. Ding H., Li Z., Ren Q., Chen H., Song M., Wang Y. Single-variable method for predicting trends in chlorophyll a concentration based on the similarity of time series. *Ecological Indicators*. 2022;14096):109027. https://doi.org/10.1016/j.ecolind.2022.109027

7. Yao J., Wang P., Wang G., Shrestha S., Xue B., Sun W. Establishing a time series trend structure model to mine potential hydrological information from hydrometeorological time series data. *Sci. Total Environ*. 2020;698:134227. https://doi.org/10.1016/j.scitotenv.2019.134227
8. De Leo F., De Leo A., Besio G., Briganti R. Detection and quantification of trends in time series of significant wave heights: An application in the Mediterranean Sea. *Ocean Eng*. 2020;202:107155. https://doi.org/10.1016/j.oceaneng.2020.107155
9. Hyndman R.J., Athanasopoulos G. *Forecasting: Principles and Practice*. 3rd ed. OTexts; 2021. 442 p. ISBN-13 978-0-9875-0713-6
10. Mann H.B. Nonparametric tests against trend. *Econometrica*. 1945;13(3):2453–259. https://doi.org/10.2307/1907187
11. Kendall M.G. *Rank Correlation Methods*. 2nd ed. Hafner Publishing Co.; 1955. 196 p.
12. Kohns D., Bhattacharjee A. Nowcasting growth using Google Trends data: A Bayesian Structural Time Series model. *Int. J. Forecast*. 2022;39(3):1384–1412. https://doi.org/10.1016/j.ijforecast.2022.05.002
13. Yahyaoui H., Al-Daihani R. A novel trend based SAX reduction technique for time series. *Expert Systems with Applications*. 2019;130(C):113–123. https://doi.org/10.1016/j.eswa.2019.04.026
14. Xie Y., Liu S., Huang S., Fang H., Ding M., Huang C., Shen T. Local trend analysis method of hydrological time series based on piecewise linear representation and hypothesis test. *J. Clean. Prod*. 2022;339(1):130695. https://doi.org/10.1016/j.jclepro.2022.130695
15. Vamoş C., Crăciun M. *Automatic Trend Estimation*. Dordrecht, Heidelberg, New York, London: Springer; 2013. 131 p. https://doi.org/10.1007/978-94-007-4825-5
16. Feng Y., Zhou C. Forecasting financial market activity using a semiparametric fractionally integrated Log-ACD. *Int. J. Forecast*. 2015;31(2):349–363. http://doi.org/10.1016/j.ijforecast.2014.09.001
17. Allen D., Chan F., McAleer M., Peiris S. Finite sample properties of the QMLE for the Log-ACD model: Application to Australian stocks. *J. Econometrics*. 2008;147(1):163–185. https://doi.org/10.1016/j.jeconom.2008.09.020
18. Epperson J. On the Runge example. *The American Mathematical Monthly*. 1987;94(4):329–341. https://doi.org/10.2307/2323093
19. Drozdov I., Petrusevich D. Water pollution time series analysis. *IOP Conf. Ser.: Mater. Sci. Eng*. 2021;1047(1):012095. http://doi.org/10.1088/1757-899X/1047/1/012095
20. Petrusevich D. Review of missing values procession methods in time series data. *J. Phys.: Conf. Ser*. 2021;1889(3):032009. http://doi.org/10.1088/1742-6596/1889/3/032009
21. Wang P., Zheng X., Ai G., Liu D., Zhu B. Time series prediction for the epidemic trends of COVID-19 using the improved LSTM deep learning method: Case studies in Russia, Peru and Iran. *Chaos, Solitons & Fractals*. 2020;140:110214. https://doi.org/10.1016/j.chaos.2020.110214
22. Kumar B., Sunil P., Yadav N. A novel hybrid model combining *βSARMA* and LSTM for time series forecasting. *Appl. Soft Comput*. 2023;134:110019. https://doi.org/10.1016/j.asoc.2023.110019
23. Abebe M., Noh Y., Kang Y.-J., Seo C., Kim D., Seo J. Ship trajectory planning for collision avoidance using hybrid ARIMA-LSTM models. *Ocean Eng*. 2022;256:111527. https://doi.org/10.1016/j.oceaneng.2022.111527
24. Arunkumar K.E., Kalaga D.V., Kumar M.S., Kawaji M., Brenza T.M. Comparative analysis of Gated Recurrent Units (GRU), long Short-Term memory (LSTM) cells, autoregressive Integrated moving average (ARIMA), seasonal autoregressive Integrated moving average (SARIMA) for forecasting COVID-19 trends. *Alexandria Eng. J*. 2022;61(10):7585–7603. https://doi.org/10.1016/j.aej.2022.01.011
25. Ning Y., Kazemi H., Tahmasebi P. A comparative machine learning study for time series oil production forecasting: ARIMA, LSTM, and Prophet. *Comput. Geosci*. 2022;164:105126. https://doi.org/10.1016/j.cageo.2022.105126
26. Anghinoni L., Zhao L., Ji D., Pan H. Time series trend detection and forecasting using complex network topology analysis. *Neural Netw*. 2019;117:295–306. https://doi.org/10.1016/j.neunet.2019.05.018
27. Box G., Jenkins G., Reinsel G.C. *Time Series Analysis: Forecasting and Control*. John Wiley and Sons; 2008. 784 p. ISBN-13 978-0470272848
28. Petropoulos F., Hyndman R.J., Bergmeir C. Exploring the sources of uncertainty: Why does bagging for time series forecasting work? *Eur. J. Oper. Res*. 2018;268(2):545–554. https://doi.org/10.1016/j.ejor.2018.01.045
29. Gramovich I.V., Musatov D.Yu., Petrusevich D.A. Implementation of bagging in time series forecasting. *Russ. Technol. J*. 2024;12(1):101–110. https://doi.org/10.32362/2500-316X-2024-12-1-101-110
30. Zhao K., Wulder M.A., Hu T., Bright R., Wu Q., Qin H., Li Y., Toman E., Mallick B., Zhang X., Brown M. Detecting change-point, trend, and seasonality in satellite time series data to track abrupt changes and nonlinear dynamics: A Bayesian ensemble algorithm. *Remote Sens. Environ*. 2019;232:111181. https://doi.org/10.1016/j.rse.2019.04.034
31. Li J., Li Z.-L., Wu H., You N. Trend, seasonality, and abrupt change detection method for land surface temperature time-series analysis: Evaluation and improvement. *Remote Sens. Environ*. 2022;280:113222. https://doi.org/10.1016/j.rse.2022.113222

About the authors

Ulyana S. Mokhnatkina, Student, MIREA – Russian Technological University (78, Vernadskogo pr., Moscow, 119454 Russia). E-mail: atlantika@live.ru. https://orcid.org/0009-0008-8756-7267

Denis V. Parfenov, Cand. Sci. (Eng.), Associate Professor, Higher Mathematics Department, Institute of Artificial Intelligence, MIREA – Russian Technological University (78, Vernadskogo pr., Moscow, 119454 Russia). E-mail: parfenov@mirea.ru. Scopus Author ID 57217119805, RSCI SPIN-code 7463-3220, https://orcid.org/0009-0004-0905-3827

Denis A. Petrusevich, Cand. Sci. (Phys.-Math.), Associate Professor, Higher Mathematics Department, Institute of Artificial Intelligence, MIREA – Russian Technological University (78, Vernadskogo pr., Moscow, 119454 Russia). E-mail: petrusevich@mirea.ru, petrdenis@mail.ru. Scopus Author ID 55900513600, ResearcherID AAA-6661-2020, RSCI SPIN-code 7999-6345, https://orcid.org/0000-0001-5325-6198

Об авторах

Мохнаткина Ульяна Станиславовна, студент, ФГБОУ ВО «МИРЭА – Российский технологический университет» (119454, Россия, Москва, пр-т Вернадского, д. 78). E-mail: atlantika@live.ru. https://orcid.org/0009-0008-8756-7267

Парфенов Денис Васильевич, к.т.н., доцент, доцент кафедры высшей математики, Институт искусственного интеллекта, ФГБОУ ВО «МИРЭА – Российский технологический университет» (119454, Россия, Москва, пр-т Вернадского, д. 78). E-mail: parfenov@mirea.ru. Scopus Author ID 57217119805, SPIN-код РИНЦ 7463-3220, https://orcid.org/0009-0004-0905-3827

Петрусевич Денис Андреевич, к.ф.-м.н., доцент кафедры высшей математики, Институт искусственного интеллекта, ФГБОУ ВО «МИРЭА – Российский технологический университет» (119454, Россия, Москва, пр-т Вернадского, д. 78). E-mail: petrusevich@mirea.ru, petrdenis@mail.ru. Scopus Author ID 55900513600, ResearcherID AAA-6661-2020, SPIN-код РИНЦ 7999-6345, https://orcid.org/0000-0001-5325-6198

Translated from Russian into English by Lyudmila O. Bychkova
Edited for English language and spelling by Thomas A. Beavitt

MIREA – Russian Technological University.
78, Vernadskogo pr., Moscow, 119454 Russian Federation.
Publication date May 31, 2024.
Not for sale.

МИРЭА – Российский технологический университет.
119454, РФ, г. Москва, пр-т Вернадского, д. 78.
Дата опубликования 31.05.2024 г.
Не для продажи.

https://www.rtj-mirea.ru